INSTRUMENTATION AND OPERATION OF A NEW FATIGUE TESTER

by

JEANETTE BIRD

Submitted in partial fulfilment of the
requirements for the degree of
Master of Science
in the
Department of Physics,
University of Natal

Pietermaritzburg
1993

PREFACE

The experimental work described in this thesis was carried out in the Department of Physics, University of Natal, Pietermaritzburg, from January 1991 to January 1993, under the supervision of Professor Paul J. Jackson.

These studies represent original work by the author and have not otherwise been submitted in any form for any degree or diploma to any University. Where use has been made of the work of others it is duly acknowledged in the text.

ACKNOWLEDGEMENTS

I wish to thank the following people for their help during the course of this work:

Professor P.J. Jackson, my supervisor, for his support and guidance and for his supervision and criticism of my thesis.

Mr A.C. Hill, of the Physics Workshop, for his willing help and expertise in adapting and improving the fatigue tester.

Mr G. Dewar, of the Faculty Electronics Centre, for all his help and advice in the design and de-bugging of the electronic circuitry of the tester.

The members of the Physics Department who were always willing to offer help when it was required.

Mintek for their financial support.

The Electron Microscope Unit for their help and the use of their SEM.

Trevor Hohls, my fiancé, for his support, encouragement and patience during this work, as well as for his help typing and proof-reading.

Thanks are also due to the Physics Department for the excellent facilities made available to me.

ABSTRACT

A computer-controlled electromagnetic fatigue tester, designed to fatigue pure copper single crystals, was instrumented and used to fatigue copper and gold specimens to failure. A computer program was written to control the fatigue tester, make measurements of stress and strain during the test, and plot mechanical hysteresis loops. A scanning electron microscope was used to make surface observations of a few fatigued specimens. The hysteresis loops and the surface observations of the specimens were used to demonstrate the present state of the development of the instrumented fatigue tester.

Chapter 1 is a general review of the subject of metal fatigue. The electromagnetic fatigue tester, which had been built in the Physics Department of the University of Natal, Pietermaritzburg, is described in Chapter 2. Electronic circuitry that controls the magnets, which apply forces to the test specimens, is described in Chapter 3. This circuitry was designed to control the strain amplitude of the fatigue tests. Measurements of the stress applied to and the strain experienced by the specimen during fatigue involve the measurement of small displacements. Various transducers for measuring small displacements are reviewed and compared in Chapter 4. In Chapter 5, the function and associated instrumentation of the specific displacement transducers chosen for use in the fatigue tester are discussed. Details of the operation and programming of the computer hardware that were used to control the strain, and to measure the applied stress are

presented in Chapter 6. The operation of the tester is described in Chapter 7, and sample results obtained are given in Chapter 8.

The results presented show that the tester is capable of fatiguing soft specimens, such as pure copper and pure gold. The tester can now be used for a comparative investigation of the fatigue behaviour of such samples, with a view to elucidating the effects of the environment on fatigue life.

TABLE OF CONTENTS

CHAPTER 1
METAL FATIGUE

1.1 INTRODUCTION

Metal fatigue is the deformation and failure of a metal subjected to repeated cyclic loading. Cyclic stresses which lead to failure are usually much smaller than the static stress required to fracture a metal, and may be even lower than the yield stress of the metal.

In the early stages of the study of metal fatigue, research was based almost entirely on a macroscopic engineering approach, and was largely restricted to the study of the mechanical fatigue behaviour of metal specimens. Design parameters were established, whereby the risk of metal fatigue could be minimised. Nevertheless, unexpected structural failure continued to plague, for example, the aircraft industry. Hence the continuing interest in the subject of metal fatigue.

The fatigue behaviour of materials was first documented using Wöhler curves or so-called S-N plots (S: stress, N: No. of cycles to failure), as shown in Figure 1.1. Such plots show the relationship between the fatigue life of the specimen and the stress amplitude of the fatigue cycle.

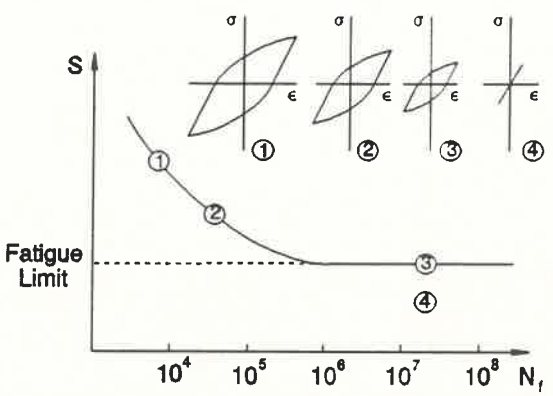

Figure 1.1 : Wöhler curve showing fatigue limit. Inserts show hysteresis loops for different stress levels (Mughrabi 1984).

Figure 1.1 shows a Wöhler curve demonstrating a well-defined fatigue limit. This limit corresponds to the value of the stress amplitude, below which failure does not occur, no matter how long the specimen is cyclically loaded.

Determination of the fatigue limit for a given material allowed safety limits to be calculated for the design of mechanical structures and components.

The existence of hysteresis in elastic deformations was first demonstrated by Bairstow in 1910. Bairstow showed that plotting the axial stress (σ) applied to a specimen undergoing fatigue against the total strain (ϵ_t) on the specimen , yielded a mechanical hysteresis loop, as shown in Figure 1.2. The total strain ϵ_t, is the sum of the elastic (reversible) strain, ϵ_e, and the plastic (irreversible) strain, ϵ_{pl}.

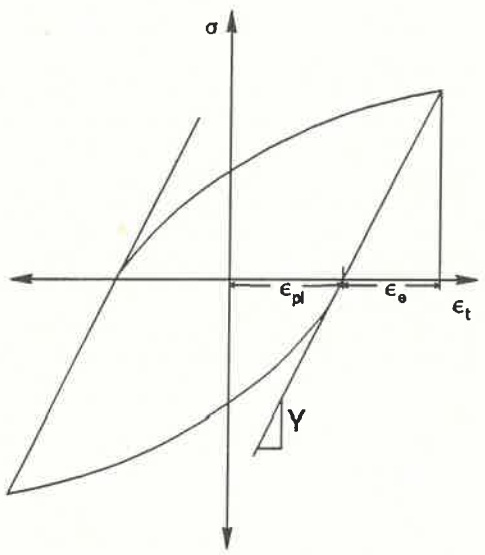

Figure 1.2 : Mechanical hysteresis loop of a fatigue cycle. Y is Young's modulus.

While stress amplitudes leading to fatigue failure are usually too small to cause macroscopic yielding, they are large enough to cause measurable cyclic plastic microstrains (Mughrabi 1984). Near the fatigue limit, these strains are of the order of 10^{-5} to 10^{-4}. Manson (1954) and Coffin (1954) established the relationship between the cyclic plastic strain amplitude, ϵ_{pl}, and the fatigue life, N_f.

The Manson-Coffin law states

$$N_f^c . \epsilon_{pl} = constant, \qquad (1.1)$$

where the power, c, is typically 0.5 to 0.6. It follows that metal fatigue is a result of small amounts of irreversible plastic deformation which occur during each stress cycle. It turns out that the plastic strain amplitude is the most physically significant loading variable, although it is inseparably interconnected with the stress amplitude.

Lukáš, Klesnil and Polák (1974) studied the behaviour of various metals and alloys in the range of very low ϵ_{pl}. They showed that ϵ_{pl} is finite at the fatigue limit and assumes well-defined values in the range of 10^{-5} and 10^{-4}.

Hence, to completely characterize the fatigue limit, the critical threshold values of both the stress amplitude and the plastic strain amplitude are required. This is illuminated by the hysteresis loops shown with the Wöhler curve in Figure 1.1. These loops correspond to the different stress amplitudes as indicated. All the hysteresis loops on the plot enclose a finite area, that is $\epsilon_{pl} > 0$. Hysteresis loops where the strain is entirely elastic (zero enclosed area), are only found at stresses below the fatigue limit.

It can be shown (Mughrabi 1984), that the cumulative plastic strain until failure is large when compared with the typical strain required to rupture a specimen subjected to unidirectional strain. Mughrabi states that, due to microstructural instabilities which result in strain localization, the local cumulative plastic strain in the regions where fatigue cracks form may be one or two orders of magnitude larger than the overall cumulative plastic strain.

During the 1950's physicists began to investigate the fundamental causes of fatigue, by studying the microstructure of fatigued specimens. The study of microstructures that occur during fatigue fall into two classes: surface microstructures and sub-surface dislocation microstructures.

Before the advent of the transmission electron microscope (TEM), microstructural observation were limited to the study of the surface. The earliest surface morphology observations were published by Ewing (1889), Ewing and Rosenhain (1899) and Ewing and Humfrey (1902), who obtained clear microscopic evidence of slip on the surface of fatigued iron. However, it was only later that serious attention was paid to surface observations, such as the work of Gough (1926) on the polished surfaces of fatigued specimens.

It was found that fine slip lines were produced in the early stages of cycling, and these slip lines became more intense as the test proceeded, producing bands of slip separated by areas relatively free of slip.

Much of the work done on microstructural studies was carried out using single crystals of metals, because they have well-defined slip planes which can be identified and orientated for single slip. The surface and sub-surface microstructure of single crystals is less complex than that of polycrystals, and lends itself to the fundamental study of fatigue.

In the late 1940's, the development of electropolishing stimulated research on surface microstructure and ultimately led to the discovery of persistent slip bands (PSBs) by Thompson *et al* (1956). These are bands of slip which, when removed by electropolishing the surface, reappear in the same positions after further cycling. Thompson and co-workers found that the PSBs appeared at about 5% of the fatigue life and were often the site of fatigue cracks.

In 1953, Forsyth discovered extrusions in Al-4%Cu alloy specimens subjected to fatigue cycling. These extrusions are thin ribbons of metal, about 1μm thick, which were extruded from slip bands. Extrusions were subsequently observed in many other fatigued specimens. Cottrell and Hull (1957) and Wood and Segall (1957) then discovered the existence of intrusions, a few microns deep, which were often associated with extrusions.

It was at this time that the role of dislocations in fatigue mechanisms began to be appreciated, as indicated in the review article by Thompson and Wadsworth (1958). Extensive work has since been performed by many researchers on dislocations and dislocation mechanisms in fatigue. Much of this work has been carried out using single crystals of copper (eg. Basinski and Basinski 1982-1989, Lisiecki and Pedersen 1990).

According to Mughrabi (1984): "fundamental studies on the nature of fatigue damage must be based on well designed cyclic deformation experiments and on a careful evaluation of the microstructural changes that occur during cyclic straining." The behaviour of dislocations and their interactions are particularly important. One can consider the localized events which lead to fatigue damage as "a consequence of the bulk microstructural changes that occur earlier in fatigue life." (Mughrabi 1984). Mughrabi summarized the scheme of events occurring during fatiguing, as shown in Figure 1.3.

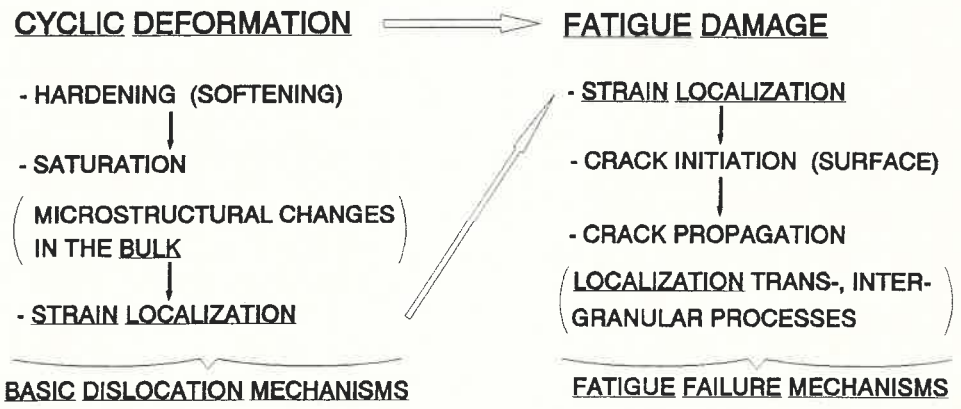

Figure 1.3 : Cyclic deformation and fatigue damage. Sequence of events and classification of mechanisms (Mughrabi 1984).

More recent studies on the application of dislocation concepts to metal fatigue have contributed to an improved understanding of some basic dislocation mechanisms, and to the development of dislocation models of the early stages of the fatigue failure process.

1.2 THE CYCLIC STRESS-STRAIN CURVE

Fatigue tests can be performed with either a constant stress amplitude, σ, or a constant plastic strain amplitude, ϵ_{pl}. In order to characterize the fatigue behaviour, the plastic strain must be monitored continuously if the stress amplitude is kept constant and vice versa. When the test first starts, rapid cyclic hardening, or softening, usually occurs. If the test is run at constant stress amplitude, ϵ_{pl} will decrease or increase, respectively. If the plastic strain amplitude is constant, σ will increase or decrease respectively. This is shown in Figure 1.4 (a) and (b). Thereafter, there is an extended period of cyclic saturation, where ϵ_{pl} and σ assume steady state values: $\epsilon_{pl,s}$ for constant σ, and σ_s for constant ϵ_{pl}. Finally fatigue failure occurs.

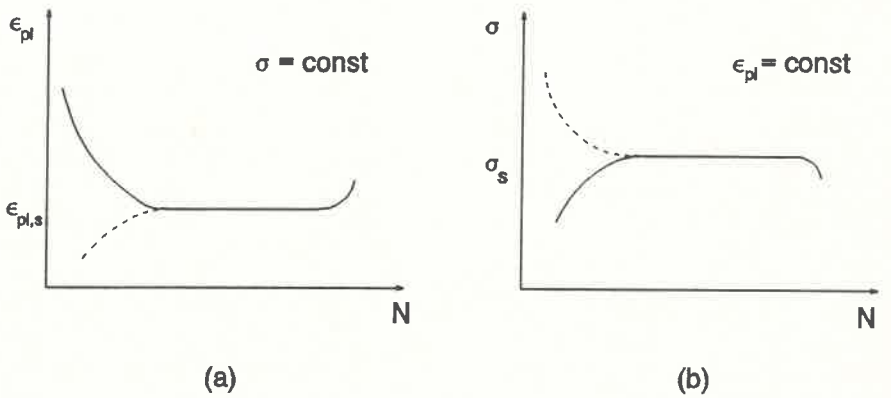

Figure 1.4 : Cyclic hardening (softening) curves. Dashed curves refer to softening. In (a) σ is constant, in (b) ϵ_{pl} is constant.

Because the saturation regime frequently dominates the fatigue life, the steady-state amplitudes, σ_s and $\epsilon_{pl,s}$, may be used as rough mean values for the stress and plastic strain amplitudes, respectively.

The resolved shear stress, τ, which is the shear stress resolved across a crystallographic slip plane, in the slip direction, is related to the tensile stress by

$$\tau = m.\sigma, \qquad (1.2)$$

where m is known as the Schmid factor of the crystal. The

resolved plastic shear strain amplitude, γ_{pl} is related to the tensile strain by

$$\gamma_{pl} = \frac{\epsilon_{pl}}{m}. \qquad (1.3)$$

Mughrabi (1978) established a useful means of representing fatigue data gathered in constant plastic strain amplitude fatigue tests. He plotted the resolved saturation shear stress, $\tau_s = m.\sigma_s$, versus the resolved plastic shear strain amplitude, γ_{pl}, for a number of single crystals. Each point on such a graph represents a single test, carried out at a different γ_{pl}. Such curves may be plotted for any metal or alloy, single crystal or polycrystal. These curves are termed cyclic stress-strain curves (CSS curves). Figure 1.5 shows the CSS curve for copper single crystals orientated for single slip.

Figure 1.5 shows the three regions (A,B and C) which are found in the CSS curve of copper single crystals. The study of the dislocation microstructure and mechanisms in each region has helped towards an understanding of the conditions which prevail in metal fatigue.

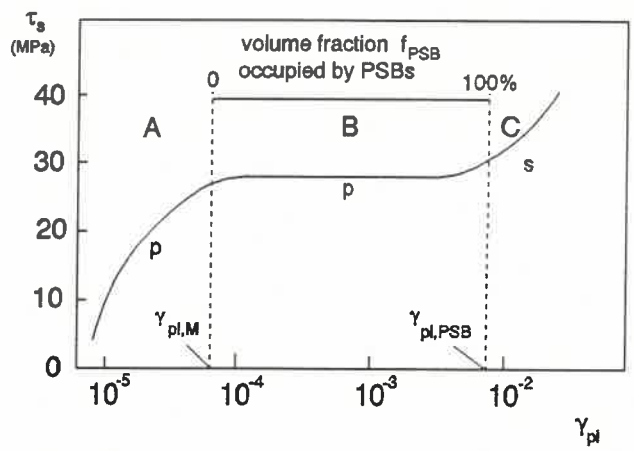

Figure 1.5 : Cyclic stress-strain curve of copper single crystals at room temperature. p: primary slip, s: secondary slip (Mughrabi 1984).

In Region A, τ_s increases with increasing γ_{pl}, while in Region B τ_s remains more or less constant for a wide range of values of γ_{pl} (6×10^{-5} to 7.5×10^{-3}). In Region C τ_s once again increases as

γ_{pl} increases. In Regions A and B single slip dominates, while in Region C secondary slip plays an important role.

1.2.1 **Region A**

At low stresses and strains, the dislocation structures found in a fatigued specimen consist of dense bundles of edge dislocation dipoles forming unit loop patches (Laird *et al* 1986). These bundles, or veins as they are termed, consist chiefly of primary edge dislocations . The roughly cylindrical veins are separated by channels which are relatively free of dislocations. Most dislocations in the channels are screw dislocations. The veins and channels lie perpendicular to the active Burgers vector, **b**. The densely packed veins are much harder than the relatively soft dislocation-free channels, and the plastic strain is therefore carried by the channels. In Region A specimens undergo homogeneous cyclic hardening.

As the imposed plastic strain amplitude increases, the volume fraction of the specimen occupied by the harder veins increases, and the saturation stress increases as well. At the plateau stress, which is approximately 28 MPa for copper single crystals, the volume fraction of veins is roughly 50%. When γ_{pl} is increased further, the imposed plastic strain can no longer be carried by the channels alone and the veins are forced to become plastic. The plateau stress is thus the stress at which the loop patches, or veins, become unstable. Persistent slip bands (PSBs) develop from the veins, forming just before the plateau stress is reached. The more open structure of PSBs supports plastic flow at a reduced stress level.

1.2.2 **Region B**

The sub-surface microstructure of the PSBs which characterize Region B, can be described as a wall or ladder structure. The PSBs are thin lamellae, about 1μm thick, which lie parallel to the primary slip plane, and which look, in cross-section, like

ladders. The rungs or walls of the ladder consist of densely packed primary edge dislocation dipole loops ($10^{15}m^{-2}$) forming a type of multipole (Laird 1986).

PSBs are regions of localized slip in which the local strain is much higher than the overall strain experienced by the crystal. Extensive dislocation glide occurs within the PSBs, and as a result of the glide, prominent surface slip traces develop, where the PSBs intersect the surface. These slip traces are frequently the site of fatigue cracks. PSBs are clearly distinguishable from the surrounding matrix, which on the surface remains flat because there is little slip activity in the matrix, as seen in Figure 1.6. The matrix has the vein structure described in Section 1.2.1 above. Figure 1.7 shows the sub-surface vein structure of the matrix and the ladder structure of the PSBs.

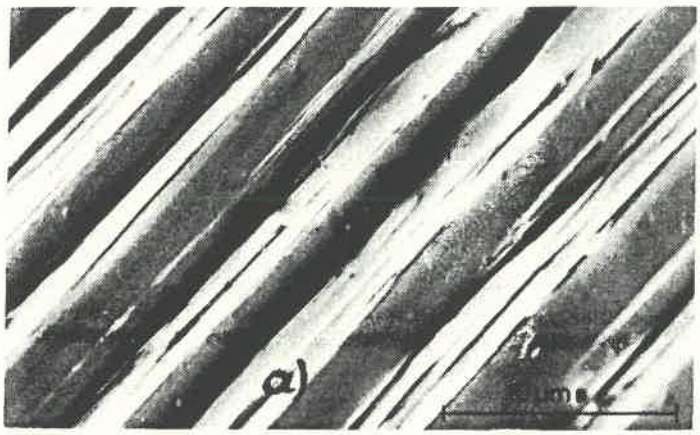

Figure 1.6 : Surface traces associated with PSBs (Mughrabi 1984).

Figure 1.7 : Electron micrograph of PSB and Matrix (Mughrabi 1984).

The heterogeneous microstructure described above is the essential characteristic of persistent slip. The soft PSBs are embedded in the hard matrix, and the strain becomes localized in the PSBs.

The plateau region is characterized by the formation of the first PSBs at its lower end ($\gamma_{pl} \approx 6\times10^{-5}$), and by PSBs occupying the entire volume of the specimen at the upper end ($\gamma_{pl} \approx 7.5\times10^{-3}$) of the plateau. The volume fraction of PSBs increases as γ_{pl} increases. On the plateau, τ_s remains constant due to the localized plastic strain in the PSBs (Section 1.3.2). PSB formation is essentially a single slip phenomenon, and as a result single crystals orientated for single slip are well suited to quantitative investigation of PSBs.

1.2.3 **Region C**

At the critical point at the end of the plateau where PSBs occupy the entire volume of the crystal, increasing γ_{pl} further results in the dislocation structure of the plateau giving way smoothly to a "cell structure of increasing refinement" (Laird *et al* 1986), and multiple slip becomes increasingly important.

The walls of the cells are similar to PSB walls, but are more complex because of secondary dislocations. They are, therefore, termed "secondary walls" (Laird *et al* 1986). On a larger scale (~10μm) the dislocation arrangement of the cell structure is more homogeneous than the dislocation arrangement in Region B.

Because the stress and strain amplitudes in Region C are high, the fatigue life of specimens fatigued in this region are short (Wöhler curve, Manson-Coffin law). Not much work has been done on dislocation structures in Region C on single crystals, perhaps because it is more difficult to fatigue single crystals at high strain amplitudes, or perhaps because high strain fatigue problems are not as prevalent as long life fatigue problems. Work carried out on polycrystals in this region (eg. Charsley 1981, Feltner and Laird 1967, Pratt 1967) show that the cell structures which form at high strain amplitudes are extremely stable. The

cells grow or shrink if the strain amplitude is decreased or increased relative to the strain amplitude at which the cells were formed.

1.2.4 **Associated Phenomena**

There are several phenomena associated with the CSS curve and the three fatigue regions.

At the onset of Region B, when the first PSBs appear, the mechanical hysteresis loop changes shape. In Region A, the hysteresis loop is characteristically slim and pointed by the time the saturation stress amplitude, τ_s, is attained. Figure 1.8(a) shows hysteresis loops for various plastic strain amplitudes in Region A. These loops are plotted as resolved shear stress, τ, versus resolved shear strain, γ.

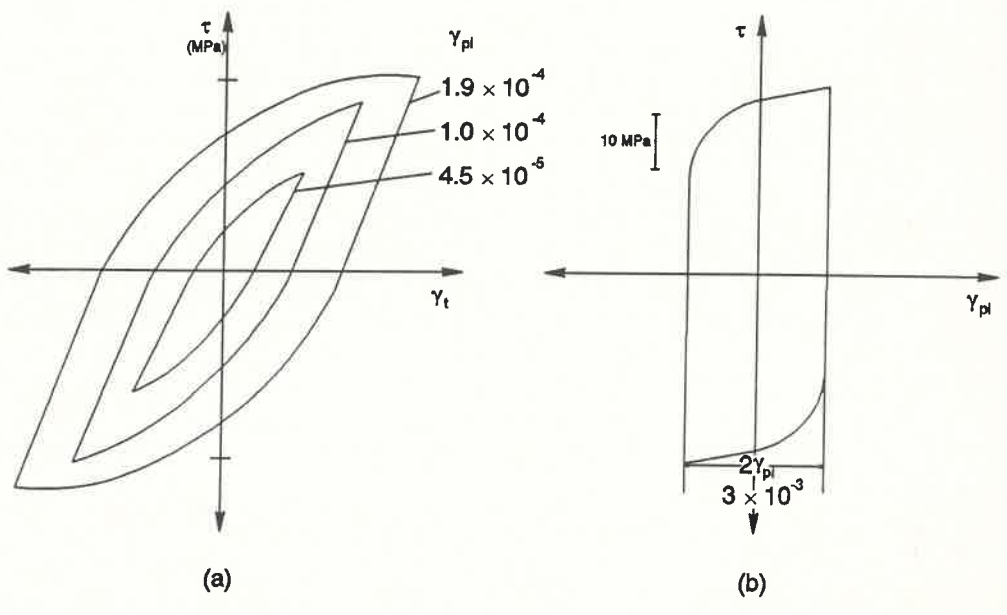

Figure 1.8 : Shapes of hysteresis loops :(a) saturation hysteresis loops in Region A and the beginning of Region B; (b) the typical shape of a hysteresis loop in Region B (Mughrabi *et al* 1979). Note that γin (a) is total strain, and γ in (b) is plastic strain.

In Region B, the loops develop flat peaks. With increasing γ_{pl} the peaks become flatter and wider, and the hysteresis loops

become more rectangular in shape, as shown in Figure 1.8(b). This mechanical behaviour can be illustrated by the performance of a two component Masing model, reviewed by Barnett (1988).

Another phenomenon is that failure only occurs in Regions B and C, not in Region A. Thus, plastic strain amplitudes in Region A are regarded as safe, that is, specimens fatigued at these strain amplitudes should not fracture, even after many thousands of fatigue cycles.

1.3 PERSISTENT SLIP BANDS AND FATIGUE CRACK INITIATION

1.3.1 Persistent Slip Bands

Because PSBs are thin and platelike and lie parallel to the primary slip plane, the matrix does not constrain the deformation of the PSBs. It can be shown that PSBs are softer than the matrix (Helgeland 1965). The soft PSBs are deformed in series with the harder matrix. This results in the strain being localized in the PSBs. The measured saturation stress corresponds to the cyclic flow stress of the PSBs and is independent of the number of PSBs present.

The formation of PSBs occurs as follows. During rapid hardening, dense bundles (veins) form. The bundles consist mainly of fragmented primary edge dislocations (Section 1.2.1). As the veins form, most screw dislocations annihilate. The vein structure becomes progressively denser as cycling continues. Thus, the individual veins harden until a certain stress level is reached. At this level of stress, the dipole structure of the veins becomes unstable, due to the imposed strain amplitude. A transient deformation process follows, whereby dislocations freed from unstable veins multiply, annihilate and rearrange until the ladder structure of the PSBs is formed (Mughrabi 1984).

Studies of copper polycrystals (eg. Mughrabi and Wang 1981) show that the CSS curve of polycrystals coincides with that of single crystals in Region A, as shown in Figure 1.9. At higher plastic

strain amplitudes, the polycrystal CSS curve deviates from the single crystal curve. A plateau region is not observed for polycrystals, although PSBs have been observed in interior grains by several groups (eg Pohl *et al* 1980, Winter *et al* 1981, Mughrabi and Wang 1981). Cyclic hardening behaviour similar to Region C in single crystals is shifted to much lower amplitudes than in single crystals, as indicated by the arrow in Figure 1.9.

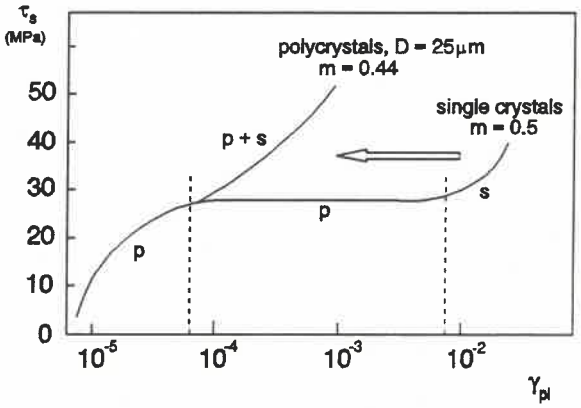

Figure 1.9 : Cyclic stress strain curves for copper mono- and polycrystals at room temperature. p: primary slip, s: secondary slip (Mughrabi 1984).

It can be shown (Mughrabi 1984), that the first PSBs to form in polycrystals are those surface grains with the highest possible Schmid factor, $m \approx 0.5$.

1.3.2 **Winter's Two-Phase Model**

When a copper single crystal is fatigued in saturation, the volume fraction of the crystal occupied by PSBs, f_{PSB}, is a constant. The value of the constant depends on γ_{pl}.

Winter (1974) measured the volume fraction of PSBs for a series of copper single crystals fatigued at different strain amplitudes. He found that f_{PSB} depends linearly on γ_{pl}, for tests carried out at constant plastic strain amplitudes. A similar relationship has been observed for crystals fatigued at constant stress amplitudes (Roberts 1969).

If $\gamma_{pl,PSB}$ and $\gamma_{pl,M}$, are the local plastic shear strain amplitudes in the PSBs and the matrix, respectively, then Winter's rule of mixture gives

$$\gamma_{pl} = f_{PSB}\gamma_{pl,PSB} + (1-f_{PSB})\gamma_{pl,M}. \qquad (1.4)$$

The linear relationship between γ_{pl} and f_{PSB}, reported by Winter (1974), implies that $\gamma_{pl,PSB}$ and $\gamma_{pl,M}$ are constants, independent of γ_{pl}. If $f_{PSB} = 1$, then the entire volume of the crystal is occupied by PSBs and $\gamma_{pl} = \gamma_{pl,PSB}$. This corresponds to the strain amplitude at the end of the plateau, so $\gamma_{pl,PSB} \approx 6\times10^{-5}$. Similarly, when $f_{PSB} = 0$ then there are no PSBs present and $\gamma_{pl} = \gamma_{pl,M}$. This corresponds to the lower end of the plateau, so $\gamma_{pl,M} \approx 7.5\times10^{-3}$. Therefore $\gamma_{pl,M} \approx 10^2.\gamma_{pl,PSB}$ (Mughrabi 1984).

Thus, a specimen fatigued at constant strain amplitude in Region B enters a steady state, which contains two phases: the soft, active PSBs, and the hard, relatively inactive matrix. For any value of γ_{pl} between $\gamma_{pl,M}$ and $\gamma_{pl,PSB}$, the PSBs are fatigued at a constant plastic strain amplitude, as is the matrix. "The crystal adapts itself to the applied strain amplitude by adjusting the relative amounts of the two phases" (Winter 1974).

Winter used his two-phase model to make several predictions, which he found to be supported by experimental observations.

Winter's model predicts that the saturation stress amplitude, τ_s, does not depend on γ_{pl}, in the region where PSBs are active. This fact is well established for copper single crystals.

Winter predicted that more PSBs would form if the plastic strain amplitude were increased after saturation. He conducted an experiment and found his prediction to be valid. If the plastic strain amplitude was decreased after stauration, existing PSBs did not disappear.

Winter's model predicts the discontinuities in the fatigue properties at $\gamma_{pl,M}$ and $\gamma_{pl,PSB}$. These discontinuities correspond to the ends of the plateau.

Winter's model is widely accepted, but Laird *et al* (1986) point out that it may be an over-simplification of the situation. The reason for their reservations is that Winter assumes that $\gamma_{pl,PSB}$ is a constant. The magnitude of the localized strain has been found to vary widely among different PSBs (Finney and Laird 1975). The accepted magnitude is thus only an average of the localized strain of all the PSBs.

1.3.3 **Dislocation Mechanisms in PSBs**

Dislocation glide processes in the PSBs and the matrix after saturation have been widely researched (eg. Winter 1974, Finney and Laird 1975, Mughrabi 1980, Basinski *et al* 1980, Laird 1983, Neumann 1983).

An important feature which is common to the PSBs and the matrix is the heterogeneous division of the dislocations into walls or veins, and into channels. The walls of the PSBs and the veins of the matrix have high densities of edge dislocations ($\sim 10^{15} m^{-2}$), while the channels have low dislocation densities, containing mainly screw dislocations ($\sim 10^{12} m^{-2}$ in matrix, $\sim 10^{13} m^{-2}$ in PSBs). The fundamental questions regarding processes in Region B, are concerned with the differences between the matrix and the PSBs with particular regard to "the compatibility of deformation of the heterogeneous dislocation structures, the establishment of steady-state conditions, the mechanical hysteresis and the local flow stresses" (Mughrabi 1984).

It would appear inadequate to describe the process in terms of a single dislocation mechanism, and a composite model is considered appropriate by Mughrabi (1983) and Pedersen and Winter (1982), among others.

Only a small microstrain ($\sim 10^{-4}$) needs to be accommodated by the matrix. According to Mughrabi (1984) this strain " can be accomplished by 'quasi-reversible' to-and-fro bowing of the screw dislocations in the channels and essentially only elastic polarization of the hard veins, perhaps with some isolated

occurrences of dipole flip-flop." He claims that there is only negligible microstructural change per cycle.

The high local plastic shear strain in the PSBs ($\sim 10^{-2}$) causes macroyielding. Mughrabi (1984) states that "this involved dislocation multiplication by edge dislocation segments that bow out from the walls and traverse the channels and the (partial) penetration of the walls by edge dislocations, as the screw dislocations glide along the channels, drawing-out edge dislocations." The hard walls of the PSBs yield plastically as a result of the compatibility requirements of the heterogeneous dislocation structure.

The processes described above have been confirmed by Yamamoto and Imura (1981) and Lepinoux and Kubin (1984), who carried out *in situ* TEM deformation studies. A very important result of the composite model of dislocation mechanisms is the predicted shape of the hysteresis loops. The cyclic microdeformation of the matrix yields a slim pointed hysteresis loop, while the macrodeformation of the PSBs leads to a broad, more rectangular loop (Mughrabi 1984). This result is in very good agreement with experiment (Section 1.2.4).

The composite model also provides a natural explanation for the periodic build-up and decay of long-range internal stresses during each fatigue cycle (Mughrabi 1983). These stresses arise due to the plastic strain mismatch between hard and soft regions during straining.

Steady-state deformation in PSBs is accomplished by a dynamic equilibrium between dislocation multiplication and annihilation (Essman and Mughrabi 1979). In order that the dislocation density does not continue to increase in saturation, screw and edge dislocations must annihilate at the same rate as they multiply.

The composite model, under the steady-state requirement, leads to simple expressions for the steady-state concentration of dislocations and point defects (Essmann and Mughrabi 1979). The model allows for steady-state plastic flow to occur down to low

temperatures, in agreement with Basinski *et al* (1980).

1.3.4 **Fatigue Crack Initiation in PSBs**

Many researchers have reported that cracks which may lead to failure are located preferentially at PSBs. Some researchers (eg. Neumann 1983, Mughrabi *et al* 1983, Ma and Laird 1989a) found that long cracks developed preferentially at PSB-matrix interfaces. Others (eg. Finney and Laird 1975, Basinski and Basinski 1985a,b) found there was a tendency for long cracks to form at isolated, narrow PSBs, termed micro-PSBs. Ma and Laird (1989a) suggest that pronounced strain localization could be caused at micro-PSBs by the abrupt change in dislocation microstructure.

Most recent fatigue models predict cracks forming at PSB-matrix interfaces or micro-PSBs due to strain localization. Some models are discussed in Section 1.4.

1.4 **MODELS FOR PSB PROFILE AND CRACK INITIATION**

1.4.1 **The EGM Model**

Essmann, Gösele and Mughrabi (1981) proposed a semi-quantitative model of the evolution of emerging PSBs, called the EGM model. Their model is based directly on the dislocation processes occurring in the bulk, as described in Section 1.3.3.

In the EGM model the annihilation of pairs of screw dislocations and the annihilation of edge dislocation dipoles represent two distinct types of irreversibility of slip. The annihilation of screw dislocations leads to unreversed slip steps at the surface, while the annihilation of edge dislocation dipoles leads to a high steady-state concentration of vacancy-type point defects.

EGM suggest that a roughness profile develops in a random manner, due to the accumulation of unreversed slip steps. The process is slow, resulting in a slow surface roughening.

In addition to the effect, EGM suggest that there is rapid extrusion growth, resulting from the annihilation of close edge dislocation dipoles and dislocation glide.

The EGM model predicts that cracks will occur in notch-like valleys in the roughness profile, and at the large steps which bound the extrusions at the PSB-matrix interfaces.

The main reservation with this model, expressed by Basinski and Basinski (1985b), is that the EGM surface profile is said to be due to statistical roughening. Basinski and Basinski suggest that, in order to account for the distinctive characteristics of extrusions and intrusions, a more systematic mechanism is required. In addition, statistical roughening predicts that progressive roughening of extrusions should occur indefinitely, whereas Basinski and Basinski showed that roughening does not continue beyond a certain number of cycles ($\sim 10^4$). A major difficulty with the EGM model is that it invokes point defect migration, which cannot occur at 4.2K. However, surface extrusions and failure do occur at 4.2K.

However, the main predictions of the EGM model have been confirmed by observation (Mughrabi 1984).

1.4.2 **Laird's Ratchetting Model**

A ratchetting mechanism which causes cracks to grow has been proposed (Ma and Laird 1989b). The mechanism was reviewed by Jackson (1989). Jackson describes the mechanism as follows: "during the tensile part of a stress cycle, an intrusion attracts dislocations, localises slip and deepens; during a compressive stroke, the intrusion closes, the slip is diffuse and the deepened intrusion retains its shape".

The model thus predicts that intrusions deepen progressively until they become cracks, which may be fatal.

1.4.3 **The Modified Mott Mechanism**

This mechanism, a modified version of the Mott mechanism (Mott 1958), has been suggested by Jackson (1989).

This model proposes that the surface of the crystal first becomes roughened, as in the EGM model. The surface profile created consists of hills and valleys. During the tensile stroke of the cycle, stress concentrations develop near the bottom of each valley as the valley opens. The stress concentrations, shown in Figure 1.10 (a), can be modelled as a climb pile-up of edge dislocations.

The stress concentration promotes plastic flow in its neighbourhood, which deepens the valley, accentuating the profile relief as shown in Figure 1.10(b).

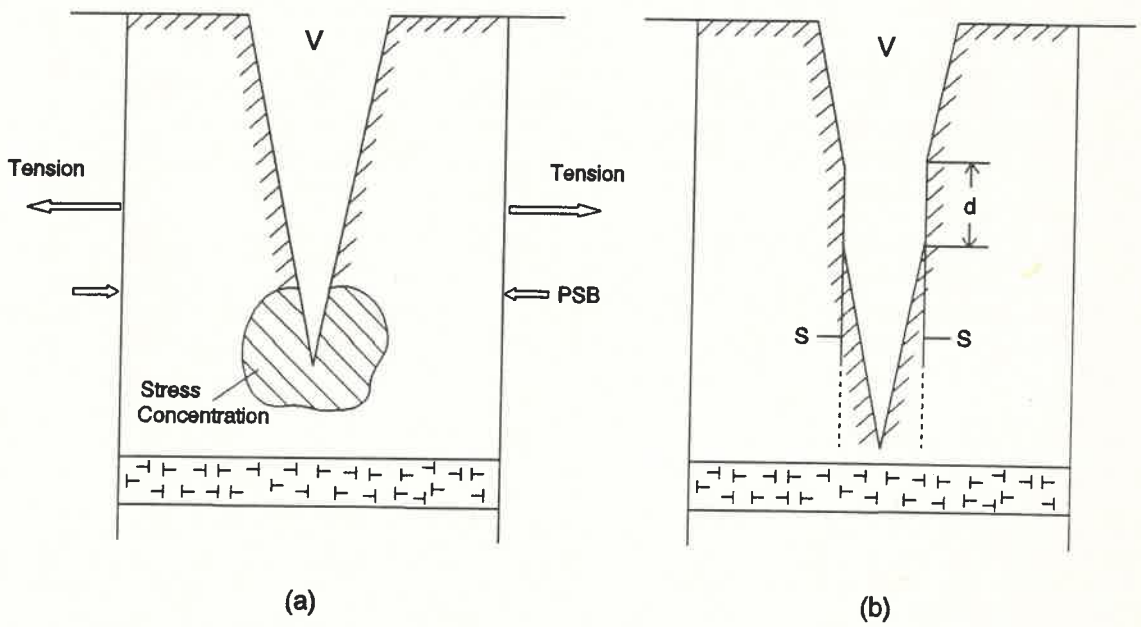

Figure 1.10 : Profile of a valley (V) in a PSB (a) before and (b) after plastic flow. d is the extent of deepening produced by the circulation of screw dislocation (s) around the valley (Descoins 1991).

Thus, the stress concentration in the valleys, which are produced by random slip (EGM, Section 1.4.1), results in plastic

deformation deepening the valleys. The deepened valleys are the intrusions observed by Basinski and Basinski (1988), among others. The intrusions are deepened further by stress concentration-driven plastic flow, until they become cracks. The cracks then propagate and finally lead to failure.

1.5 **ENVIROMENTAL EFFECTS**

There are several environmental effects which may affect the fatigue behaviour of a material. Among these are temperature, atmosphere and pressure.

The effects of temperature have been studied by many researchers (eg. Basinski *et al* 1980, Cortie 1989, Lisiecki and Pedersen 1990) and will not be described here.

The effects of the composition and pressure of the atmosphere were studied by Wadsworth and Hutchings (1958). They fatigued polycrystals of copper, aluminium and gold in air at various pressures, and in water vapour and some inert gases.

They found that the logarithm of fatigue life of copper in air depended linearly on the logarithm of the air pressure, with the life at 10^{-5}mmHg 20 times longer than the life at atmospheric pressure.

The fatigue life of aluminium also increased as the pressure was reduced, although the relationship was not linear. The life of aluminium at 10^{-5}mmHg was about 5 times longer than that in air at atmospheric pressure.

The fatigue life of gold was found to be approximately the same in vacuum (10^{-5}mmHg) and at atmospheric pressure.

Wadsworth and Hutchings also found that the fatigue life of copper at room temperature was affected mainly by the partial pressure of oxygen present during testing, with water vapour increasing the effect of oxygen slightly, but having no effect

on its own. The effect of the inert gases tested was found to be compatible with the probable oxygen pressure present in the gas.

Wadsworth and Hutchings also investigated the formation of intrusions and found that number and size were the same for copper fatigued in air and in a vacuum of 10^{-5}mmHg.

They concluded that the effect of the presence of oxygen was to speed crack propagation in copper and aluminium, but not in gold. They concluded that "chemical attack at the root of the crack" was the reason for this increased rate of crack propagation, and suggested two possible mechanisms to explain this.

In 1965, Grosskreutz and Bowles carried out tests to investigate the effects of enviromental gases on aluminium single crystals during the early stages of fatigue. They argued that at the pressure of 10^{-5}mmHg a monolayer of oxygen can form in 1 second, so that effects on surface slip and crack formation would probably not be observed at low fatigue test frequencies.

Snowden (1963) showed that crack tip oxidation is suppressed at higher pressures because of the additional time required for a gas to flow into a fine crack. Thus, although surface slip and crack formation may not be affected at 10^{-5}mmHg, propagation of existing cracks will be affected.

Grosskreutz and Bowles fatigued aluminium for short periods at atmospheric pressure and at 10^{-9}mmHg, which is ultra high vacuum (UHV). At this level of vacuum, a monolayer of gas would take 20 minutes to form. They found that the slip bands which formed in air at atmospheric pressure were more numerous and intense than those formed at the same strain amplitude, in the same number of cycles, in vacuum. They found that cycling in a partial pressure of dry oxygen produced surface slip equivalent to that obtained under atmospheric conditions. They also did a test on polycrystalline gold in air and under vacuum, and could detect no difference in surface slip. They concluded that "the rate of cyclic hardening in aluminium is decreased by the removal of atmospheric gases", and that "admission of a partial pressure of

dry oxygen is sufficient to restore the rate observed under atmospheric conditions."

They also found that the near-surface dislocation distribution was different in air and in vacuum. Those fatigued in air had clusters of dislocation dipoles along the primary glide plane. Those fatigued in vacuum showed slip line contrast, which is due to trapped or partially trapped edge dislocations.

They suggested two models to explain the effect of oxidation at surface slip steps. In one model the oxidation reaction provides obstacles which lead to rapid hardening, while absence of the reaction leads to continued reversal of surface dislocation sources with only little slip step formation. The other model states that the reduction of surface energy due to oxidation causes increased cross slip and hardening at atmospheric pressure.

Thus, the work carried out indicates that fatigue crack initiation and propagation may be affected by the presence or absence of oxygen. Further qualitative and quantitative comparison between copper, which oxidizes rapidly, and gold which does not oxidize, could provide further information about crack initiation and propagation mechanisms, and add to the understanding of metal fatigue. This is the motivation behind the present study.

CHAPTER 2
THE FATIGUE TESTER

2.1 INTRODUCTION

The most versatile and commonly used push-pull fatigue testers are computer-controlled servo-hydraulic testers. They are brute-force hydraulic machines which employ sophisticated modern electronic control systems. They can be operated in several modes and are available in a range of sizes.

The only shortcoming of these testers is their prohibitive cost. The smallest have a maximum load capacity of about 10 kN, which is quite adequate for small samples, but they cost about R300000.

It was for reasons of economy that Descoins (1992) built a cheaper electromagnetic fatigue tester, for fatiguing small specimens of copper. The labour and materials cost of this tester was approximately R25000: a fraction of the cost of a commercial servo-hydraulic tester. The electromagnetic tester was designed with computer control in mind, to allow the performance to be comparable with that of the accurate servo-hydraulic testers available.

Figure 2.1 shows the basic components of the fatigue tester, in section and plan view.

The tester is built primarily of steel. It has a solid steel base (**B**) and three primary uprights (**U**). The uprights form the corners of an equilateral triangle. Two horizontal triangular platforms (**P_1 and P_2**) are bolted to the uprights. The lower platform (**P_1**) is solid 20mm thick perspex, while the upper platform (**P_2**) is a triangular steel frame.

Two identical electromagnets with a common vertical axis attract one another to generate the forces required to fatigue the specimens. The lower magnet (**M_1**) is bolted to the perspex platform. The upper magnet (**M_2**) is suspended from the upper

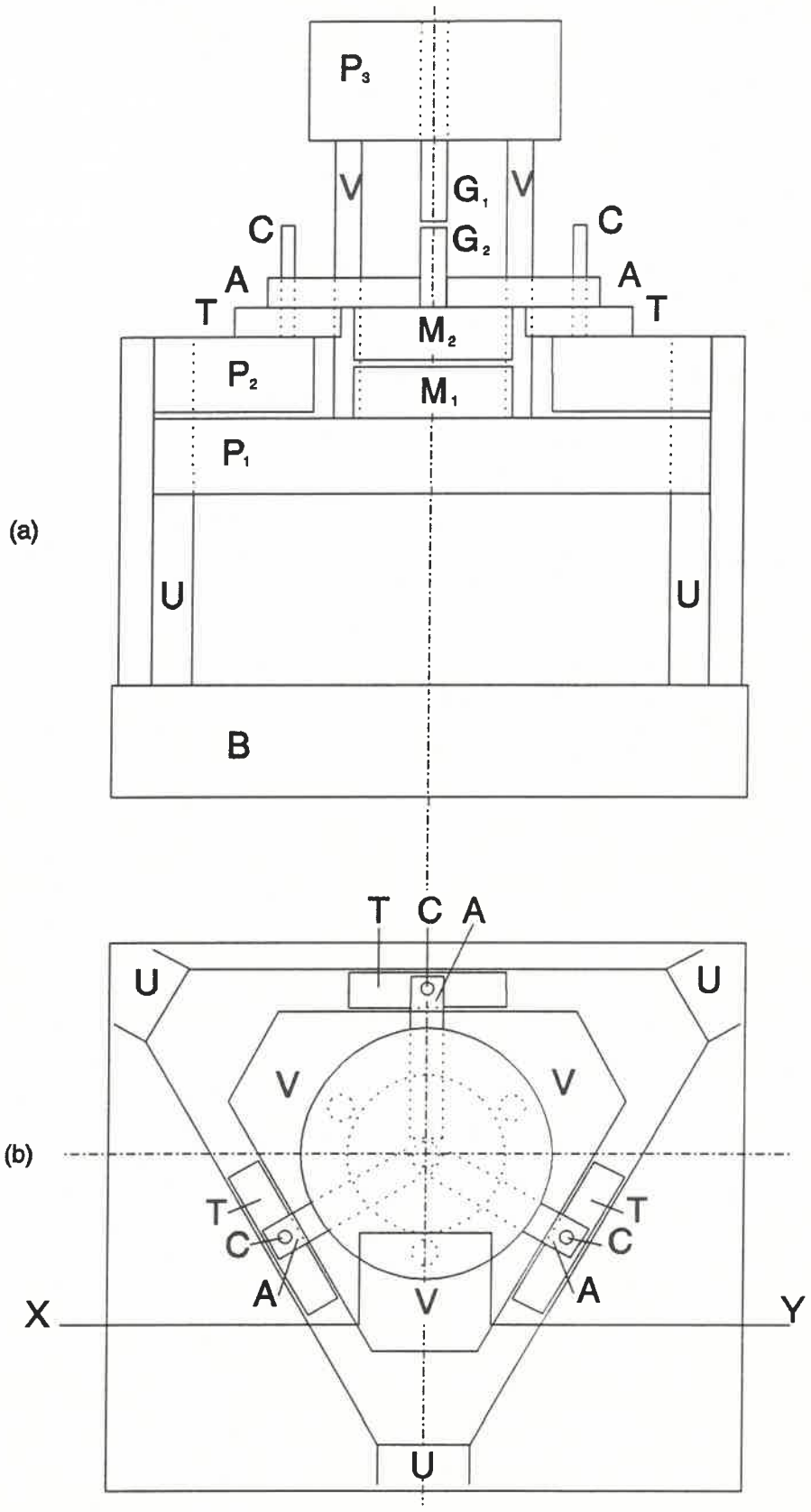

Figure 2.1 : A section (a) and a plan view (b) showing the components of the fatigue tester. the section is taken along X-Y, as shown in (b).

platform by three stiff radial linked arms (**A**). One end of each arm is fixed to the upper magnet, while the other end rests on a stiff spring (**T**). Each arm has a low-friction bush in the outer end. A column (**C**) passes through the bush and guides the movement of the arm. The flat top of M_1 and the flat bottom of M_2 have an adjustable separation which is set to approximately 1 mm.

The vice-like specimen grip (G_1) which is fixed to the top of M_2, grips one end of the crystal to be tested. The other end of the crystal is held by the upper specimen grip (G_2). Three secondary uprights (**V**) extend up from the lower platform to hold a smaller circular platform (P_3). This platform is a load cell and carries the upper grip G_2. The separation of the two grips is adjusted by setting the height of the upper grip. This separation is set to approximately 4 mm.

The current is supplied to the magnets by a Kepco bipolar 200 Watt dc unit, whose output can be controlled either manually or by an external control signal. The Kepco supply is called bipolar because it can act as a current source and, if needed, as a current sink. The magnets are connected in parallel, and since they were constructed to be identical they have the same resistance. Therefore a given current results in equal magnetic fields being generated by both magnets.

To operate the fatigue tester, a biasing or offset current of approximately 0.5 A is supplied to each magnet.This offset current was chosen because it lies in the middle of the operating range of the apparatus. The magnets attract one another and M_2 moves towards M_1, thereby compressing the springs. The crystal is then placed into the grips and locked into place. The axial load on the specimen is thus zero. Increasing the current increases the attractive force between the magnets and results in a tensile force on the specimen. Decreasing the current reduces the attractive force between M_1 and M_2, and since the springs are compressed they push M_2 upwards resulting in a compressive force on the specimen.

Thus, by varying the magnet current above and below the offset

current, the axial load or stress on the specimen is cycled between tension and compression. The displacement or strain amplitude can be changed by adjusting the amplitude of the control voltage.

2.2 MECHANICAL DESIGN

2.2.1 The Electromagnets

The two electromagnets M_1 and M_2 are identical. Figure 2.2 shows the upper magnet M_2. They were machined from soft iron, since it has negligible magnetic remanence. If the remanence were not small, the magnetic flux would not be able to follow an oscillating current accurately.

The magnets are cylindrical, with an outside diameter of 130 mm and a height of 45 mm. The coil (**E**) of each magnet is recessed into the soft iron and consists of 1500 turns of insulated copper wire, 0.55 mm in diameter.

Air cooling ducts (**D**) allow compressed air to be forced through the magnets to dissipate the Joule heating of the driving current. The top magnet has 6 ducts and the lower magnet has 8. The compressed air escapes through the gap between the magnets.

The magnets each have a resistance of 32 Ω and are designed to carry currents of up to 2 A without overheating.

2.2.2 The Suspension Springs

There are 3 suspension springs, one for each arm of the upper magnet. Figure 2.3 shows one of the springs (**T**). Each spring has 2 upper leaves (L_1) and two lower leaves (L_2) each. Each leaf is made of 8 mm x 12 mm K460 gauge plate and is 130 mm long. The leaves are prevented from touching the column (**C**) by a thick teflon bush (**Tb**). These leaves are separated by two fulcrums (**F**). Varying the separation of the fulcrums adjusts the stiffness of

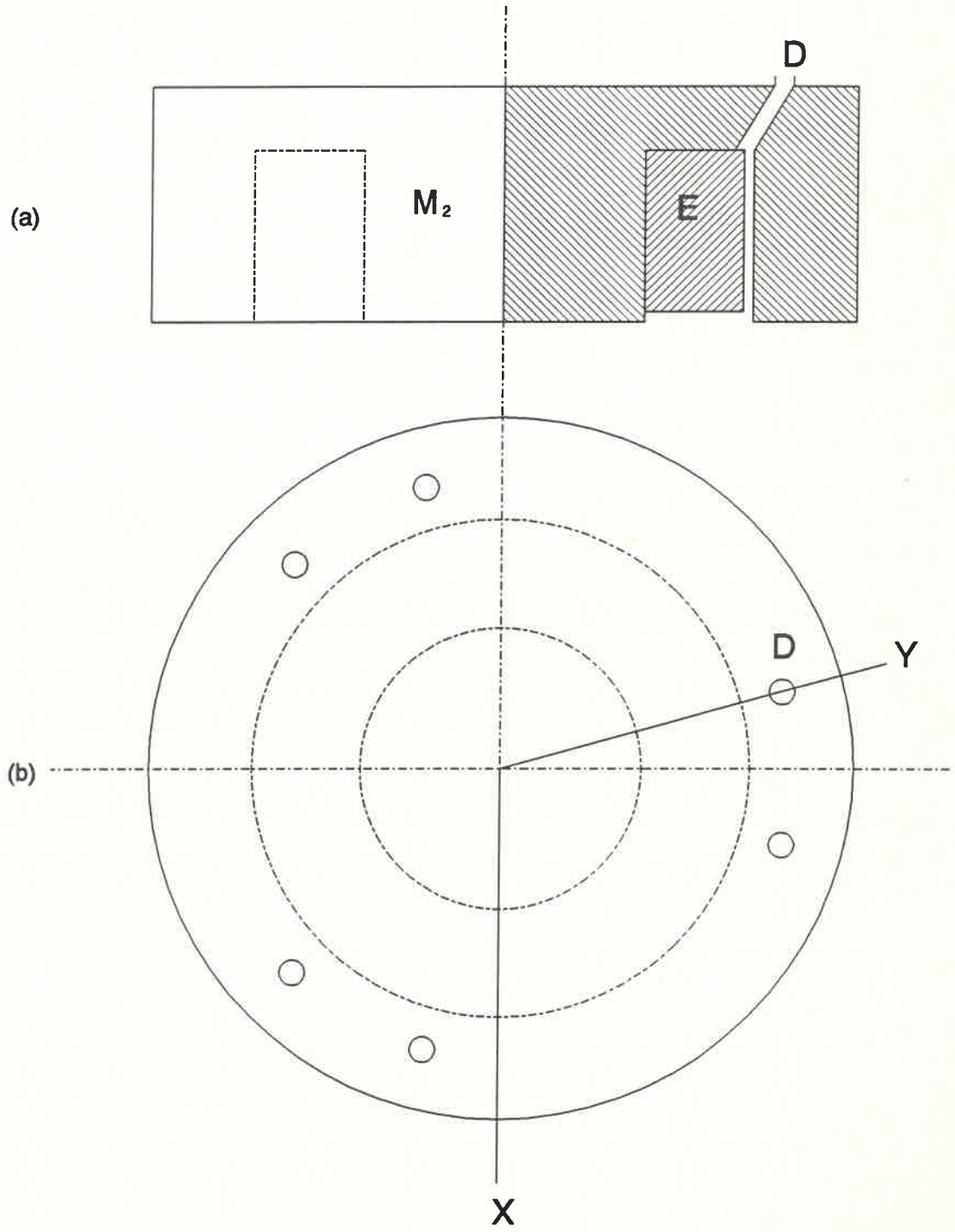

Figure 2.2 : A section (a) and a plan view (b) of the upper electromagnet (M_2). The section is taken along X-Y, as shown in (b). The left half of (a) is a front view.

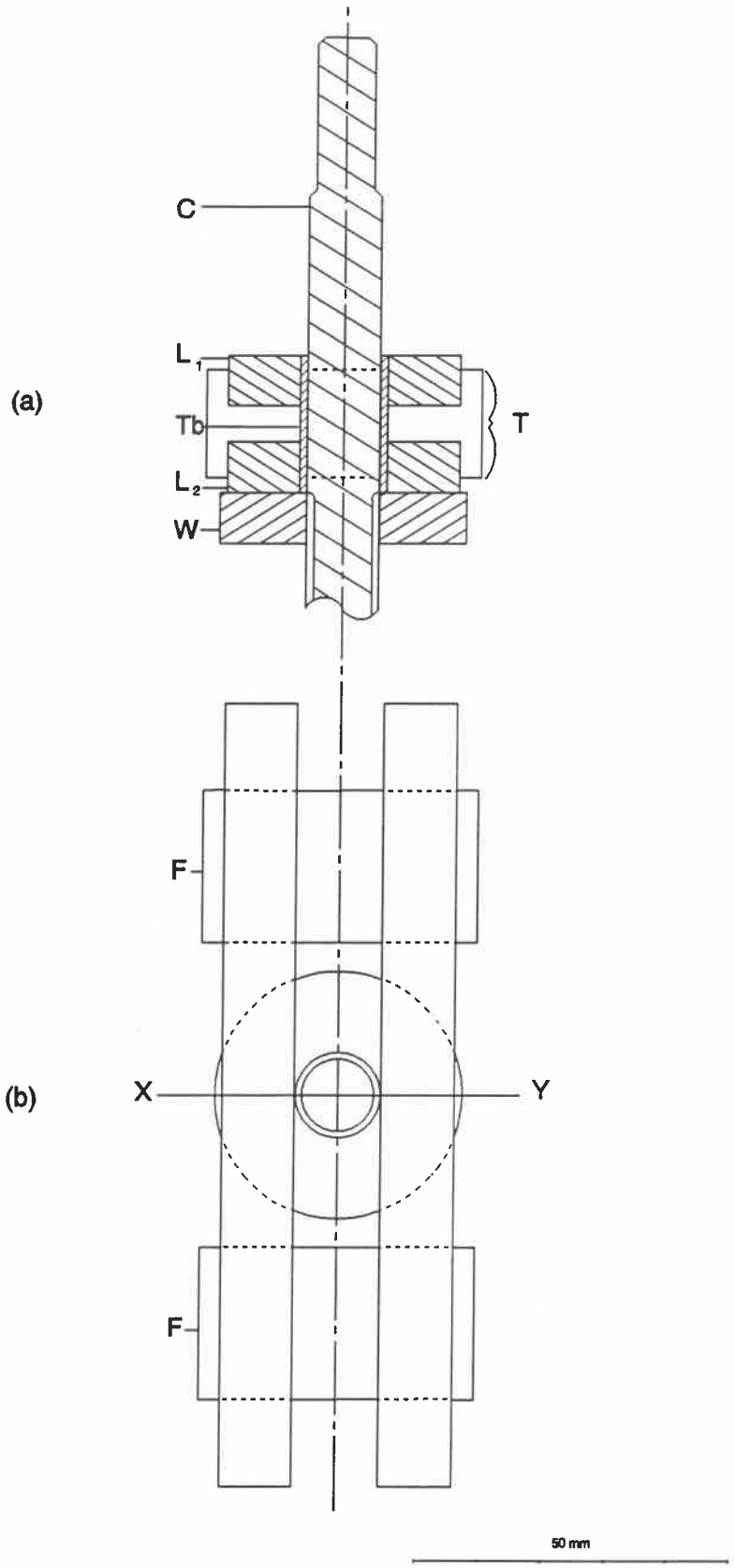

Figure 2.3 : A section (a) and a plan view (b) of a suspension spring and column (C). The section is taken along X-Y, as shown in (b).

the springs. That is, the closer together the fulcrums are, the stiffer the spring.

When the magnets attract one another, the springs are loaded. The springs were designed to be able to generate at least 120 N of compressive force each for a deflection of 0.02 mm. In fact, by moving the fulcrums very close together (50 mm) forces greatly in excess of the minimum requirement could be achieved for the same displacement (Descoins, 1991).

The suspension spring system employed in the tester is very versatile, allowing easy adjustment as well as a large range of spring stiffness.

2.2.3 **The Specimen Grips**

When the machine was first built, the specimen grips were made of silver steel, and are described by Descoins (1991).

The grooves in the original grips were serrated with a chisel to hold the specimen firmly in place. Unfortunately, the upper grip broke during the testing of copper crystals. A fatal crack originating at one of the serrations in the groove of the grip resulted in the failure of the fixed jaw of the specimen grip. This failure was due to fatigue taking place in the grips, probably hastened by the presence of stress concentrations at the chiselled serrations.

A new set of grips was designed, and these are shown in Figure 2.4. They were machined from fatigue resistant chrome-molybdenum steel (SAE 4340).

Each grip consists of two parts: a fixed jaw (J_1) and a separate detachable jaw (J_2). J_2 is bolted to J_1 with the crystal between them. A V-shaped groove, with a right-angled corner, in J_1 and J_2, keeps the specimen in alignment. The grooves are designed so that the jaws (J_1 and J_2) do not quite meet when the crystal is gripped between them. This arrangement enables the test specimen

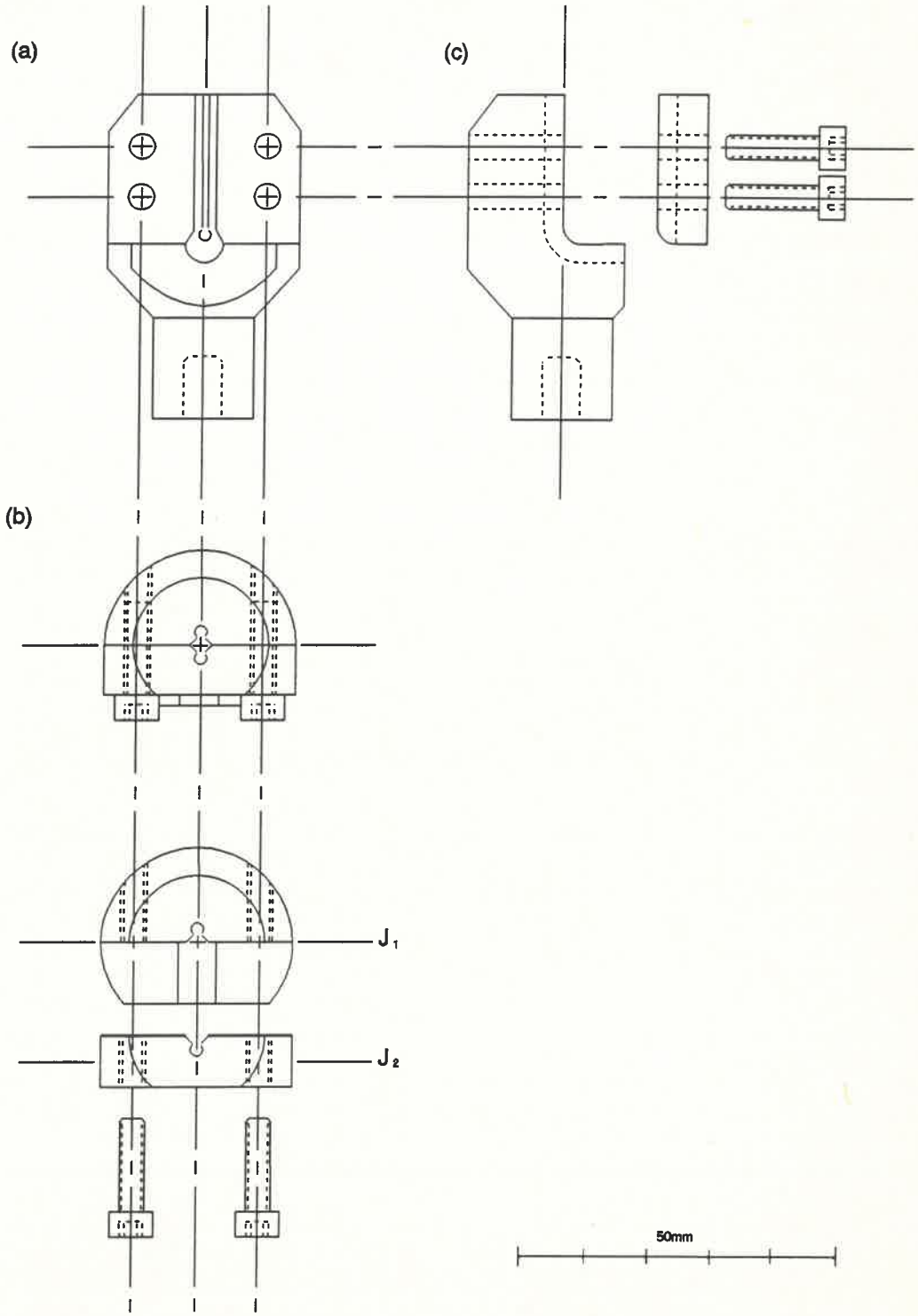

Figure 2.4 : The components of the lower grip (G_1) are shown. The front view (a) shows only the jaw, J_1. The plan (b) and left-side (c) views show the assembly of the grip.

to be securely gripped.

Because the serrations chiselled into the original grips may have contributed to the failure of the top grip, the new grips were not chiselled in this fashion, and there does not appear to have been any slippage between grip and specimen.

To further reduce any stress concentrations in the grips, a rounded channel was drilled along the junction of the V-shaped groove in both jaws. This can be seen in Fig. 2.4 (b). In addition, the top of the groove in the fixed jaw ends in a rounded hollow. Also, the new grips are almost 100% larger than the original grips and wherever possible, are more rounded.

Hopefully, these precautions will considerably extend the life of the new specimen grips. After at least six months of use they have shown no visible signs of fatigue.

2.2.4 **The Load Cell**

In a load cell a small elastic displacement is measured when a load is applied. The magnitude of the displacement can be related to the load. The displacement must be elastic so that the relationship is linear. The load cell must be as stiff as possible, so that its movement does not interfere with the strain on the specimen more than necessary. On the other hand, if it is too stiff the displacement might not be measurable in practice. The measurement of the displacement of the load cell and its correlation to load is discussed in Section 2.3.1.

The load cell is shown in Figure 2.5 and Figure 2.6 below. The load cell shown consists of 3 phosphor-bronze discs (**Pd**) clamped together by four silver-steel discs (**Sd**). A threaded cylinder (**Cy**) passes through holes in the centres of the phosphor-bronze discs and bolted securely by two large nuts ($\mathbf{N_1}$ and $\mathbf{N_2}$). Two spacers (**Sp**) are positioned between the phosphor-bronze discs and clamped firmly into place when the nuts are tightened. A drawbar (**Db**), with a threaded end, pulls the narrow end of the upper grip

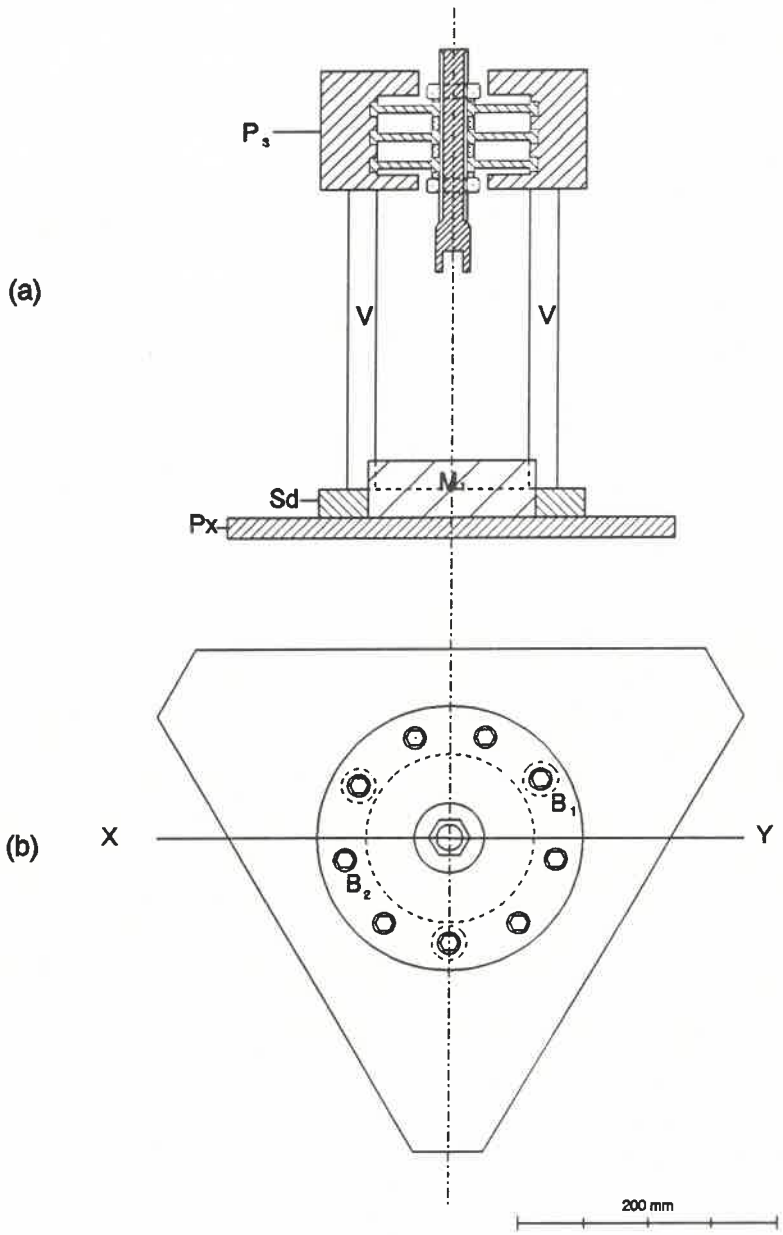

Figure 2.5 : A section (a) and a plan view (b) showing how the load cell (P_3) is fixed to the lower platform (P_1). The section is taken along X-Y, as shown in (b).

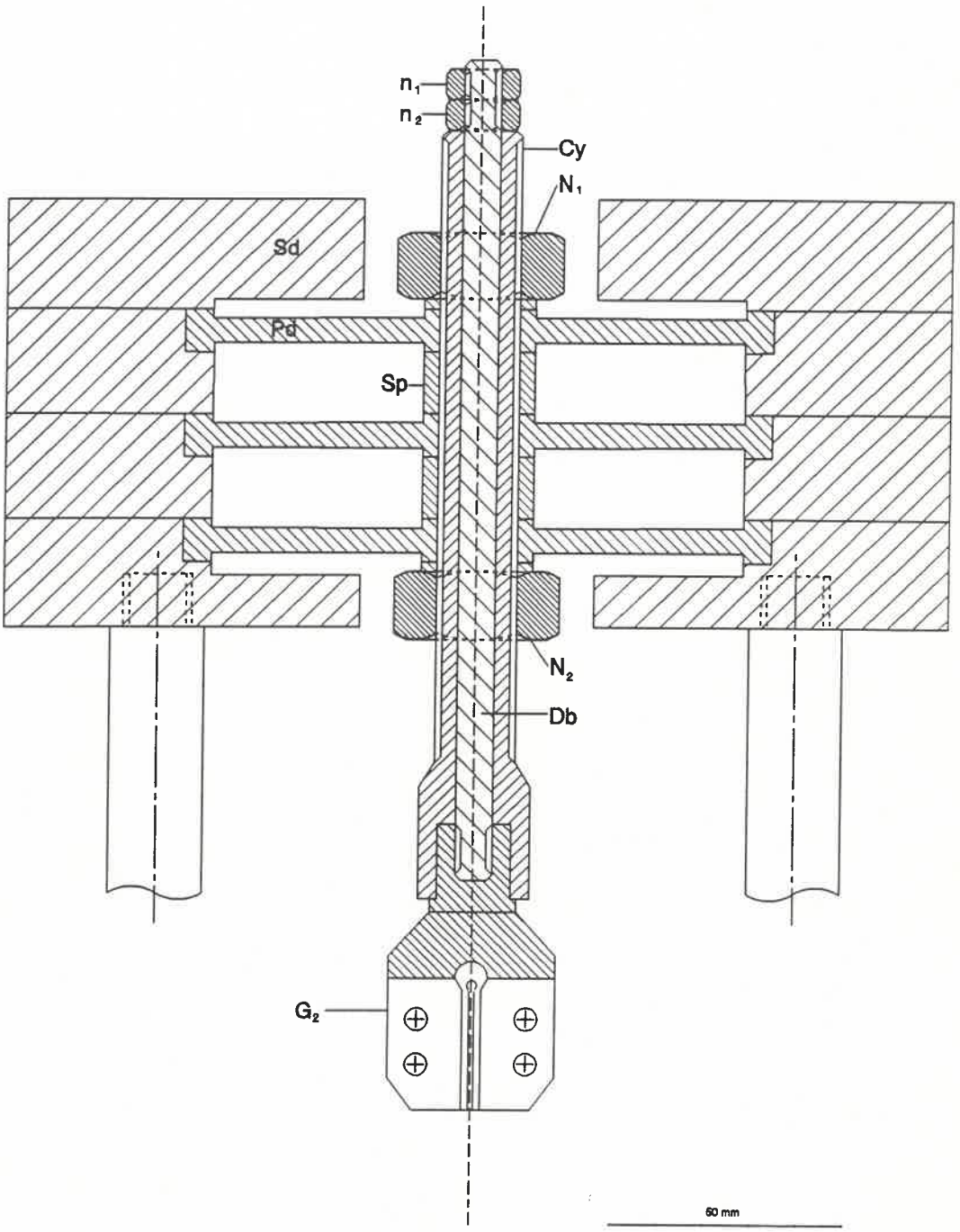

Figure 2.6 : An enlarged section of the load cell. The section is taken along X-Y (See Figure 2.5(b)).

(G_2) up into the lower end of **Cy**. Two smaller nuts (n_1 and n_2)

fix the drawbar and grip firmly to the cylinder.

The silver-steel discs are bolted together with six accurately machined bolts (B_2). Three more bolts (B_1) fix the load cell to the uprights (**V**). The uprights are then bolted to a silver-steel ring, which is bolted to the lower perspex platform (P_1).

With the load cell in place, the upper grip (G_2) rests just above the lower grip (G_1) and the separation of the grips is adjusted by moving **Cy** and then tightening the nuts (N_1 and N_2). During a fatigue test the axial load on G_2 is transferred by **Cy** to the load cell. The load cell is designed to allow small but measurable movements of **Cy**, which can be calibrated to give the stress on the fatigue specimen.

Although the figure shows three phosphor-bronze discs and four silver-steel discs, it was designed so that one or two of each could easily be removed to vary the stiffness. It was found that removing one of each of the discs made the load cell more sensitive and reduced the settling which occurred when a load was first applied to the load cell and the separate components shifted slightly into place. With only two inner discs in place no significant settling occurred. If there is settling within the load cell, successive load measurements may not be reproducible.

2.3 **INSTRUMENTATION OF THE FATIGUE TESTER**

It is necessary to measure both the stress and strain of the specimen during the fatigue test.

2.3.1 **Load Measurements**

Measurement of the load (or stress) on a specimen is achieved by measuring the displacement of the central cylinder (**Cy**) of the load cell (section 2.2.4). This displacement is proportional to the axial stress (Hooke's Law). The constant of proportionality is determined by calibrating the load cell with dead weights.

The displacement is measured using a Linear Variable Displacement Transducer (LVDT), which is mounted on top of the load cell. The operation and function of a LVDT is described in Section 4.3. LVDT's are capable of accurately measuring small linear displacements, of the order of microns.

A LVDT measures the differential displacement between its body and its separate movable core. The core of the LVDT is mounted on top of **Cy** by a brass cap, with an internal thread, which screws onto **Cy** over the two small nuts, $\mathbf{n}_1$ and $\mathbf{n}_2$. The body of the LVDT is attached to a rack bolted to the uppermost silver steel disc of the load cell. Thus when **Cy** moves as the specimen is loaded, the core of the LVDT moves relative to its body and a voltage proportional to this movement is produced.

In order to measure the voltage output of an LVDT, a lock-in amplifier is used (Section 5). For the stress measurement, an ITHACO Lock-in Amplifier is employed. This is a computer operated amplifier and the output is read using a computer program (Section 6.2).

The voltages read by the amplifier are proportional to the displacement of **Cy**. These displacements are in turn proportional to the load on the specimen, and thus to the stress.

By applying known loads to a specimen, the lock-in amplifier output is calibrated with respect to load. To determine the stress on a given specimen the calibrated load is first converted to a force, and then divided by the cross sectional area of the specimen.

A function generator or oscillator was used as an input for the LVDT and as a reference signal to the amplifier. For the stress measurement, a Philips Low Frequency Synthesizer was used to supply a 19710 Hz signal.

2.3.2 **Strain Measurement**

The axial strain on a specimen is equal to the change in length per unit of length of the specimen. The original gauge length of the specimen is determined before the test using a travelling microscope. The change in length of the specimen must be measures continuously during a fatigue cycle.

The fatigue tests performed using the electromagnetic tester were carried out in strain amplitude control mode at a frequency of about 1 Hz. This means that a constant strain amplitude is imposed throughout the test (Section 1.1). Thus, it was necessary to measure the strain during each cycle at intervals of approximately 10 - 20 ms, depending on the cycle frequency.

This was achieved by using another LVDT (Section 5.2). The relative displacement of the two specimen grips was measured by mounting the LVDT alongside the crystal. The change in this displacement is therefore equal to the change in length of the specimen, and since the length of the specimen was known, this displacement was easily converted into strain.

As in the stress measurement, a lock-in amplifier was used to measure the voltage output of the LVDT. For the strain measurement, a Princeton Applied Research Lock-in Amplifier (PAR) was used. An Escort Function Generator was used to supply a 9997 Hz signal as the input to the LVDT and the reference to the lock-in amplifier.

In order to control the strain amplitude during the tests, a feedback system was employed. This is described in detail in Chapter 3.

CHAPTER 3
POWER CONTROL

3.1 INTRODUCTION

When running a fatigue test, it is convenient to impose a strain cycle of given amplitude. This amplitude may be different for different tests, but for any one test the amplitude should remain constant. The reason for imposing a constant strain amplitude is discussed in Section 3.4.

The stress is measured continuously during each cycle of the test so that a stress-strain fatigue cycle, as described in Section 1.1, can be plotted at any stage of the test.

The strain is measured using an LVDT (Section 2.3.2) which gives a voltage output proportional to the strain on the specimen. In order to control the strain, a voltage is generated which is the same as the desired LVDT output, and the current to the magnets is varied until they produce a displacement corresponding to the desired strain.

This is achieved by generating a voltage signal of the desired form and size, using computer driven hardware. This signal is then fed into a comparison or feedback circuit which adjusts the control voltage to the KEPCO power supply until the output from the strain LVDT follows the computer generated signal.

Some introductory material regarding the basic electronics used is given in Appendix 2.

3.2 THE COMPARISON CIRCUIT

3.2.1 The Differential Amplifier

One of the major assets of the operational amplifier (op amp) is its ability to amplify the algebraic difference between two voltages. If an op amp is used as a two input amplifier with feedback, the resultant amplifier circuit is called a differential amplifier with feedback.

Figure 3.1(a) shows such a differential feedback amplifier. the circuit in Figure 3.1(b) is an inverting amplifier and the circuit in Figure 3.1(c) is a non-inverting amplifier.

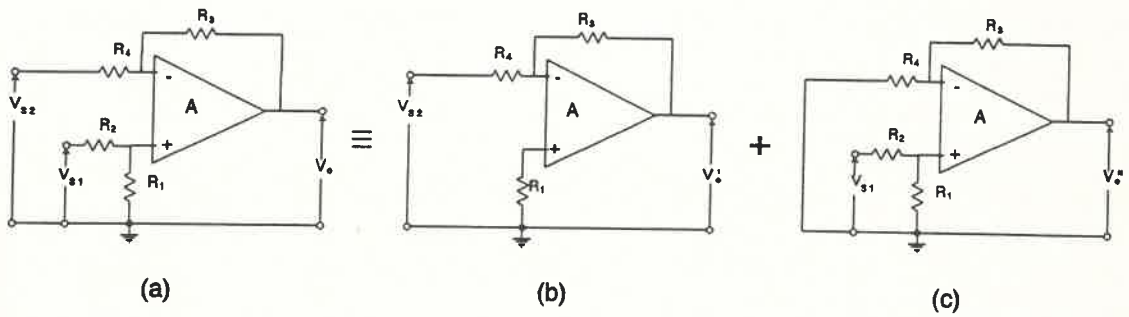

Figure 3.1 : Circuit diagrams of (a) a differential feedback amplifier, (b) an inverting amplifier and (c) a non-inverting amplifier.

The output from the diferential feedback amplifier, V_o, may be regarded as the sum of V'_o (the output of the inverting amplifier) and V''_o (the output of the non-inverting amplifier), by the principle of superposition. This is indicated in Figure 3.1. Thus,

$$V_o = V'_o + V''_o \ . \qquad (3.1)$$

The output of the non inverting amplifier is given by

$$V'_o = -V_{s_2} \cdot \frac{R_3}{R_4} \ , \qquad (3.2)$$

(Kahn 1970) and the output of a non inverting amplifier is given by

$$V''_o = V''_{s_1}(1+\frac{R_3}{R_4}) \ , \qquad (3.3)$$

(Kahn 1970), where

$$V''_{s_1} = V_{s_1} \frac{R_1}{R_1+R_2} \ , \qquad (3.4)$$

since the resistors R_1 and R_2 form a potential divider at the non-inverting input.

Therefore, from equations 3.1 to 3.4

$$V_o = V_{s_1} \frac{R_1}{R_1+R_2} \frac{R_3+R_4}{R_4} - V_{s_2} \frac{R_3}{R_4} \ . \qquad (3.5)$$

A differential amplifier amplifies the difference between the two source voltages, and the gain depends only on the values of the resistors used in the circuit.

The comparison or feedback circuit used to control the strain on the specimen during the fatigue tests, is shown in Figure 3.2. This circuit is equivalent to the differential feedback circuit shown in Figure 3.1(a), with $R_1 = \infty$, $R_2 = R_4 = 10k\Omega$, $V_{s1} = V_{ref}$ and $V_{s2} = V_\epsilon$. In Figure 3.2 the combination of a 10MΩ rheostat in series with a set of parallel resistors, each with a switch, is equivalent to R_3 in Figure 3.1(a). Thus R_3 is of the order of 10MΩ. This combination can be adjusted to optimise the performance of the feedback system. Optimum response was obtained with the highest gain consistent with no oscillation of the system as a whole. A value of 10 kΩ was chosen for the R_2 and R_4 resistors, as this value is high enough to protect the integrated circuit from any externally induced transients, without affecting circuit operation.

In Figure 3.2, $V_{control}$ is the output of the amplifier which is connected to the voltage programming input of the Kepco magnet

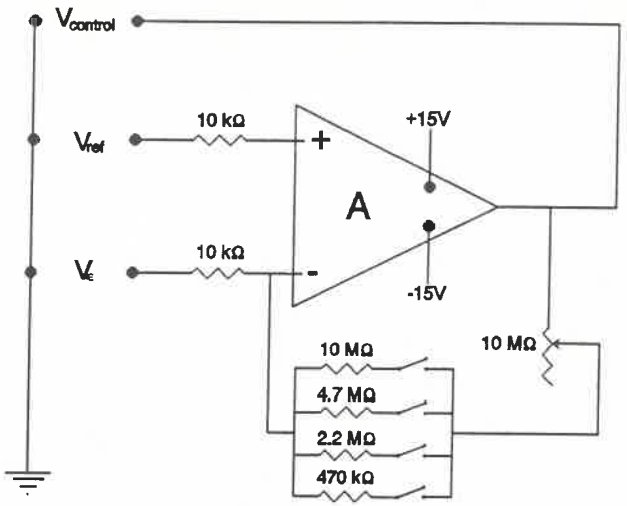

Figure 3.2 : Schematic diagram of the differential feedback amplifier for the fatigue tester.

power supply. $V_{control}$ determines the voltage across the magnets and therefore, the strain on the specimen. V_{ref} is the computer generated waveform, which acts as a reference for the feedback system. V_{ϵ} is the output voltage of the lock-in amplifier and is proportional to the strain.

If R_1 is infinite (open circuit)

$$\frac{R_1}{R_2+R_1} \approx \frac{R_1}{R_1} = 1 \ , \qquad (3.6)$$

and for the circuit in Figure 3.2 equation 3.5 can be reduced to

$$V_{control} = V_{ref} \frac{R_3+R_4}{R_4} - V_{\epsilon} \frac{R_3}{R_2} \ . \qquad (3.7)$$

Since R_3 is of the order of MΩ and R_4 is 10kΩ, $R_3 >> R_4$, so $R_3 + R_4 \approx R_3$, and equation 3.7 becomes

$$V_{control} = (V_{ref}-V_{\epsilon}) \frac{R_3}{R_4} \ . \qquad (3.8)$$

The combination of resistors which forms R_3, was designed to allow easy adjustment of the value of R_3. The combination of

resistors chosen provides a range for R_3 of 20MΩ to 0.35MΩ. Thus, the gain of the feedback amplifier can be adjusted to optimise the performance of the control circuit.

3.2.2 **The Magnet Control Circuit**

The differential feedback amplifier is the heart of the circuit used to control the strain on specimens during fatigue tests. Figure 3.3 shows a schematic diagram of the magnet control circuit.

The output of the strain measuring LVDT is amplified by the PAR lock-in amplifier. The output of the lock-in amplifier is connected to the inverting input of the differential feedback amplifier. The voltage, V_ϵ, from the lock-in amplifier is proportional to the strain on the specimen.

The computer generated reference voltage, V_{ref}, is connected to the non-inverting input of the feedback amplifier. So, the output of the amplifier will be proportional to $V_{ref} - V_\epsilon$.

The output of the feedback amplifier, $V_{control}$, is connected to the voltage programming input of the Kepco power supply. The voltage supplied to the magnets is proportional to the voltage across the programming input. So, $V_{control}$ determines the voltage across the magnets and therefore affects the strain on the specimen.

Equation 3.8 in Section 3.2.1 gives the relationship of the output voltage to the input voltages. If V_ϵ is much lower than V_{ref}, then the differential feedback amplifier amplifies the difference according to equation 3.8. $V_{control}$ becomes large and the voltage across the magnets increases rapidly. As the magnet voltage increases, the magnets move closer together and the strain increases. The difference, $V_{ref} - V_\epsilon$, decreases and $V_{control}$ starts decreasing. So, V_ϵ approaches V_{ref}, rapidly at first and then more gradually until they are almost equal. At this point the system reaches equilibrium.

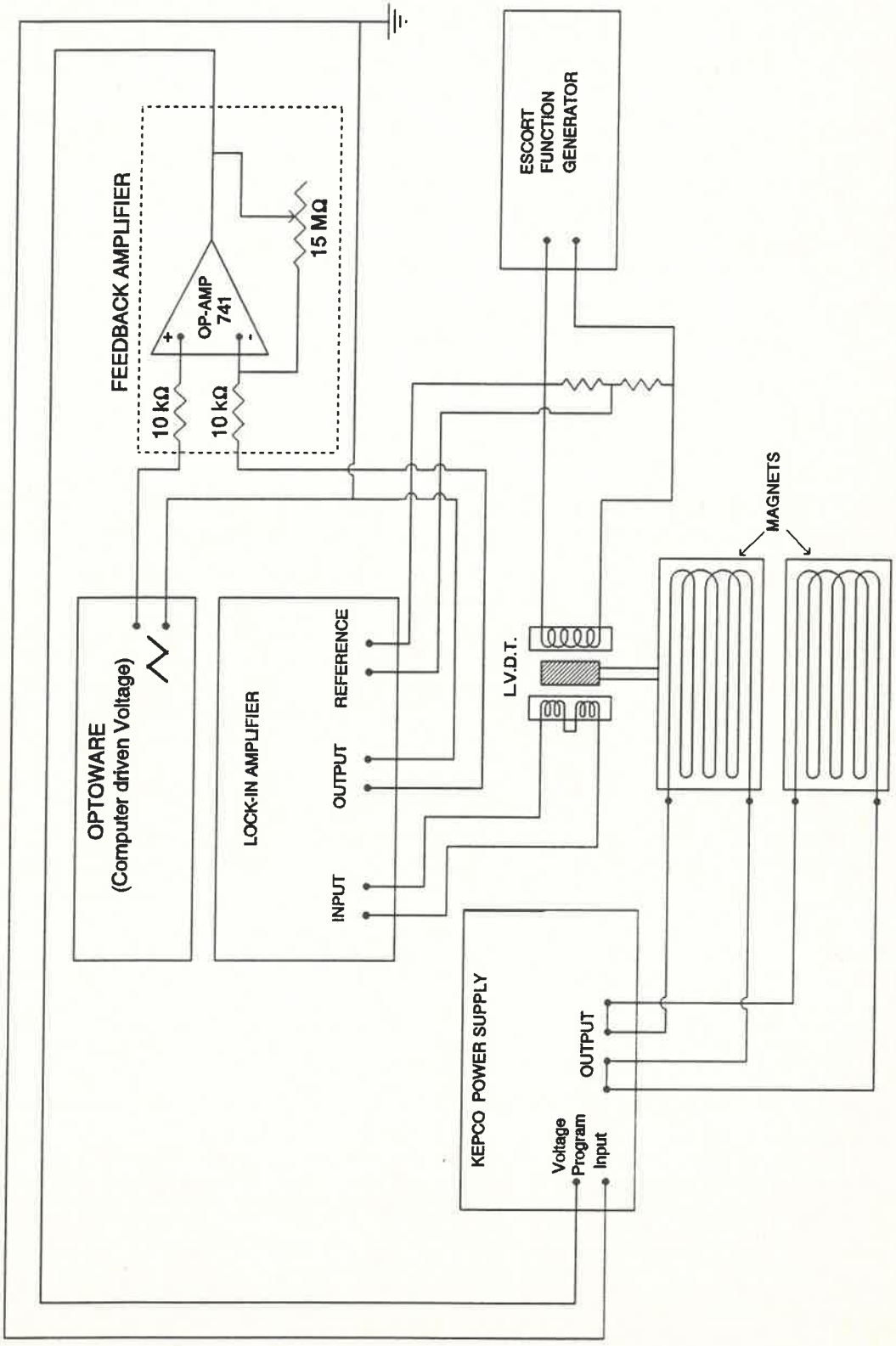

Figure 3.3 : Schematic diagram of the magnet control circuit.

If V_ϵ and V_{ref} were exactly equal then $V_{control}$ would become zero and the magnets would start moving back to their original position. V_ϵ would then decrease as the strain decreased, and $V_{ref} - V_\epsilon$ would no longer be zero, and $V_{control}$ would increase again. There has to be a small difference between V_{ref} and V_ϵ, so that $V_{control}$ is non-zero. This difference is practically immeasurable, and may be regarded as zero.

Similarly, if V_ϵ is greater than V_{ref}, $V_{control}$ becomes large negative, and the magnets start moving further apart. The strain decreases and V_ϵ approaches V_{ref}. $V_{control}$ becomes less negative and the magnets move apart more slowly, until V_ϵ is almost equal to V_{ref}, where an equilibrium is reached as described previously.

If V_{ref} is changing slowly, then the magnet control circuit acts as described above to force V_ϵ to follow V_{ref}. There is, however, a limit to the speed with which the control circuit can change V_ϵ. If the frequency of V_{ref} exceeds this limit then V_ϵ will no longer be able to follow the reference.

3.3 **OPERATION AND LIMITATIONS OF THE CONTROL CIRCUIT**

One of the limitations which govern the behaviour of the magnet control circuit is the inductance of the magnets.

Another constraint on the frequency at which the tester may be operated, is the power limitation of the Kepco power supply. With the feedback circuit operating and a step control voltage applied, the system attempts to force the magnet voltage to increase as quickly as possible, by setting the voltage much higher than the desired final value and then decreasing the voltage as the magnet voltage approaches the final value. This means that the magnet voltage will follow the step more closely the higher the maximum voltage of the power supply. That is, the voltage limit of the power supply limits the rate at which the magnets can respond. The Kepco power supply can supply a maximum voltage of 40V. A control voltage of 10V results in an output of 40V from the Kepco . The control voltage of the Kepco is the

output of the op amp, which has a saturation voltage, V_{sat}, of approximately 12V.

Because of these considerations, low frequencies of the order of 1 Hz are used for the fatigue tester.

The reference waveform, V_{ref}, may have any shape that can be programmed by computers or supplied by a function generator. Since, for the fatigue test, the waveform should have a constant amplitude, the following waveforms will be considered; a sinusoidal waveform, a sawtooth or triangular wave, and a step function or square wave. The reference waveforms for this test were generated by a Hewlett-Packard function generator.

Figures 3.4 to 3.6 show the behaviour of the control system for various waveforms and frequencies. These figures were redrawn from printouts of oscilloscope traces. There was no sample in the grips during the test. Each figure shows the reference voltage, V_{ref}; the strain voltage, V_{ϵ}; the voltage across the magnets, V_{magnet}; and the current through the magnets, I_{magnet}. Figure 3.4 shows the behaviour for a sinusoidal reference waveform; Figure 3.5 shows the behaviour for a sawtooth reference and Figure 3.6 shows the behaviour for a step function. Each waveform is shown at 1 Hz and 3 Hz. The most important information is whether V_{ϵ} follows V_{ref}. V_{magnet} and I_{magnet} are of secondary importance as long as V_{ϵ} follows V_{ref}. V_{magnet} and I_{magnet} show the response of the power supply to the reference signal.

It can be seen from Figure 3.4 (a), that for a sine wave of approximately 1 Hz, the actual displacement (and therefore the strain), is the same as the reference signal. The voltage across the magnets is also a sine wave, but with a high-frequency noise superimposed. This was visible on the original oscilloscope trace. The current is not perfectly sinusoidal.

Figure 3.4 (b) shows a 3 Hz sinusoidal reference waveform, V_{ref}. The displacement voltage is again equal to the reference voltage, but the voltage is slightly irregular in shape and the current is not sinusoidal, although it still varies smoothly.

If the frequency of the sinusoidal reference signal is increased beyond about 5 Hz then the displacement voltage no longer follows the reference exactly, but flattens out on the peaks. This is due to the voltage limitation of the power supply, as V_{magnet} was observed to reach to voltage limit of 40V at this frequency.

Figure 3.5 (a) shows a sawtooth reference voltage of 1 Hz. The displacement voltage follows the reference voltage closely. If superimposed there is no visible difference between the two signals. The voltage across the magnets has sharp spikes where the displacement changes direction, and has a large mains frequency signal superimposed. The current through the magnets is also slightly noisy and shows clearly that the current and the displacement are not directly proportional.

In Figure 3.5 (b), it can be seen that at 3 Hz the displacement is no longer following the reference properly, but has small kinks in its waveform. The voltage has large overshoot spikes which are then slowly damped. The current also shows damped oscillations at this frequency.

If the frequency of the sawtooth reference voltage, V_{ref}, is increased further, the displacement will follow the reference less closely, with the amplitude decreasing and rounding of the sharp corners.

Figure 3.6 (a) shows the response to a square wave reference voltage. Even at 1 Hz the displacement cannot follow the reference exactly, since, due to the effective inductance of the magnets and the resultant time constant, the magnets cannot follow the step function. The control circuit attempts to make it do this, but cannot prevent the overshoot, or damp it rapidly enough. Even at lower frequencies (0.5 Hz) this phenomenon still occurs, though less conspicuously.

Figure 3.6 (b) shows how the response to the step function has deteriorated by 3 Hz. The magnet voltage is overloading, and the current shows large oscillations.

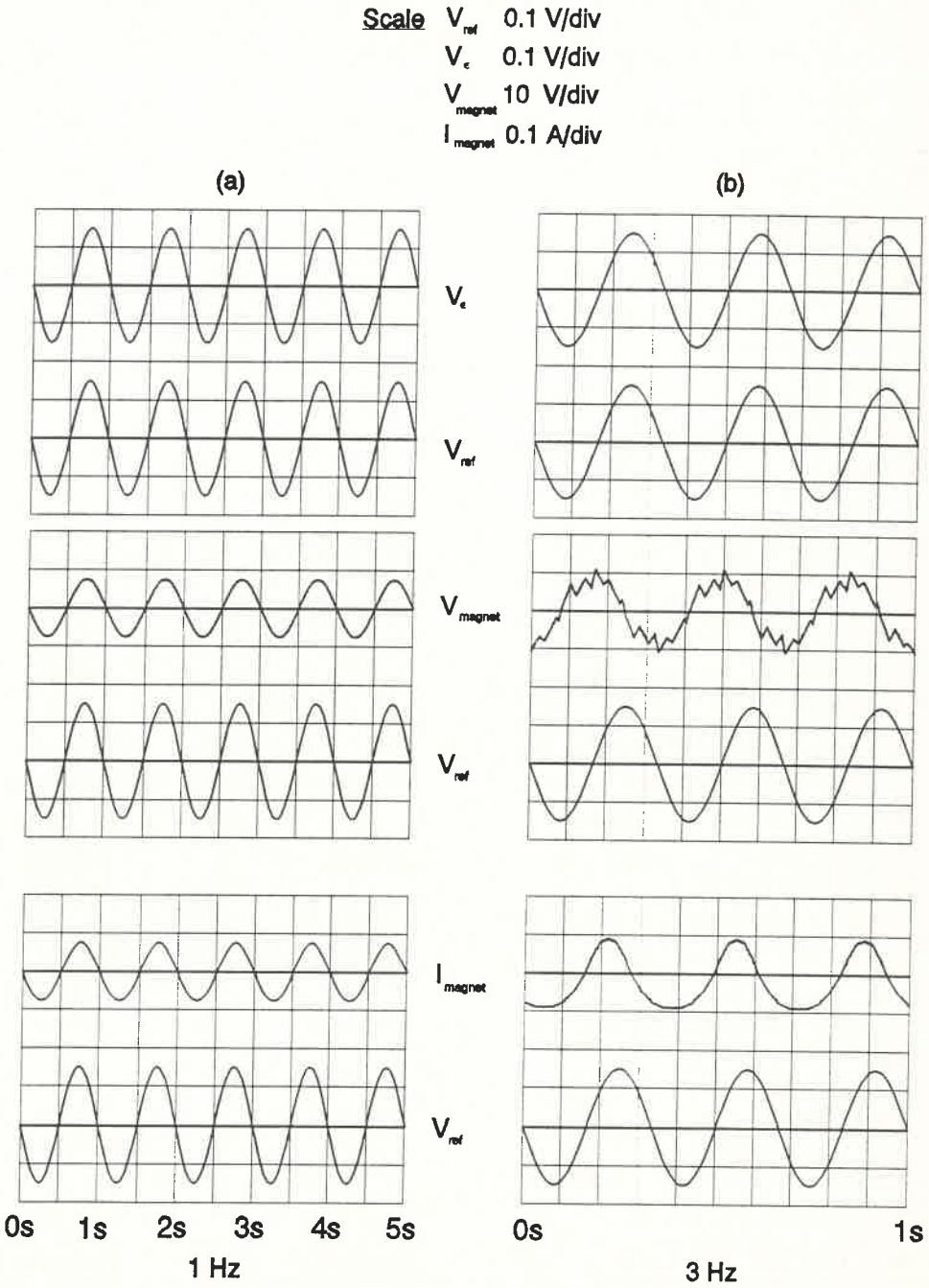

Figure 3.4 : Graphs showing the behaviour of the magnet control circuit when V_{ref} is sinusoidal. In (a) V_{ref} is 1 Hz, and in (b) it is 3 Hz. The scale refers to both (a) and (b).

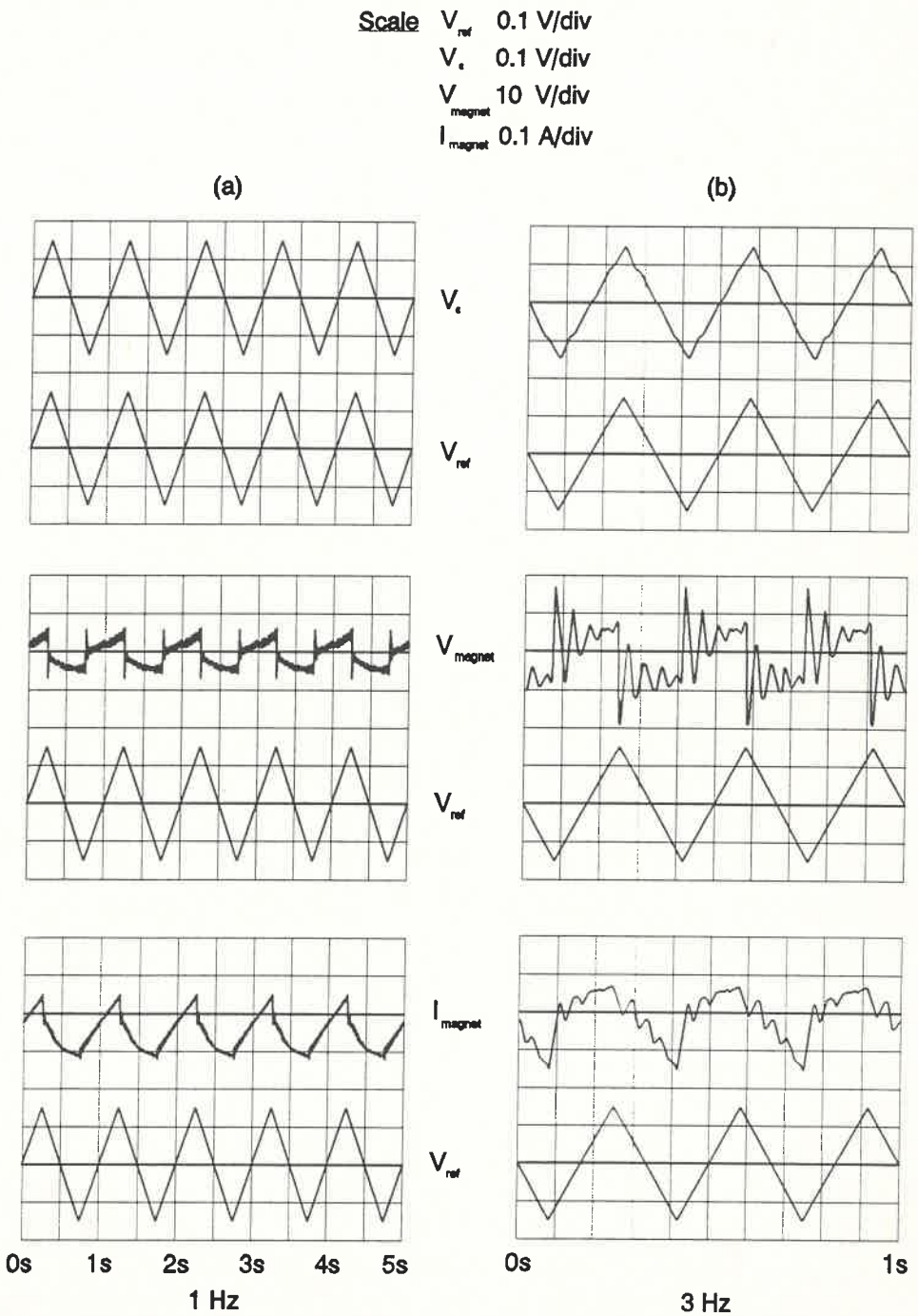

Figure 3.5 : Graphs showing the behaviour of the magnet control circuit when V_{ref} is a sawtooth waveform. In (a) V_{ref} is 1 Hz, and in (b) it is 3 Hz. The scale refers to both (a) and (b).

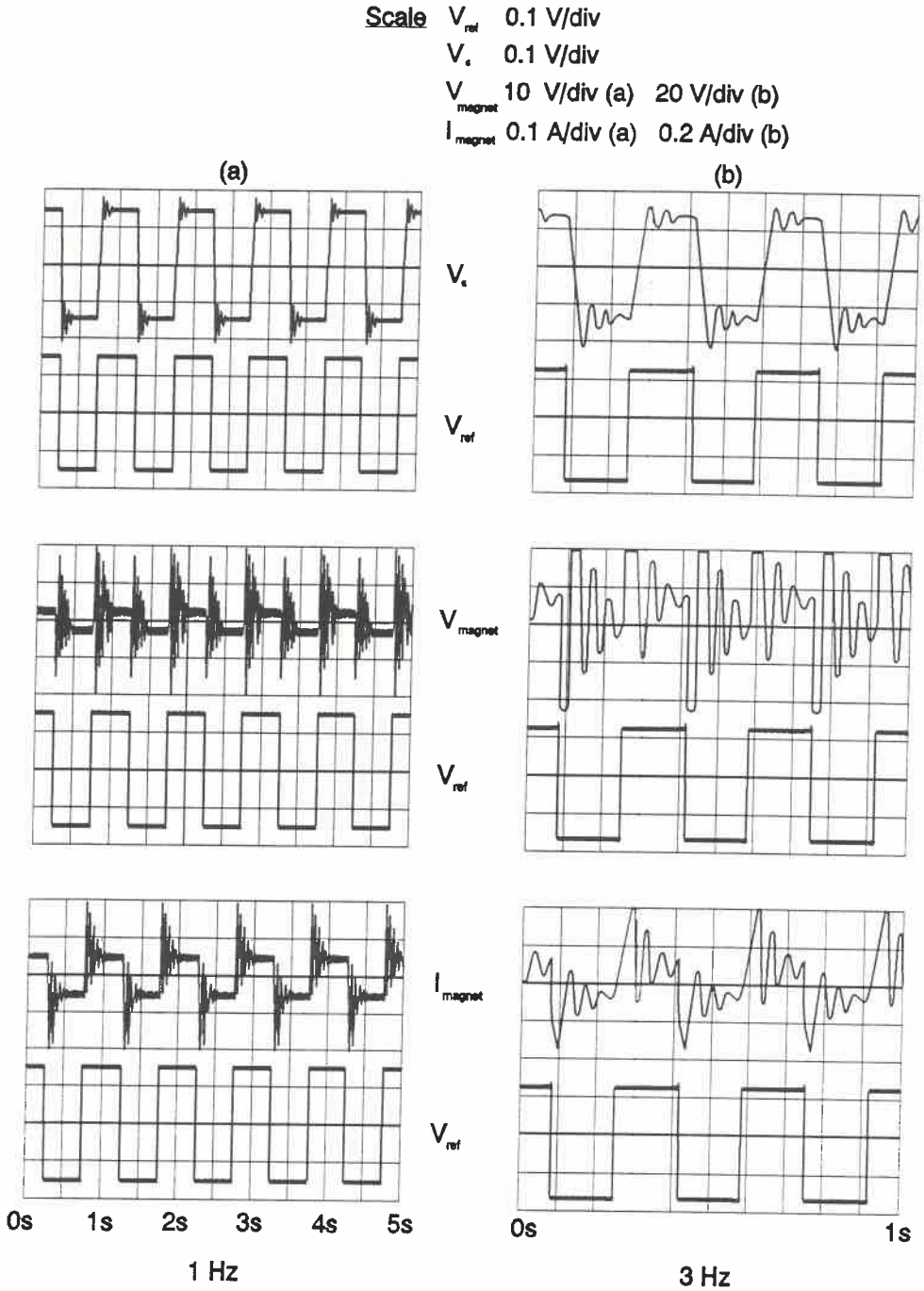

Figure 3.6 : Graphs showing the behaviour of the magnet control circuit when V_{ref} is a step function. In (a) V_{ref} is 1 Hz, and in (b) it is 3 Hz.

From Figures 3.4 to 3.6 it can be seen that the more gradual the required change in displacement, the better the magnets follow. The magnets follow the sinusoidal waveform, where there are no sharp changes in displacement or direction, best. The step function and the sawtooth function , are composed of a superposition of sinusoidal harmonics of the fundamental frequency. It is impossible for the magnets to follow the high frequency sinusoidal harmonics. This confirms the effect of the limitations imposed by the inductance of the magnets and the voltage limitations of the KEPCO power supply.

Another factor which affects the behaviour of the control system, is the amplitude of reference voltage. The amplitude was the same in all the figures shown and is typical of the tester's operating amplitudes. If, for the same frequency of the reference, the amplitude was increased, there would be a point at which the displacement could no longer follow the reference. This is because increasing the amplitude at a given frequency increases the rate of change of the displacement required. The higher the rate of displacement, and therefore, voltage, the greater the power required of the power supply. Thus the voltage limits of the Kepco power supply impose limits on the amplitude of oscillation it can support.

Thus, the magnet control circuit operates most effectively at low frequency and amplitude. The magnet cannot respond to very drastic changes in voltage, such as the step in a square wave, but follows signals such as sinusoidal and sawtooth waveforms very well within the frequency limitations.

3.4 **APPLICATION TO FATIGUE CYCLING**

It has been shown (Basinski 1959) that the flow stress of a specimen undergoing plastic deformation is influenced by two factors: temperature and strain rate. The temperature in the laboratory fluctuates no more than a few degrees during a fatigue test, and this is not sufficient to affect the stress. However, the strain rate on a specimen should be kept constant during a

fatigue test, so that changing rates of strain do not alter the stress during the test.

The sinusoidal reference waveform yields the best magnet response, in that it can be followed at higher frequencies and amplitudes than the sawtooth waveform. However, the strain rate is then not constant, whereas the voltage of the sawtooth waveform changes at a constant rate, except at the peaks where the slope changes abruptly. This constant rate of change of the reference results in a constant rate of strain and this is desirable in fatigue testing.

If the limits on the frequency and amplitude of the reference voltage are observed, the magnet control circuit effectively constrains the magnets to produce strains with a sawtooth form. The reference signal, $V_{réf}$, used during all tests performed using the fatigue machine has been a sawtooth waveform, with a frequency not more than 1 Hz and amplitudes not much greater than 0.3V. This amplitude corresponds to strain amplitude of approximately 6×10^{-3}, depending on the specimen.

CHAPTER 4

THE MEASUREMENT OF SMALL DISPLACEMENTS

4.1 INTRODUCTION

Measuring the stress and the strain during a fatigue test, requires the measurement of small displacements. To measure the stress, the displacement of the central cylinder, C_y, of the load cell has to be measured accurately. Measuring the strain involves measuring the small changes in length of the specimen.

There are several methods of measuring small displacements. Most involve the use of some form of transducer. A transducer is an instrument for converting a physical quantity into a convenient electric form, such as a voltage. This voltage can then be measured and calibrated in terms of displacement.

4.2 DISPLACEMENT TRANSDUCERS

4.2.1 Strain Gauges

The electrical resistance of a length of conductor depends on its length and cross sectional area. For a resistor of length L and constant cross section, the resistance R is given by

$$R=\rho\frac{L}{A}. \qquad (4.1)$$

The resistance of the wire changes under applied loads. If the resistor is stretched the resistance increases. If the length of the resistor decreases, the resistance also decreases.

After differentiation of equation 4.1, it can be shown (Neubert 1975) that, at constant temperature

$$\frac{\Delta R}{R}=\frac{\Delta L}{L}-\frac{2\Delta D}{D}+\frac{\Delta\rho}{\rho}, \qquad (4.2)$$

where D is the diameter of the resistor. The strain sensitivity or gauge factor, K, of the strain gauge is defined as the fractional change in resistance per fractional change in length, and therefore, from equation 4.2

$$K=(1-2\frac{\Delta D/D}{\Delta L/L}+\frac{\Delta\rho/\rho}{\Delta L/L}) . \qquad (4.3)$$

According to Poisson's Law of lateral contraction

$$\frac{\Delta D}{D}=-\nu\frac{\Delta L}{L}, \qquad (4.4)$$

where ν is Poisson's ratio. Thus

$$K=1+2\nu . \qquad (4.5)$$

where $\Delta\rho/\rho = 0$ because, to a first approximation the resistivity, ρ, does not depend on the lattice parameter of the strain gauge. Poisson's ratio $\nu = 0.25 - 0.44$ for various metals, so K may vary between about 1.5 and 1.8. Most strain gauges have a gauge factor of approximately 2. Thus

$$\frac{\Delta R}{R} \simeq 2\frac{\Delta L}{L} = 2\epsilon, \qquad (4.6)$$

where ϵ is the strain. That is, the fractional change in resistance is proportional to the strain on the resistor.

The alloy Constantan (45% nickel, 55% copper) is often used for strain gauges as it has a constant gauge factor of 2.1 and a low thermal coefficient of resistance ($\pm 0.002\%\ ^{\circ}C^{-1}$).

Semiconductor strain gauges are also available. They have gauge factors of the order of 100, but have very high thermal coefficients of resistance (Usher, 1985). This makes it difficult to design measuring circuits that have long-term stability.

The linearity of a strain gauge is a function of the constancy of the gauge factor with varying strain. Constantan and some other nickel-copper alloys have almost constant gauge factors over a wide range of stains, and are therefore linear over this range.

Because strain gauges have a finite width, they are sensitive to a small extent to transverse strains. The transverse sensitivity may be between 0.3% and 2% of the longitudinal sensitivity (Neubert, 1975). Foil strain gauges are designed to eliminate transverse sensitivity to a certain extent.

Strain gauges are usually etched foil resistance elements mounted on a plastic backing. The element may be etched from foil such as Constantan. If the strain gauge is glued on to a surface, its resistance will change if the surface is distorted. The change in the resistance can then be measured by a suitable circuit. Figure 4.1 shows the grid formation of a strain gauge.

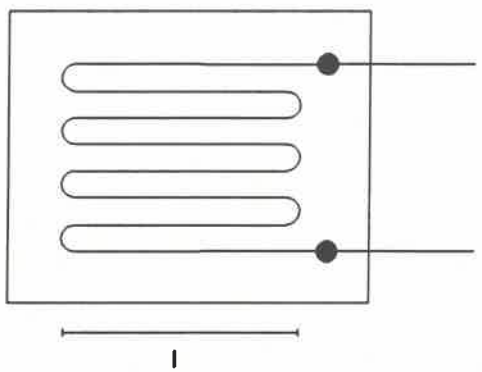

Figure 4.1 : Schematic diagram of a strain gauge of length , l.

In principle, measurements could be made using a single strain gauge connected as part of a potential divider circuit. In practice however, this kind of measurement is seldom used since much more accurate results can be obtained using Wheatstone bridge circuits.

Usually, measurements are made using a Wheatstone bridge circuit. The bridge usually has 2 or 4 strain gauges. Two strain gauges in combination with two fixed resistors is termed a half-bridge circuit, while a bridge with four strain gauges is a full bridge. Figure 4.2 shows these two configurations.

It can be shown (Philips "Guide to Strain Gauges") that for one active strain gauge, the voltage across the bridge, V_d, is given

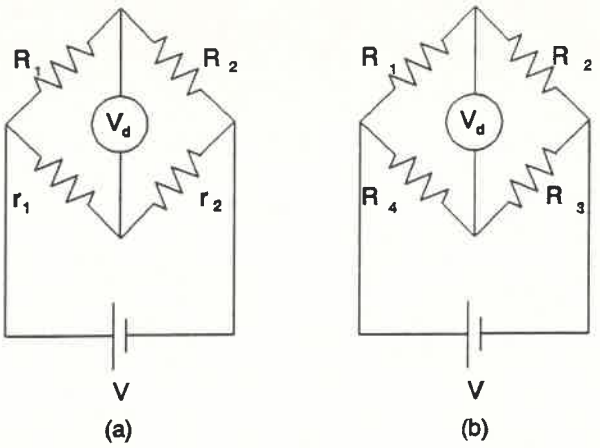

Figure 4.2 : Wheatstone bridge circuits for measuring strain. A half-bridge is shown in (a), while (b) shows a full bridge. R_1, R_2, R_3 and R_4 are strain gauges, and r_1 and r_2 are resistors.

by

$$V_d = \frac{V}{4}\frac{\Delta R}{R} = \frac{V}{4} K \epsilon. \qquad (4.7)$$

For two active gauges experiencing equal but opposite strain

$$V_d = \frac{V}{2}\frac{\Delta R}{R} = \frac{V}{2} K \epsilon. \qquad (4.8)$$

If four active strain gauges are used (two pairs with equal but opposite strain), then

$$V_d = V\frac{\Delta R}{R} = V K \epsilon. \qquad (4.9)$$

Thus, using more strain gauges in a wheatstone bridge increases the sensitivity of a strain measurement.

Strain gauges can also be used to measure load. For example, if a surface, such as that of a cantilever beam, is stretched or compressed by the application of a load, then the change in the resistance is proportional to the load applied, provided Hooke's law applies.

For a small strain gauge (L = 2.5mm), with a gauge factor of 2,

a 1μm displacement of the ends of the gauge will result in a voltage change

$$V_d = \frac{V}{4}\, 2\, \frac{1\times10^{-3}}{2.5}, \qquad (4.10)$$

if it is arranged as the one active gauge in a bridge. For an input voltage of 3V,

$$V_d = 0.6 \text{ mV}/\mu\text{m}.$$

If four such strain gauges were used in a full bridge then,

$$V_d = 2.4 \text{ mV}/\mu\text{m}.$$

4.2.2 **Capacitance Transducers**

The capacitance, C, of a parallel plate capacitor of area, A, plate separation, d, and containing a dielectric of relative permittivity, ϵ_r, is given by

$$C = \frac{\epsilon_r\, \epsilon_0\, A}{d}. \qquad (4.11)$$

Capacitance transducers give an electrical signal when the distance between the plates of a capacitor, or the area of the capacitor, changes. Figure 4.3 shows some typical devices. In Figure 4.3(a) the area changes with the horizontal displacement of the top plate, and in Figure 4.3(b) the separation of the plates change.

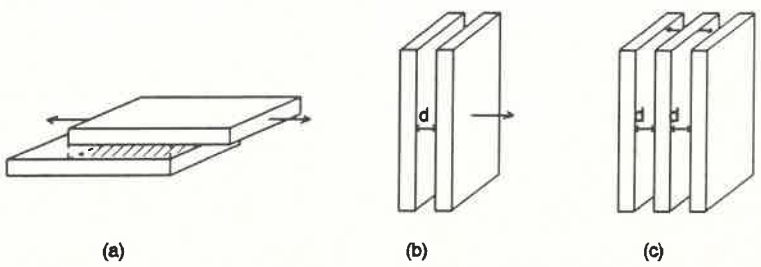

Figure 4.3 : Three capacitance transducers: (a) is a variable-area capacitor; (b) is a two-plate variable-separation transducer; and (c) is a three-plate transducer.

The capacitor may form part of a resonant circuit whose resonant frequency depends on the capacitance. Displacement of one of the

plates changes the capacitance of the transducer, and thus the resonant frequency of the circuit. Changes in the frequency can be calibrated in terms of the displacement of the plate. As with a strain gauge, the frequency change could also be calibrated in terms of the physical quantity such as load, which resulted in the displacement.

The most common variable capacitance transducer, as seen in figure 4.3(c), is the three-plate variable separation transducer. The three plates are identical and form two capacitors. When the central plate is displaced transversely, the capacitance of the one capacitor will increase, while the capacitance of the other will decrease. It can be shown (Usher, 1985) that,

$$\frac{\Delta C}{C} = \frac{\Delta d}{d}, \qquad (4.12)$$

where d is the separation between each outer plate and the central plate when Δd is zero. To provide a reasonable capacitance (~10pF), d is usually about 1mm, so the range of displacement is small (<1mm). Usher (1985) gives the sensitivity of the transducer as approximately 2 mV/μm.

However, the measurement circuitry for capacitive transducers is complex, and does not lend itself to dynamic measurement. Thus, although the sensitivity quoted is comparable to that of the strain gauge described, the capacitance transducer would not be practical for use in the fatigue tester.

4.2.3 **Linear Variable Differential Transformers**

The Linear Variable Differential Transformer (LVDT) is an electromechanical transducer. The LVDT produces a voltage proportional to the displacement of its core relative to its body. The body of the LVDT is a cylinder containing three equally-spaced coils. The core of the LVDT is a magnetic rod placed axially inside the body. The core provides a path for magnetic flux linking the coils. Figure 4.4 shows a cross sectional view of the LVDT.

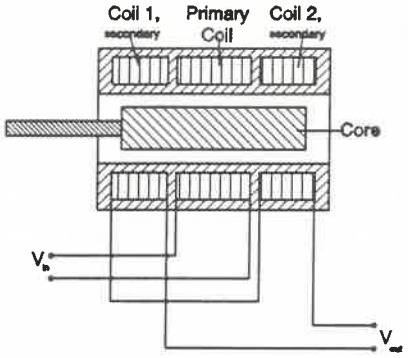

Figure 4.4 : Cross sectional view of an LVDT.

Energising the primary or centre coil with a.c., induces voltages of the same frequency in the two outer coils. The two outer or secondary coils are connected in series opposition. The two secondary voltages are therefore opposite in phase and the net output of the LVDT is the difference between these two voltages.

One central position of the core within the coils produces equal secondary voltages. Therefore, at this position, the output of the LVDT is zero. This is called the balance point or null position of the LVDT.

Moving the core from the balance point, increases the voltage induced in the coil towards which the core is moved, while decreasing the voltage induced in the opposite coil. This produces a differential output voltage from the LVDT, which varies linearly with change in the position of the core. If the core is moved in the opposite direction, then beyond the null position, a similar differential output voltage is produced, but with a 180° phase shift. Plotting voltage output versus core position yields a straight line through the origin, as shown in Figure 4.5. Opposite algebraic signs indicate opposite phases.

The magnetic flux inside the LVDT is uniform over most of the length of the LVDT. However, near the ends of the LVDT, the flux is non-uniform, as shown in Figure 4.6. When the core of the LVDT is lying in the uniform flux region, then the voltage induced in the secondary coils varies linearly with displacement; but, if the core moves beyond the uniform flux region, the linearity breaks down. This is shown in Figure 4.5.

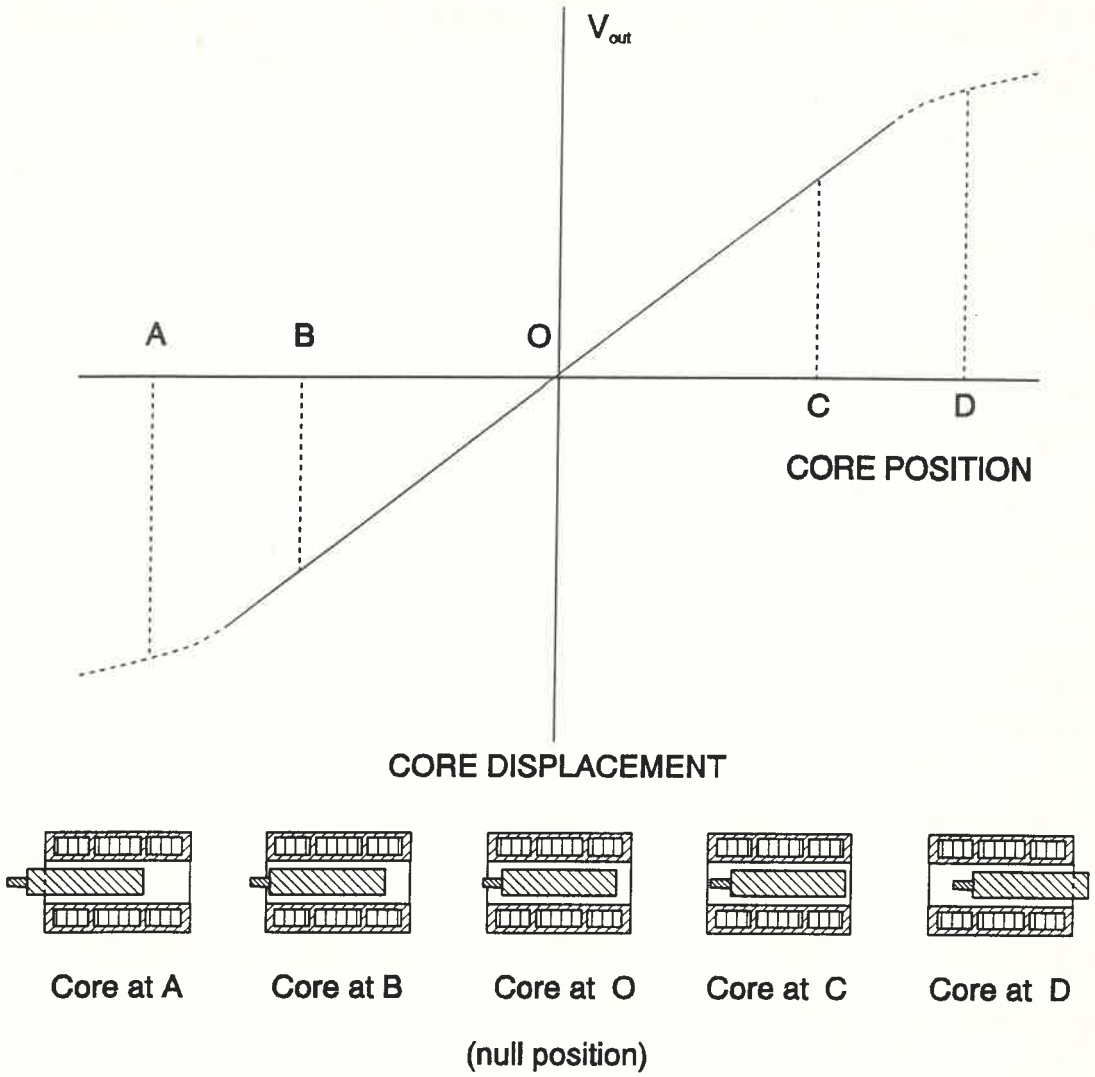

Figure 4.5 : Graph of the output voltage of an LVDT versus the position of its core. Cross sectional views of the LVDT indicate the core position at points A, B, O, C and D on the graph.

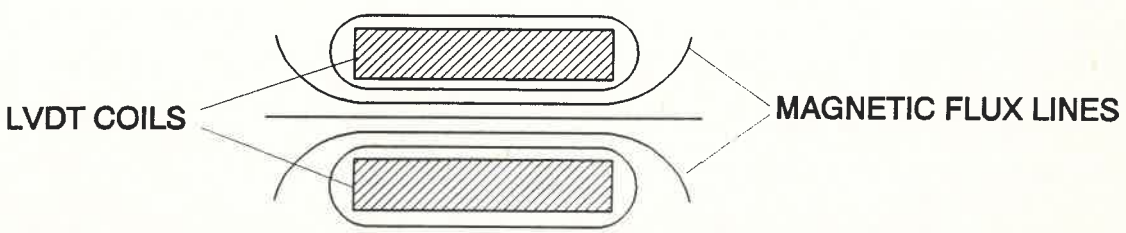

Figure 4.6 : Schematic diagram showing the magnetic flux through an LVDT.

The range of an LVDT depends on its size. Miniature LVDTs, with bodies about 1 cm long have a range of ± 0.1 mm. Larger LVDTs about 2 or 3 cm long may have a range of the order of ± 1 mm.

LVDTs are available in a wide range of sizes and types. A major advantage of the LVDT is that because the mechanical moving parts do not touch one another, there is no friction and therefore no wear. Hermetically sealed LVDTs are available for use in corrosive atmospheres, as well as heat-resistant LVDTs, high pressure sealed LVDTs, nuclear radiation resistant LVDTs and LVDTs for use at cryogenic temperatures (Schaevitz Catalog #101).

The sensitivity of an LVDT depends to a certain extent on its size. For example, a Schaevitz 005 MHR miniature LVDT, with a $3V_{rms}$ input at 10kHz, has a sensitivity of 1 mV/μm (Schaevitz Catalogue #101). The Schaevitz 050 HR LVDT, with a $3V_{rms}$ input at 2.5kHz, has a sensitivity of 0.8 mV/μm. Thus the sensitivity of a LVDt is comparable with that of a strain gauge.

4.3 COMPARISON OF LVDT'S AND STRAIN GAUGES

LVDTs and strain gauges have comparable sensitivities, although strain gauges may effectively be more sensitive when arranged in a full wheatstone bridge, as described in Section 4.2.1.

Strain gauges are very easy to attach to a surface, and produce a direct measurement of the surface strain, while LVDT's are not always as straightforward to mount as strain gauges.

Strain gauges may be subject to temperature variations, but most general purpose strain gauges have low thermal coefficients of resistance, and the temperature changes in the laboratory are not rapid or extreme, so this should not be a significant problem.

One problem with the strain gauge is that even the smallest strain gauges available were mounted on backings of approximately 3mm by 5mm. To get the best sensitivity, four strain gauges should be used, but this is limited by the size of the specimen.

Another consideration is the presence of electrical noise in the measuring circuits. The noise levels of an LVDT and a strain gauge were compared, using apparatus available in this laboratory. The displacements of a cantilever were measured. The strain gauge was glued longitudinally on its upper surface. The body of the LVDT was mounted on the end of a parallel beam above the cantilever. The core of the LVDT was fastened to the end of the cantilever below the LVDT body. Small weights were hung from the end of the cantilever. The LVDT output was measured using the lock-in amplifier, and calibrated with respect to the applied load. The strain gauge was incorporated into a Wheatstone bridge and the changes in resistance determined from the off-balance voltage, which was measured using a null-detector. The reading of the null detector was calibrated with respect to the load.

The noise of the LVDT was found to be 1.1% of the signal for a load of 100g, whereas the noise of the strain gauge was found to be 6.7% of the voltage for the same load. In addition, the strain gauge output was found to drift with time, whereas no drift was detected in the LVDT output.

Taking all of the considerations into account, LVDTs were chosen to measure the stress and strain in the fatigue tester.

CHAPTER 5
THE LVDT AND THE LOCK-IN AMPLIFIER

5.1 THE MEASUREMENT OF SMALL DISPLACEMENTS IN THE FATIGUE TESTER

5.1.1 Stress Measurements

Since the measurement of stress on the fatigue specimens involves measurement of small axial displacements in the load cell, a miniature LVDT (Schaevitz 005 MHR) was chosen to measure displacement in the load cell, and therefore the stress applied to the specimen.

The Schaevitz 005 MHR LVDT is 9.6mm long, with an outside diameter of 9.5mm and an internal diameter of 3.2mm. The core is 4.6mm long with a diameter of 2.7mm. The body has a mass of 2g and the mass of the core is 0.1g. The displacement range of the LVDT is ±0.125mm. The input voltage should not exceed $3V_{rms}$ at a frequency of between 400Hz and 20kHz.

The sensitivity of the Schaevitz 005 MHR LVDT, with $3V_{rms}$ input, is 0.3mV/μm at 2.5kHz, and 1mV/μm at 10kHz.

5.1.2 Strain Measurements

Measuring the strain of the specimen could be achieved by glueing a strain gauge to the specimen, or by using a clip-on extensometer. However, although very small strain gauges are available, even the smallest would completely cover one side of the gauge length of the specimen. In addition, the surface of a specimen plays a role in fatigue, and glueing a strain gauge to the surface would interfere with the fatigue mechanisms. Because of the short gauge length (5mm), an extensometer would also not be practical. For these reasons, an LVDT is used to measure the strain, rather than a strain gauge or a clip-on extensometer.

The Schaevitz 050 HR LVDT is 28.5mm long, with an outside

diameter of 20.6mm, an inside diameter of 9.5mm, and a mass of 32g. The core is 20mm long, with a diameter of 6.4mm and a mass of 4g. The displacement range is ±1.25mm. The maximum input voltage is $3V_{rms}$ at frequencies between 400Hz and 10kHz. With $3V_{rms}$ input at 2.5kHz, the sensitivity is 0.8mV/μm.

5.2 **THE LOCK-IN AMPLIFIER**

A major problem with measurement of small voltages is background or random noise. In many cases the noise can be more than an order of magnitude larger than the signal.

A lock-in amplifier is very useful for measuring very small signals buried in noise many times larger than the signal itself.

Lock-in amplifiers lock into a reference frequency and only measure signals of the same frequency, within a narrow bandwidth, as the reference. These amplifiers are also sensitive to the relative phases of the measured and reference signal, and are known also as phase-sensitive detectors. This technique effectively eliminates any random noise, as well as any large unwanted signals of different frequencies, such as mains pick-up signals.

If the ac voltage supplied to an LVDT, for example, is also used as the reference signal for the lock-in amplifier, then the voltage output of the LVDT will have the same frequency as the reference signal and will be measured and amplified by the lock-in amplifier. The gain depends on the sensitivity scale of the amplifier. The Princeton Applied Research (PAR) Model 5210 lock-in amplifier available in the present work, produces a full scale d.c. output signal of ± 1 V for inputs down to 1μV.

Once the amplifier has locked into the reference signal, it is possible to optimise the signal by adjusting the reference phase. Some lock-in amplifiers, such as the PAR lock-in amplifier, detect only the component of the signal with the selected phase. The component 90° out of phase is not measured. A signal of

opposite phase (180° out of phase) is measured as a negative quantity. Other lock-in amplifiers, such as the ITHACO Model 3981 lock-in amplifier used to measure the stress, measure both the in-phase and the 90° out of phase components. The latter are termed two-phase amplifiers, while the former are termed single-phase amplifiers.

By selecting the exact frequency and phase of the signal of interest, signals of other frequencies are eliminated. The only noise would be random noise, which happened to have the same frequency and phase as the signal being measured.

5.3 THE MEASUREMENT OF STRESS AND STRAIN IN THE FATIGUE TESTER

5.3.1 Strain Measurements

As was pointed out in Section 2.3.2, the strain is evaluated by measuring the change in the separation of the grips. To this end, an LVDT (Schaevitz 050 HR) was mounted next to the crystal, as shown in Figure 5.1. The body of the LVDT is fixed in an aluminium mounting, $\mathbf{Am_1}$, which is attached to the lower specimen grip, $\mathbf{G_1}$. The core of the LVDT is attached to the top grip, $\mathbf{G_2}$, by a similar mounting, $\mathbf{Am_2}$, and is positioned axially within the body of the LVDT.

When the specimen grips move relative to one another the position of the core changes and the LVDT measures this displacement. The relative displacement of the grips corresponds to the change in length of the specimen and is, therefore, directly proportional to the strain. Given the original length of specimen, the LVDT output can be calibrated in terms of strain.

The LVDT was calibrated as follows. The body of the LVDT was held horizontally in a clamp while the core of the LVDT was fastened to a micrometer screw gauge, as shown in Figure 5.2. The micrometer was clamped to the same base as the LVDT body, and was positioned so that the core lay axially inside the body. The LVDT's output was measured using a lock-in amplifier, and the

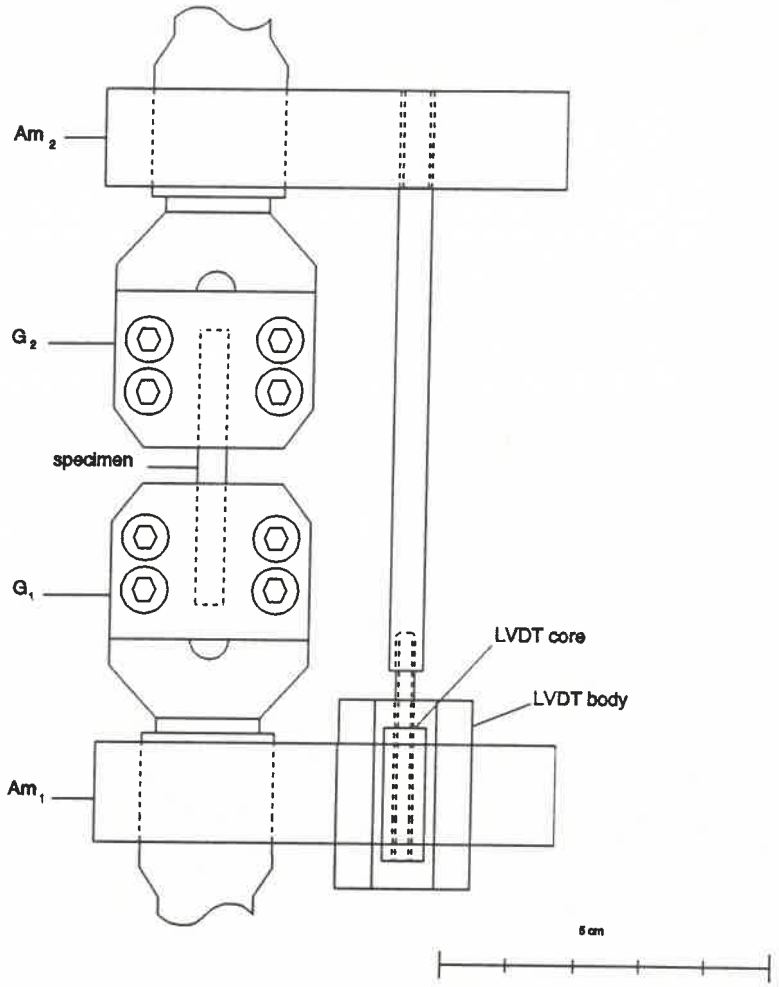

Figure 5.1 : A front view of the specimen grips, showing the mounting of the LVDT.

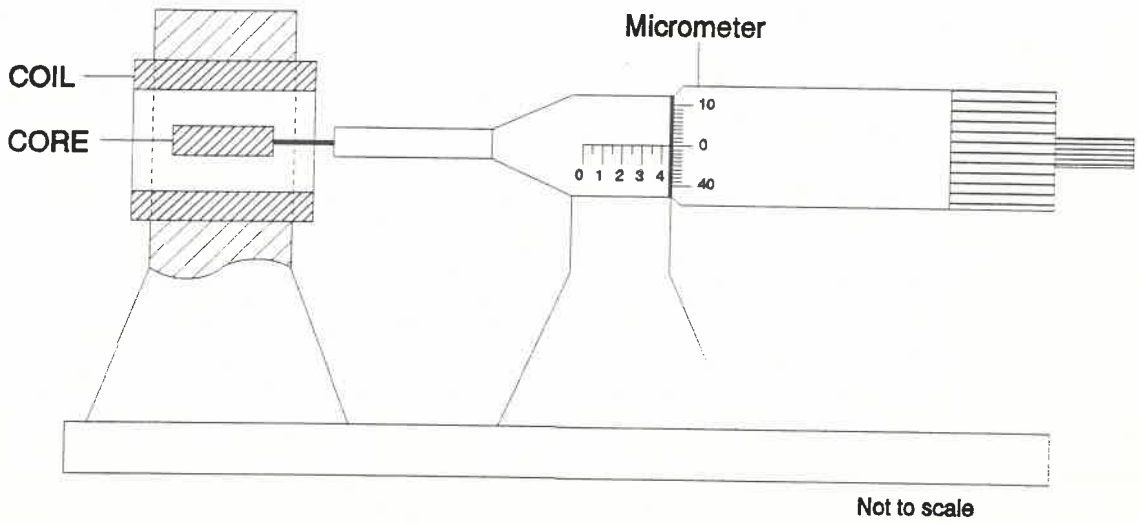

Figure 5.2 : Apparatus for calibrating an LVDT.

LVDT output was plotted versus position, which was read off the micrometer gauge.

The graph should be a straight line, and its slope gives the voltage output of the LVDT per unit length. Because the magnitude of the voltage output of the LVDT depends on the magnitude of the voltage supplied to it, it is important to quote the input voltage when calibrating the LVDT.

The LVDT output may be quoted as the ratio of V_{out} to V_{in}. If the calibration curve is plotted using the values of V_{out}/V_{in} versus displacement, the curve is valid for other values of V_{in}.

The Schaevitz 050 MH LVDT has a nominal input voltage of $3V_{rms}$, but the Escort Function Generator used to supply the input voltage could only produce 2.759 V_{rms}, due to the low impedance of the primary coil of the LVDT (430Ω). The frequency of the input voltage was 9997 Hz. This is the frequency used during fatigue testing.

Figure 5.3 shows the calibration curve of the LVDT used to measure the strain on the specimen during fatigue tests.

The slope of the calibration curve is

$$255.7 \text{ mV/V}_{in}.\text{mm}^{-1}.$$

The value of V_{in} was 2.759 V rms. Therefore the output of the LVDT is 705 mV/mm, or .705 mV/μm.

The displacement measured corresponds to the change in length of the specimen. To determine the strain, the original length, L, is required. Given the gauge length of the specimen, the tensile strain is given by

$$\epsilon = \frac{\Delta L}{L} = \frac{V_{out}}{0.705\ mV/\mu m} \cdot \frac{1}{L} .$$

The PAR lock-in amplifier used to measure the strain produces an output of 1V dc for a full scale deflection (FSD). A FSD ranges from a manually selected 1μV to 250mV.

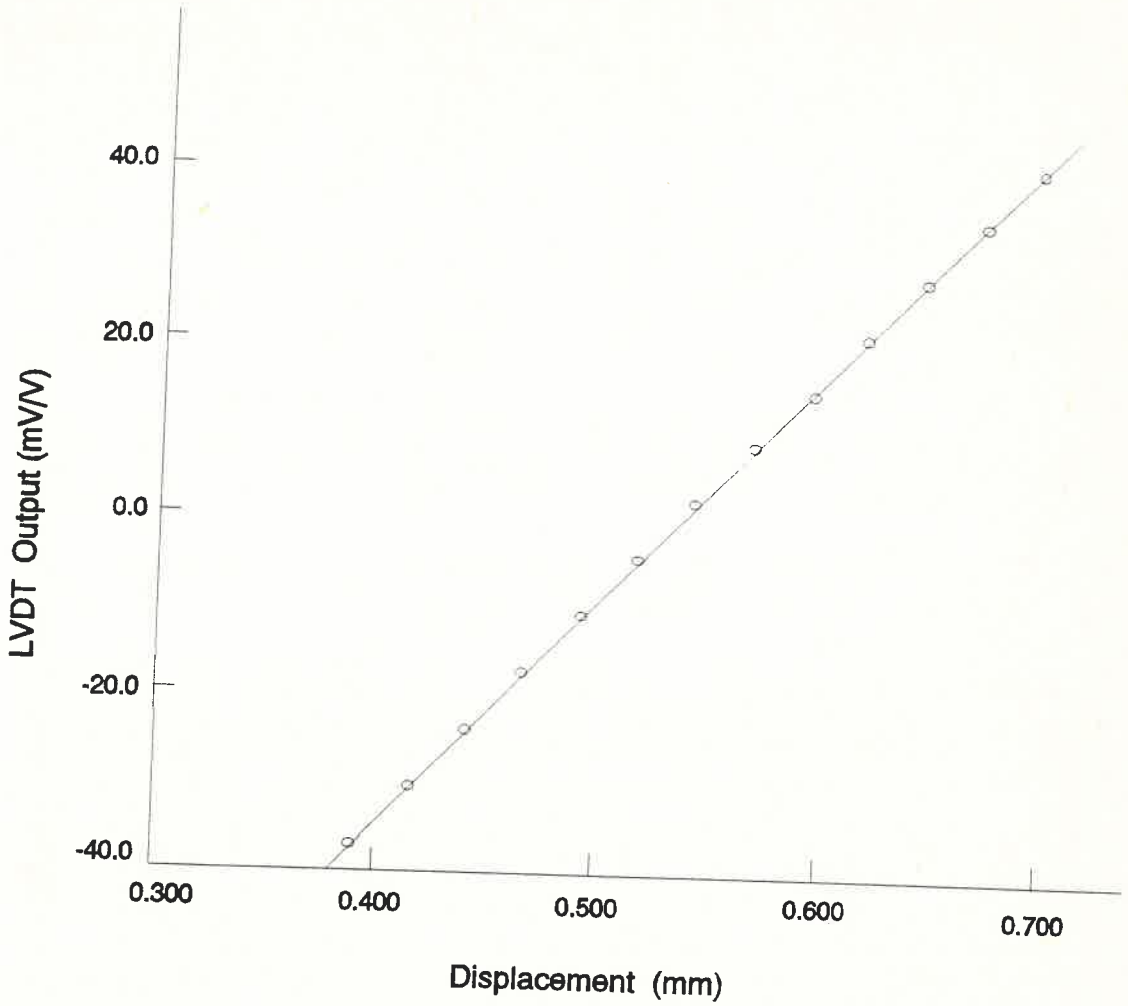

Figure 5.3 : The calibration curve of the strain measuring LVDT. The LVDT output is given as the ratio of the output voltage, V_{out}, and the voltage supplied to the LVDT, V_{in}.

The lock-in amplifier output is proportional to the strain, but the constant of proportionality depends on the sensitivity setting. The output of the LVDT is 705 mV/mm. This means that a 1mm displacement results in an LVDT output of 705 mV. The output of the lock-in amplifier will therefore be G_{PAR}.705 mV for 1mm of displacement ie. G_{PAR}.705 mV/mm, where G_{PAR} is the gain of the PAR lock-in amplifier. Therefore the tensile strain, is given by

$$\epsilon = \frac{V_{PAR}}{G_{PAR}\ 0.705\ mV/\mu m} \cdot \frac{1}{L}$$

V_{PAR} is connected to the input of the feedback amplifier (Figure 3.6) and the magnet control circuit forces V_{PAR} to follow the reference voltage, V_{ref}. Therefore, for a given V_{ref}, the strain applied to the specimen depends on the gain of the lock-in amplifier, and therefore, on the sensitivity setting. For example, if the sensitivity setting is changed from 10 mV to 100 mV, then for the same value of V_{ref}, the strain on the specimen will increase by a factor of 10.

The accuracy and reproducibility of the calibration curve depends on the correct setting of the phase. Since, as described earlier, the PAR amplifier only measures the component of the input signal which is in phase with the reference signal, if this phase is not equal to the phase of the signal to be measured, the output voltage will be only a fraction of what it would be if the phase was set correctly. If the error in the phase is Θ_E then the output voltage will vary as the cosine of the phase ie.

$$V_{PAR}=G_{PAR}.V_{LVDT}\cos\Theta_E.$$

Thus V_{PAR} is a maximum if the phase is equal to the phase of the input voltage from the LVDT, V_{LVDT}. If the error in the phase of the reference is exactly 90°, then V_{PAR} will be zero.

The PAR locks into the frequency of the signal connected across its reference input. The phase of the reference can be altered continuously over a range of 90°, and discretely with push buttons by either 90° or 180°. The lock-in amplifier only amplifies the component of the signal with the phase indicated on the dial.

It is far easier to locate a minimum in the amplifier response than to find a maximum response, because near the minimum there is a greater change in the response for a given change in phase than near the maximum. Therefore, in order to set the exact phase desired, it is most convenient to first find the phase at which the amplifier response is a minimum, indicating that the phase set is 90° out of phase with the signal. The phase is then changed by 90°.

The amplifier response is then maximized, because it is in phase

with the input signal. Once the phase is set it should not be necessary to reset it. However, it is possible to check the setting, by pushing the 0°-90° button. If this results in the amplifier response dropping to a minimum, the phase is correctly set. If not, the phase must be reset.

5.3.2 **Stress Measurements**

When a load is applied to a specimen fixed in the grips of the fatigue tester, this load is transferred from the upper grip, G_2, to the central cylinder, **Cy**, of the load cell (Section 2.2.4). The phosphor-bronze discs, **Pd**, bend very slightly, and **Cy** is displaced vertically. The discs have been designed to allow small, but measurable, displacements of **Cy** (Descoins 1992). The displacement of **Cy** is proportional to the applied load, and therefore to the stress on the specimen.

In order to measure the displacement of **Cy** a LVDT was mounted on top of the load cell as described in Section 2.3.1. The body of the LVDT, mounted firmly to the top steel disc of the load cell, is stationary. The core is mounted directly onto **Cy**, so the LVDT measures the displacement of **Cy** relative to the outside of the load cell.

In an ideal tester the load cell should not itself contribute to the elastic component of the total strain. To approach this ideal as closely as possible, the displacement of **Cy** must be as small as possible.

The load cell is calibrated by plotting the LVDT output versus load applied to the cell. In order to apply a known load to the cell , the top grip and drawbar are removed from the load cell, and replaced by a long steel shaft with a metal disc attached to the lower end. Lead weights lowered onto the disc load the cell and displace **Cy**.

Alternatively, with a specimen in the grips, a similar shaft can be passed through a hole in the centre of the bottom magnet, M_1,

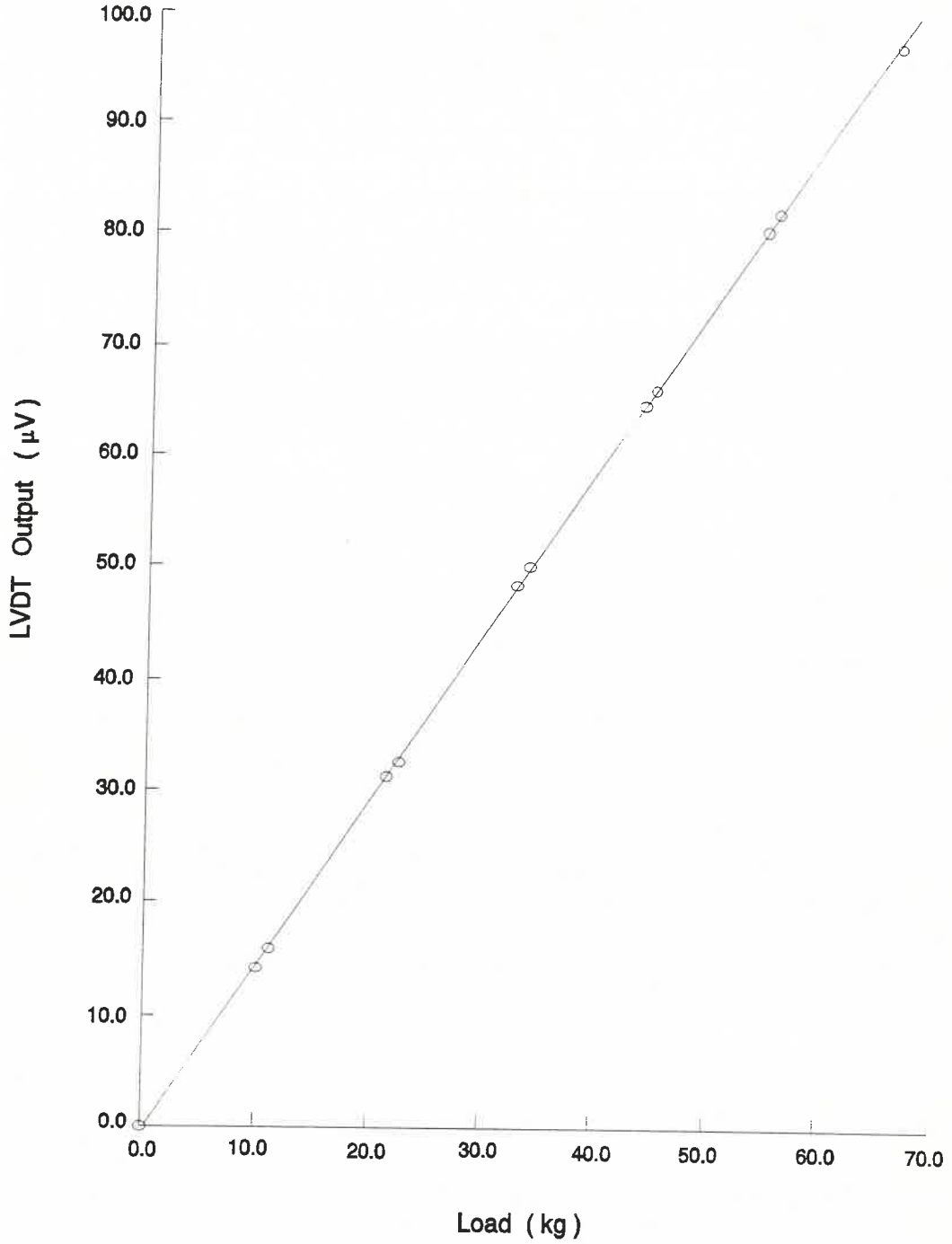

Figure 5.4 : The calibration curve of the stress-measuring LVDT.

and screwed into the top magnet, M_2.

Figure 5.4 shows the calibration curve for the load cell.The input voltage, V_{in}, was a 19710 Hz signal with an amplitude of 0.334 Vrms. The graph is a straight line with a slope of 1.47 μV/kg.

To determine the stress given by an LVDT output, V_{LVDT}, it is necessary to know the cross sectional area , A, of the specimen. Axial stress is equal to the force per unit area on the specimen, and can be calculated as follows

$$\sigma = \frac{V_{LVDT}(\mu V)}{1.47 \mu V/kg} \frac{9.79 ms^{-2}}{A(m^2)} \quad (5.3)$$

The output of the LVDT is measured using an ITHACO computer operated lock-in amplifier. The ITHACO Model 3981 PC Lock-in Amplifier may be controlled using the software provided by ITHACO, or it may be programmed in a computer language, such as QuickBASIC.

The ITHACO Model 3981 PC Lock-in Amplifier consists of three components: a main board; a remote signal input module; and a 3 metre interconnecting cable. The main board slots into an IBM compatible AT computer. The remote signal input module contains a current preamplifier and a programmable voltage input amplifier, and is connected to the main board by the cable. The LVDT signal is connected to the remote input module, and the reference frequency signal is connected to the main board. This arrangement is designed to minimise interference between the computer's microprocessor and the sensitive input amplifiers.

All control functions of the lock-in amplifier are programmed from the host computer, which acquires data from the lock-in amplifier using ITHACO MS-DOS based driver software. The driver can be accessed by computer programs written in any MS-DOS based language: in this case, QuickBASIC. The driver can also be accessed by the ITHACO User Program, which allows one to operate the lock-in amplifier from the computer keyboard.

The Model 3981 lock-in amplifier operates as a two-phase instrument. That is, it produces two dc outputs: $X = M \cos\phi$ and $Y = M \sin\phi$ (where M is the magnitude of the signal), which are proportional to the signal components in-phase and in-quadrature (90° out of phase) with the reference input, respectively, as

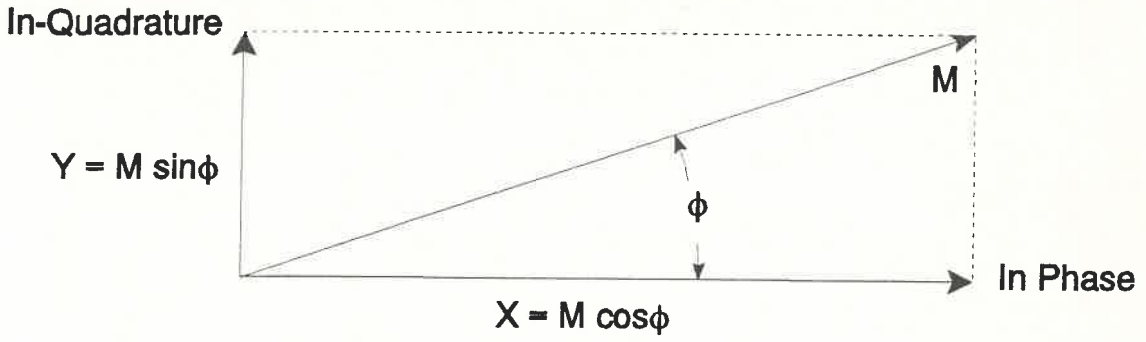

Figure 5.5 : Vector diagram for a two-phase lock-in amplifier.

shown in Figure 5.5.

The ITHACO lock-in amplifier works on the same principle as the PAR lock-in amplifier described in Section 5.3.1, in that it locks onto the frequency of the reference signal and only amplifies the portion of the input signal with this frequency. The ITHACO lock-in amplifier can make measurements in the presence of interference up to 320 times larger than the signal of interest (ITHACO Instruction Manual).

5.3.3 **The Nulling Circuit**

In what follows, it is important to remember that the PAR is a single phase amplifier while the ITHACO is a two-phase amplifier. The PAR lock-in amplifier amplifies only the in-phase component of the input signal, as described in section 5.3.1; while the ITHACO lock-in amplifier amplifies both the in-phase component and the in-quadrature component of the signal (Section 5.3.2).

If there is a signal of the same frequency as the signal of interest, but having a different phase, the PAR lock-in amplifier ignores all but the component of the extraneous signal which is in phase with the primary signal. The ITHACO lock-in amplifier, on the other hand, is a more sophisticated instrument which amplifies both the in-phase and out-of-phase components of this

signal, which are then available as separate outputs.

In practice this distinction creates problems for the stress measurement in contrast to the relatively straightforward measurement of strain. It was found that superimposed on the primary LVDT signal, which is proportional to the displacement, there is an additional extraneous signal. This extraneous signal has the same frequency as the primary LVDT signal, but of a different phase. It is independent of the displacement of the magnetic core of the LVDT, persisting even when the magnetic core is removed entirely.

It appears that the extraneous signal is due to a magnetic flux pick-up across the coils of the LVDT. It depends only on the frequency of the excitation of the primary coil of the LVDT.

The presence of this signal means that even at the null position of the LVDT there is an output, albeit of a different phase to the reference.

The PAR lock-in amplifier will only amplify the in-phase component of this signal, and since it is constant for a given frequency, it should still be possible to null the measured output of the LVDT, although the physical position of the apparent null will be different to the true null position. The difference will depend on the magnitude and phase of the extraneous signal, but does not affect the linearity of the LVDT.

The ITHACO lock-in amplifier reads and amplifies both the in-phase component and in-quadrature component of the total signal from the LVDT. If the primary signal is much larger than the extraneous signal, their vector sum is approximately equal to the primary signal, and the phase can be set so that ϕ in Figure 5.5 is zero. This means that the magnitude of the in-phase component is equal to the magnitude of the sum signal. This in-phase component behaves exactly the same as the in-phase component measured by the PAR.

However, as the primary signal approaches zero (null position),

the extraneous signal becomes significant and the vector sum of the two signals is no longer equal to the primary signal, and the phase ϕ will no longer be zero. This means that the in-quadrature component of the sum is no longer zero.

If the primary signal is much smaller than the extraneous signal then although the in-phase component of the sum may be small, the magnitude of the sum is much larger than the magnitude of the primary signal.

For the ITHACO lock-in amplifier, the magnitude of the input signal determines the sensitivity scale which may be used. If a particular scale is chosen, say 1mV, then if the magnitude of the input signal exceeds this value, 1mV, then the ITHACO shows an error and only gives an output slightly higher than the sensitivity limit.

This means that even if the primary signal is less than 1mV, if the vector sum of the primary and extraneous signal is greater than 1mV, the ITHACO output will not exceed approximately 1.01mV.

The displacements measured by the stress LVDT are very small, and the corresponding voltage produced by the LVDT are of the order of microvolts. The extraneous signal however has a magnitude of at least 10mV. Therefore, to measure the primary signal accurately, it is necessary to set the sensitivity to at least the 1mV scale. But, because the extraneous signal is greater than 10mV, the sum of the two signals is greater than 10mV, and the ITHACO lock-in amplifier will not amplify on the 1mV scale. Thus the primary signal is masked by the extraneous signal over almost the entire range of displacements of the load cell.

This situation was obviously unacceptable, and a solution had to be found. As the extraneous signal was intrinsic to the LVDT, it could not be eliminated at its source, so it was necessary to cancel it out before the signal reached the lock-in amplifier. Since the phase and magnitude of the extraneous signal were constant for a given reference signal, it could be cancelled by adding a signal in series, with the same magnitude as the

extraneous signal but opposite in phase. The sum of the extraneous signal and this nulling signal would be zero, and only the primary LVDT signal would persist.

A circuit to provide a nulling signal was designed and built with the help of the Faculty Electronics Centre. This circuit was connected in series with the voltage out of the LVDT. The circuit is shown in Figure 5.6.

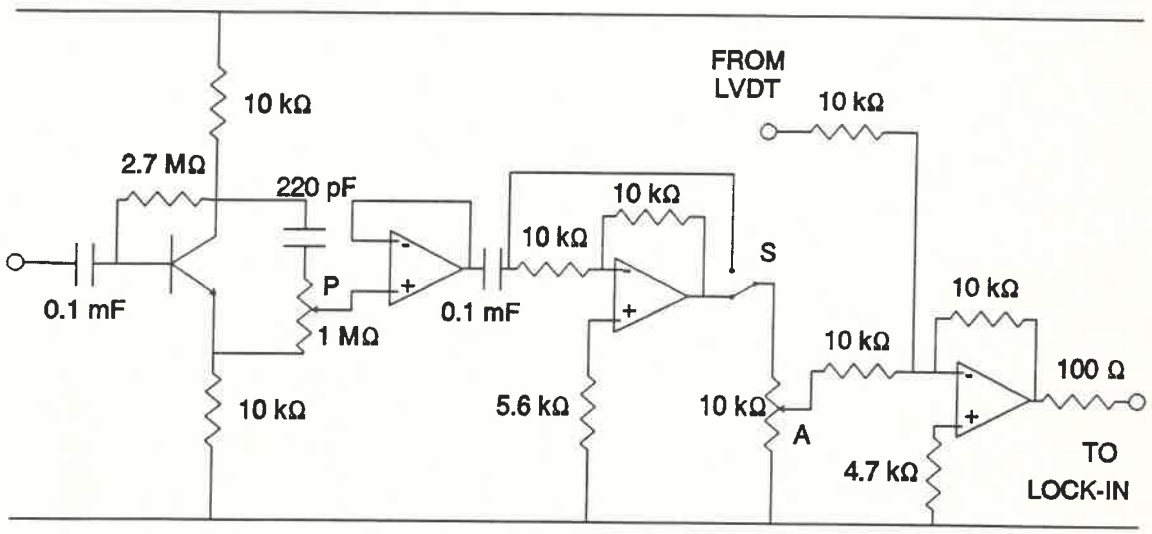

Figure 5.6 : The nulling circuit.

The nulling circuit is connected in parallel with the input signal to the LVDT, and produces a voltage which is connected between the LVDT output and the lock-in amplifier input. Figure 5.7 shows how the nulling circuit is connected. The frequency of the voltage is equal to the frequency of the LVDT input voltage (which also acts as the reference to the lock-in amplifier). The magnitude and phase of the voltage produced by the nulling circuit can be adjusted. The phase is adjusted using a rheostat, P, which shifts the phase between 0° and 180°, and a switch, S, which changes the phase by another 180°. The magnitude of the voltage is adjusted by a rheostat, A.

Thus the nulling voltage can be adjusted to cancel out the extraneous signal from the LVDT. With the nulling circuit shorted, the signal to the lock-in amplifier should be monitored

on an oscilloscope. The position of the core can then be adjusted to minimise the amplitude of the signal. The nulling circuit is then activated and the phase and magnitude adjusted alternately until the signal displayed on the oscilloscope is as close to

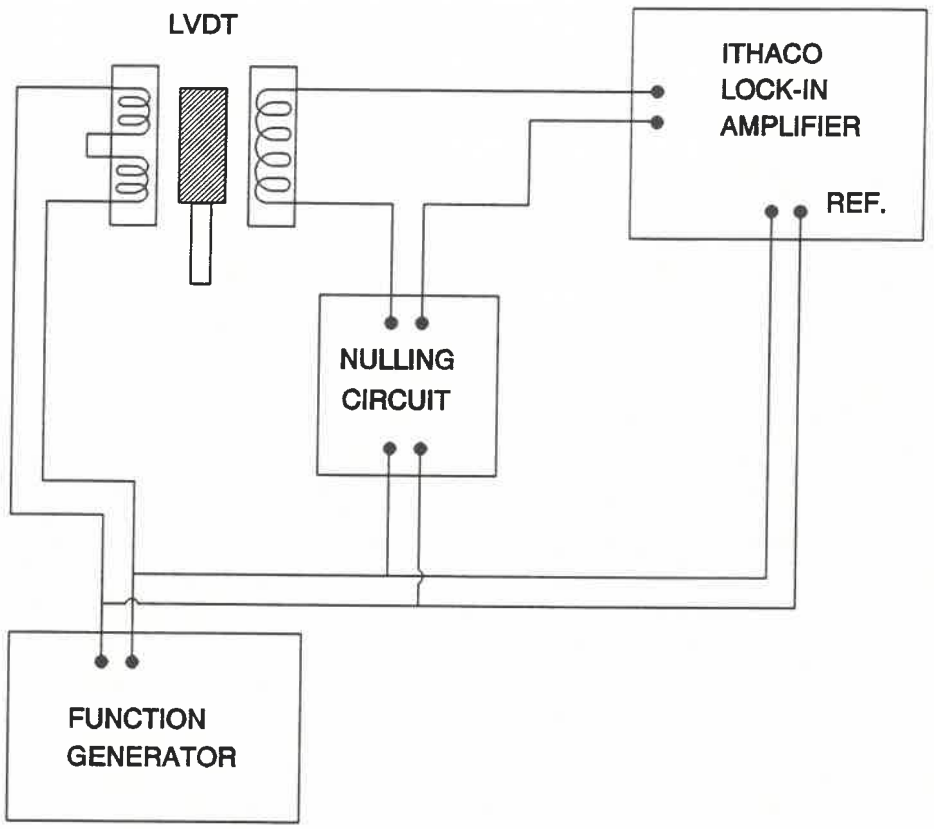

Figure 5.7 : Block diagram showing how the nulling circuit is connected between the LVDT and the lock-in amplifier.

zero as possible. It is possible to adjust the nulling voltage to cancel the extraneous signal to within less than a millivolt. The resultant voltage can then be connected to the lock-in amplifier, and measured on the 1mV scale.

Therefore, the nulling circuit effectively reduces the extraneous signal, so that the LVDT output can be accurately read for the small displacements of the load cell as described in Section 5.3.2.

CHAPTER 6
PROGRAMMING

6.1 INTRODUCTION

Both the stress measurement and the strain control of the fatigue tester were computer controlled. The stress was measured with the PC-board based ITHACO Lock-in amplifier, and the strain was controlled by a computer generated voltage signal sent to the magnet control circuit. The voltage signal was produced by OPTO hardware. The controlling programme was written in MS-DOS based QuickBASIC.

The fatigue test is controlled by the program. The amplitude of the strain cycle can be set, and calibration factors for the stress and strain entered. The program communicates with the OPTOWARE hardware to generate a sawtooth reference voltage with the desired amplitude. The program reads the LVDT output continuously during the test, and converts the voltages into stress values. At any stage during the test a stress-strain cycle can be plotted on the screen and printed out on a printer. Every thousandth cycle is saved to a random access file. The test may be paused or stopped at any time, and the program detects when a specimen has broken and stops the test automatically.

The programming of the OPTOWARE computer hardware is discussed in section 6.3, and the programming of the ITHACO lock-in amplifier is discussed in section 6.4.

6.2 PROGRAMMING IN QUICKBASIC

The most important programming feature of QuickBASIC is the sub-program. A sub-program is a self-contained unit whose variables, unless otherwise specified, are local. This means that changing a variable with a given name in a sub-program does not change the value of a variable of the same name in the main program, or any other sub-program, unless that variable is declared as a common

variable in the main program.

Sub-programs are very useful where a particular task is repeated often in a program, and using sub-programs keeps the main program uncluttered. Sub-programs make editing easier, as it is easier to pin-point where errors occur since each sub-program usually has only one main function.

A sub-program can be called anywhere in a program: either from the main program, or from within another sub-program. Once a sub-program which has been called, is completed, the program returns to where the sub-program was called from.

Another feature of QuickBASIC is that line numbering is not required, unless a particular line will be called by a GOTO statement, in which case it is only necessary to assign a unique number to the line in question. This feature is a great advantage when programming and editing.

An important programming technique is the loop. There are several types of loop which the computer can perform. The advantage of a loop is that the same task can be performed repeatedly by the computer, possibly with variations, until some condition is met.

The QuickBASIC program used to run the fatigue test is listed in Appendix 1.

6.3 **THE OPTO SYSTEM**

OPTOMUX (Optically Isolated Multiplexing Hardware) is a range of external analog and digital input-output (I/O) devices which communicate with a host computer via a serial link which may be several hundred metres long. An OPTOMUX station is composed of two parts: a "brain board" and an I/O mounting rack. The brain board contains a microprocessor which communicates with the host computer and the I/O modules. Each OPTOMUX station has a unique address, allowing the host computer to communicate with as many as 256 different stations, on a single serial communications

link.

OPTOWARE is a software driver package which is designed to communicate with the OPTOMUX stations. The OPTOWARE driver is an assembly language subroutine that acts as an interface between an OPTOMUX network and an application program written in a high level language such as QuickBASIC.

The OPTOWARE driver allows communication with an OPTOMUX network by calling a subroutine from the applications program. The driver then builds and transmits OPTOMUX command messages, and converts the data returned by the OPTOMUX network to a form which may easily be manipulated in high level languages. The driver also does extensive error checking and returns diagnostic error codes.

In order to use the OPTOWARE driver in a program, it is necessary to know how to call an assembly language subroutine from the program, how to tell the driver what OPTOMUX command to send, and how to interpret the data passed back by the driver.

There are two types of OPTOMUX station: a digital station, and an analog station. A digital station is composed of a digital brain board (designated B1 by the manufacturer) and a digital Input/Output (I/O) mounting rack for individual I/O modules. An analog station has an analog brain board (designated B2 by the manufacturer) and an analog I/O mounting rack.

6.3.1 **The OPTOWARE Driver Parameters**

The OPTOWARE driver subroutine is called from the application program using a CALL statement. The CALL statement contains six parameters which address and control the operation of individual modules. These parameters provide the driver with all the data necessary to specify which command is to be sent to which OPTOMUX station. Data values and error commands are passed back to the application program in the parameters.

A CALL statement in QuickBASIC is written as follows:

```
CALL OPTOWARE (ERRORS %, ADDR%, CMD%, POSITIONS%(0),
MODIFIER%(0), INFO%(0)),
```

where the section in brackets is the parameter list, containing the six variables to be passed to the driver. The parameters are all 16 bit integers, as specified by the percent sign after the variable name.

The ERRORS parameter is an integer variable used to return error codes. A value of zero indicates that there were no errors and the command was successfully executed. A value of less than zero indicates that an error was detected and the command was not executed. The values of the ERRORS parameter indicates what type of error occurred, and may be an integer from -1 to -34. For example, a value of -29 means that the driver sent a command to the OPTOMUX, but the OPTOMUX did not answer.

The ADDRESS parameter contains the OPTOMUX station address to which the command must be sent, and is an integer from 0 to 255.

The COMMAND parameter is an integer variable which contains the number of the desired command. There are 85 possible commands.

The POSITIONS parameter is a 16-element integer array which specifies which module positions the command applies to. On a 16-position mounting rack the modules may be placed in 16 locations numbered 0 to 15. The desired position numbers are entered in consecutive array elements, with the element following the last position number set to -1. If all 16 module positions are entered the -1 is not required. For example, to specify module positions 1, 3, 7 and 14, the POSITIONS array parameter will contain the following values:

```
POSITIONS%(0)=1
POSITIONS%(1)=3
POSITIONS%(2)=7
POSITIONS%(3)=14
POSITIONS%(4)=-1
```

The MODIFIERS parameter is a two-element integer used to hold the

command modifiers, when a command has several different modes. For example, the command "Set Output Waveform" (command number 43), sets a waveform at any output which may be a square wave, a triangular wave or a ramp function. The first element of the MODIFIERS array contains a value from 0 to 14, which specifies the period of the waveform. The second element of the array contains a value from 0 to 7, which specifies the type of waveform to be initiated.

The INFO array parameter is a 16-element array which is used to hold data necessary to execute a command, and to hold all returned data. If the data values returned are not associated with specific module positions they will appear in the first array element. Data values associated with specific modules appear in the corresponding elements of the array. For example, data relating to module position 3 would be returned in INFO%(3).

All the parameter variables must be dimensioned (if they are arrays) and initialised before calling the driver. If the serial communications are not connected to communication port one, the Set Serial Port Number command (command 102) must be used to specify which serial port the OPTOMUX network is connected to.

6.3.2 **The OPTOWARE Commands**

There are 3 types of OPTOWARE commands: Analog, Digital and Driver commands.

There are 42 possible analog commands which fall into six categories: System commands; Configure commands; Read and Write commands; Input Range commands; Gain and Offset commands; and Waveform commands. The 47 possible Digital commands fall into seven categories: System commands; Configure commands; Read and Write commands; Latch commands; Counting commands; Time Delay and Pulse commands; and Duration measurement commands. There are a total of 80 analog and digital commands, numbered from 0 to 79. There are nine commands (0, 1, 2, 4, 5, 6, 7, 8 and 70) which are both analog and digital commands. There are five Driver commands

from 100 to 105.

The first command which must be sent to the OPTOMUX is command number 0, the "Power Up Clear" command. This command prevents the OPTOMUX from returning a Power Up Clear Expected Error in response to the first instruction following the application of power. It has no effect on the OPTOMUX operation. If this command is the first command sent to the OPTOMUX, then if there is a Power Up Clear Expected Error during the program, it means that there has been a power failure. This is important as a power failure resets the OPTOMUX configuration. The Power Up Clear command is a system command and should be carried out for both analog and digital optomux stations.

The next commands which should be sent are the necessary driver commands, such as Set Serial Port Number (command number 102) and Set Number of Retries (command number 103). The Set Serial Port Number tells the driver which serial port to use. The first element of the INFO array contains the number of the desired serial port to be used in the host PC. The default setting is COM1. The Set Number of Retries command sets the number of times the driver will attempt to send a command to the OPTOMUX before returning an error message. The desired number of attempts is contained in the first element of the INFO array. The default setting is 1 retry. A value of zero in INFO array will select the retry count to 65536.

The next system command which should be carried out at the beginning of a program is the Reset command (command 1) which sets all operating characteristics of the addressed OPTOMUX station to power up conditions. For example, it sets all analog output modules to zero scale, turns off all digital outputs and configures all positions as inputs.

Once the Power Up Clear and Reset commands have been sent, the module positions may be configured as inputs or outputs, as the case may be. There are three configure commands which may be used. Command number 6 (Configure Positions) configure the module positions specified in the POSITIONS array as outputs, and all

module positions not specified as inputs. Commands 7 and 8 (Configure as Inputs and Configure as outputs) configure the positions in the POSITIONS array as inputs or outputs, respectively, and leave the other positions unchanged.

Other commands which have been used are the Write Analog Outputs command (number 35), the Activate Digital Outputs command (number 9) and the Deactivate Digital Output command (number 11).

The Write Analog command instructs the OPTOMUX to write a specified value to one or more analog outputs. The POSITIONS array contains the output positions that are to be written to, while the first element in the INFO array contains the value that will be written to each position specified in the POSITIONS array. The values range from 0 to 4095, where the value 4095 corresponds to the full scale value of the output.

Commands 10 and 11, Activate and Deactivate Digital Outputs, turn the specified outputs on and off, respectively. The output positions to be switched on or off are contained in the POSITIONS array.

6.3.3 **Control of the Fatigue Cycle**

To provide the reference voltage for the magnet control unit an analog OPTOMUX station with a module, designated model DA7 by the manufacturer, was used. The DA 7 module is a -10 to +10 V DC Output Module, and provides a single channel of optically-isolated Digital to Analog conversion. The address of the station is 1, and module position 0 is configured as an output. The desired reference voltage is a sawtooth waveform of a given amplitude. To provide such a waveform, the output module uses FOR...NEXT loops.

The program allows one to enter the desired offset and amplitude. These values are entered into the variables ov and aml. The maximum and minimum voltage of the waveform are then calculated. The maximum voltage (variable t) is given by t = ov + aml, while

the minimum (variable b) is given by b = ov - aml. The values of b and t are then tested to check that they fall in the voltage range of the module.

The sawtooth is generated by either incrementing or decrementing the value of the output in small even steps in three FOR...NEXT loops. The first loop increases the voltage from the offset value to the maximum in 25 steps, the second decreases the voltage from the maximum to the minimum in 50 steps, and the third loop increases the voltage from the minimum to the offset in another 25 steps. Thus each cycle consists of 100 steps, each one twenty-fifth of the amplitude. Within each loop, the variable f is increased by 1/25 of the amplitude and a sub-program called "voltout" is called from within the loop. The "voltout" sub-program converts the value f into the corresponding value, between 0 and 4095 of the INFO array for the Write Analog Output command. The "voltout" sub-program then calls the "sendit" sub-program, which calls the OPTOWARE driver.

Once all three loops have been completed, the variable nc, which gives the total number of cycles completed, is incremented by 1. The three FOR...NEXT loops are contained in a DO...LOOP UNTIL loop, which repeats the entire cycle until the condition specified in the UNTIL line is met, ie. until the string variable stp$ = "y".

It was found, that with the number of steps per cycle set at 100, the duration of a cycle is approximately 1.6s. Thus, the frequency of V_{ref} is approximately 0.6 Hz. It was found that using few steps per cycle, and thus increasing the frequency, produced an unacceptably rough waveform because the discrete steps involved become larger as the number of steps decreases. It was found that 100 steps per cycle produced a superior waveform. Increasing the number of steps per cycle decreases the frequency without improving the waveform appreciably. This is due to the fact that a change in voltage has a discrete minimum magnitude, since the INFO array value which determines the output voltage is an integer. Thus the smallest change in voltage is 1/4096 of the total voltage range of the module.

6.3.4 **Practical considerations**

The low frequency at which the fatigue test is conducted, means that a single test may take more than 12 hours. It is therefore necessary to be able to leave the tester unattended overnight.

This could be a problem, because sudden voltage changes in the mains supply can cause the system (computer and control system) to drive the KEPCO power supply to overload the magnets. Although the power supply is designed to sustain continuous overload, the magnets would overheat if this condition persisted for any length of time. Overheating of the magnets could lead to damage of the magnet coils, and may even result in a fire, since large currents are supplied when the power supply overloads. The power supply may also overload if there is a short circuit in the magnet coils.

Another problem with leaving the tester unattended, is that the magnets will continue cycling and counting cycles even once the specimen has fatigued to failure. This is unnecessary and should be avoided if possible, since it is desirable to know the number of cycles to failure as accurately as possible.

For these reasons, it was decided that the mains power to the KEPCO power supply should be supplied via a DC relay, which could be operated by the computer. To this end, a digital OPTOMUX station was connected in multidrop mode to the existing analog station and assigned the address 255. The connections are shown in Figure 6.1. The first OPTOMUX station acts as a host to the next OPTOMUX.

The digital station used consists of a B1 digital brain board and a 16 channel integral DC output rack (PB16L). This rack provides 16 individual channels of optically-isolated output for controlling or switching small DC loads. It is useful for controlling low power DC relays.

The first channel (position 0) of the rack is used to operate a high-voltage low power relay. This relay is connected between the

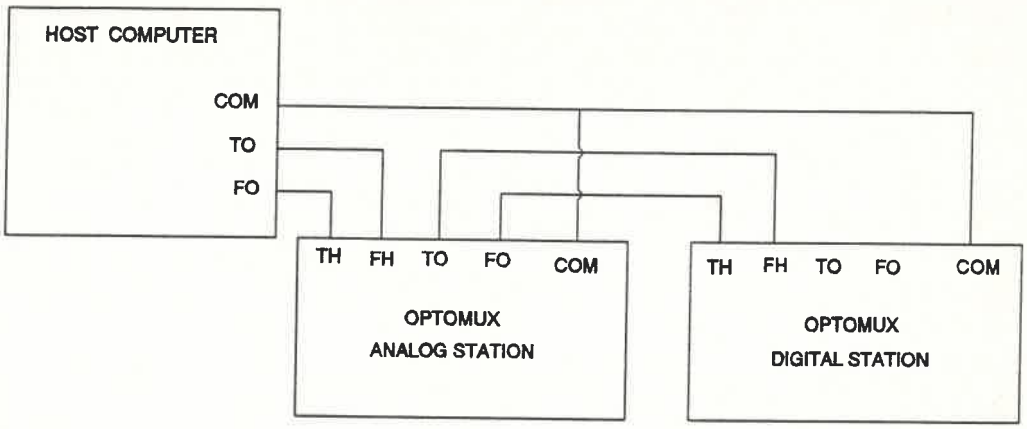

Figure 6.1 : The connections between the host computer and the two OPTOMUX stations. The abbreviations are: TO - to OPTOMUX; FO - from OPTOMUX; TH - to host; FH - from host; and COM - common.

plug to the mains power and a socket. With the KEPCO power supply plugged into the socket, the relay can switch the KEPCO power supply on and off. The commands Activate Digital Output and Deactivate Output are used to switch the relay on and off from the program. Figure 6.2 shows the relay circuit.

When the program starts running the test, the command, Activate Digital Output, is used to switch the KEPCO on. Conditions are set within the program for switching the power supply off using the Deactivate Digital Output command.

The two conditions for which the magnets should be switched off are: the magnets overloading, and the specimen breaking. Both conditions are tested for by monitoring the stress which is read each time the voltage output is changed.

If the magnets overload, the stress will exceed the sensitivity scale (see Section 5.3.3). The stress-LVDT output voltage is read into the computer by the ITHACO lock-in amplifier (see section 6.4). If this voltage reaches the sensitivity limit, the magnets must have overloaded. They must then be switched off and the test terminated.

An overload flag is set to zero before each cycle and is changed

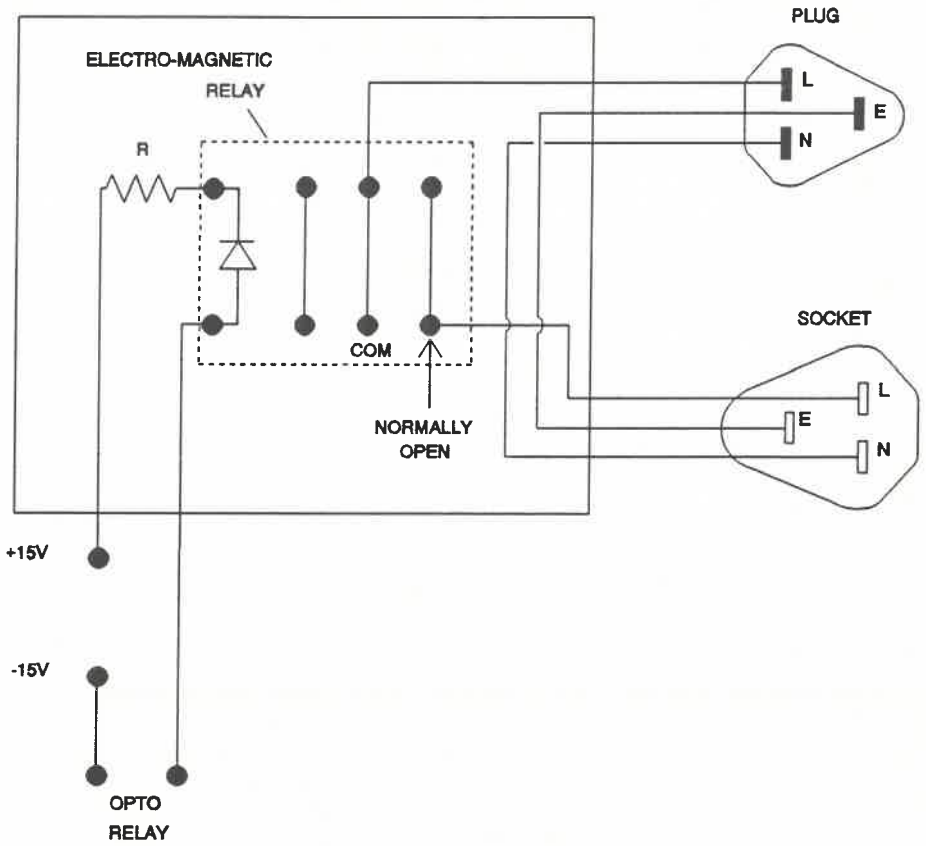

Figure 6.2 : Schematic diagram of the dc relay circuit.

to 1 if the LVDT voltage exceeds given limits. At the end of the cycle, if the flag equals one, the relay cycle is switched off, the last cycle is saved to a random access file, and the test is terminated by setting stp$ to equal "y" (the condition for stopping the DO...LOOP UNTIL loop).

Testing whether the specimen has failed is more complicated. During the tensile part of the cycle there will be no stress on the top grip as the lower piece of the specimen will merely move away from the upper portion. During the compressive part of the cycle, there will be a negative stress on the specimen. This means that where the strain is positive, the slope of the stress-strain curve should be zero.

In practice, due to noise on the LVDT voltage, it was found that the most effective method of determining whether the slope was approximately zero, is to average the stress for the 10 lowest

positive strain values and average the stress for the 10 highest positive strain values, and test the difference between the two averages. If the difference is below a set value, the relay is switched off, the last cycle saved to a random access file, and the test stopped.

These precautions enabled tests to be left running unattended, without damage to the equipment or risk of fire.

6.4 **THE ITHACO LOCK-IN AMPLIFIER**

The installable device driver for the ITHACO lock-in amplifier (DRV3981.SYS) is an assembly language interface between application programs and the model 3981 lock-in amplifier hardware. The driver responds to over 100 commands which control the lock-in amplifier and can perform numerous calculations on the measurements taken by the amplifier.

All communication between the amplifier and an application program occurs through the driver. The program communicates with the driver as though the driver were a file, which must be opened, written to, read from and then closed. The program writes to the driver to send commands and reads from the driver to get returned values.

6.4.1 **ITHACO Software Driver Commands**

The general form of a command is:

COM[nnnn/?/!] where: 'COM' is a three-letter code,
'nnnn' is an optional integer,
'/' separates options in the list,
'?' is an optional request for data, and
'!' is an optional demand for data.

All commands written or values read are ASCII strings. After a command which requests or demands data, there should be a READ statement to read the data.

Often a returned value will be preceded by a status number which reports any error condition that occurred while data was being accumulated. The value of the status number indicates which error was encountered. If more than one error occurred, the status number is the sum of error numbers.

It is possible that data may be requested faster than it becomes available. If data is requested, data is not returned if it has already been read before. If data is demanded, it is returned whether or not it has been read before.

The commands fall into seven categories: data Acquisition commands, Program Control commands, Autocalibration commands, State and Status Query commands, Control commands, General Purpose Timers, and Ratio Functions.

The commands used for the stress measurement are:

ENI - Enable Interrupts,
DSI - Disable Interrupts, and
CXC{?/!} - Current X Channel
SIN{ } - Set Integration Number.

Enable Interrupts enables and starts interrupts so that the lock-in amplifier can gather data. The Disable Interrupts command disables the interrupts so that the amplifier will discontinue functioning. Current X channel returns the most recent X channel data, that is the in-phase component of the LVDT signal. The Set Integration Number command .

6.4.2 **Reading the Stress**

In section 6.3.3 the FOR...NEXT loops which control the strain cycle of the fatigue test are described. In each loop, after the voltage output has been changed, a sub-program is called to read the stress. In the first and last loop, where the strain is being incremented, the "stressup" sub-program is called. This sub-program calls the "readstress" sub-program which issues the AXC (Averaged X Channel command) and reads the returned data. The

data is then converted to a floating point variable, that is returned to the "stressup" sub-program, which stores the data in an array, up(r).

During the second loop, where the strain is decreasing, the "stressdn" sub-program is called. This sub-program also calls the "readstress" sub-program and stores the returned LVDT output in an array, dn(r).

Thus, at the end of each strain cycle, the stress for that cycle is stored in the up(r) and dn(r) arrays. This data can either be stored or plotted on the screen and printed on a printer.

CHAPTER 7
OPERATION OF THE FATIGUE TESTER

7.1 PREPARATION

In order to run a fatigue test, the first step was to run the ITHACO software program. In this program the following conditions were set:

1. External Signal - OFF
2. Sensitivity Scale - 1mV
3. Time Constant - 3.33ms
4. Integration Count - 1
5. Averaging Count - 2.

The ITHACO lock-in amplifier has autocalibration facilities which automatically calibrate the zero offset, the gain and the phase of the amplifier. These autocalibrations were performed each time a test was run, in order to set the same initial conditions.

The Offset Autocalibration was run. Once this was completed, the external signal was switched back on, and the Gain and Phase Autocalibrations were run. The ITHACO has a phase nulling circuit which zeros the out-of-phase component of the measured signal. The Phase Shifter was enabled and the phase was nulled.

Using the oscilloscope to monitor the stress LVDT voltage, the LVDT position, and the nulling circuit phase and magnitude were adjusted to minimise the LVDT voltage.

With the stress LVDT and lock-in amplifier conditions set, the ITHACO software program was terminated.

The computer that was used has a monochrome screen with a Hercules graphics card. A locally written, commercially available program called HERCPRIN was run. This program "dumps" the screen of a computer, with a HERCULES graphics card, to a dot matrix printer when the keys, CTRL-\, were struck. This facility is necessary to plot the stress-strain cycles when running the

fatigue test. When the HERCPRIN program was finished, a program called MSHERC was run. This program enables graphics emulation with the HERCULES graphics card.

The specimen to be tested was fixed into the lower specimen grip as tightly as possible. The output of the strain LVDT was set to zero by adjusting the position of the LVDT body in its mounting.

7.2 **THE FATIGUE TEST PROGRAM**

The program which runs the fatigue test FATGDIFF.BAS, was loaded into Quickbasic and run.

7.2.1 **Layout of the Program**

The FATGDIFF.BAS program consists of a main module and sub-programs. The main module declares all the sub-programs, dimensions all the variable arrays and declares all the common shared (global) variables. The main module then calls the following sub-programs: "startup", "init", "setup", and "softkey".

"Startup" opens communication port two, for the OPTO communications; opens the ITHACO software driver file and enables the ITHACO interrupts.

"Init" initialises all the OPTOWARE driver parameters, setting the addresses of the analog and digital stations and the positions of the modules being used. All other parameters are set to zero.

"Setup" performs all the OPTOWARE commands necessary (see Section 6.3.2). The Set Serial Port command sets the port to COM2. The Power Up Clear and Reset commands are sent to both analog and digital addresses. The number of retries is set to six. The Configure as Outputs command configures the first module of each station as outputs. The voltage out of the DA7 module, V_{ref}, is

set to zero.

The "softkey" sub-program sets and activates six soft keys. A soft key is a keystroke or combination of keystrokes which instruct the program to perform some task. A soft key may be pressed at any time during a program. The program will run the desired subroutine and then continue running from where it was interrupted.

The following soft keys are created in the "softkey" sub-program: CTRL-c, CTRL-v, CTRL-a, CTRL-p, CTRL-r and CTRL-s. They are numbered 15 to 20, and instruct the computer to perform the following subroutines:

CTRL-c - plot, which activates the "plotcycle" subprogram at the end of the current cycle;

CTRL-v - volt, which allows the user to change the offset voltage of the output signal;

CTRL-a - amplitude, which allows the user to change the amplitude of the output signal;

CTRL-p - pausecycle, which sets the amplitude to zero and effectively pauses the strain cycle until CTRL-r is pressed;

CTRL-r - restart, which restarts the cycle after a pause by returning the amplitude to its original value; and

CTRL-s - stopcycle, which stops the program at the end of the current cycle.

These subroutines are found at the end of the main module.

The main module then calls the sawtooth sub-program. This sub-program runs the fatigue cycling of the tester.

The "sawtooth" sub-program first prompts the user to enter the desired offset voltage and amplitude of the reference signal to be generated, and checks that the maximum and minimum voltages requested are within the range of the output module. A value for the lag is requested (Section 8.3.1). It then prompts the user to enter the stress and strain calibration factors, and the name of the file that data should be saved to. Sawtooth then calls the

menu sub-program and the "switch (i)" sub-program. "Menu" is a sub-program which prints a menu of the available soft keys on the screen; the current offset, amplitude and cycle number, and the current status of the relay. The "switch" sub-program is called with either a 1 or a 0. If "switch" is called with a 1, then "switch" uses the Activate Digital Outputs to switch the relay to the KEPCO power supply on.

Then the principal loop (DO...LOOP UNTIL stp$="y") begins. This loop performs one complete stress-strain cycle and repeats itself until the string variable, stp$, is equal to "y".

Within the principle loop, the variables used to test for failure and the overload flag (Section 6.3.4) are set to zero. Thereafter, the three FOR...NEXT loops generate V_{ref} (Section 6.3.3). Within each loop the variable f is calculated and "voltout (f)" is called to change the output voltage. Then, "stressup (n)" or "stressdn (n)" are called to measure and store the stress LVDT voltage (Section 6.4.2). In the first two loops, the variables to test for failure are adjusted, and the overload condition is tested for.

After all three FOR...NEXT loops have been completed, ie. a cycle has been executed, the cycle counter, nc, is updated. The cycle number, amplitude, and offset are printed on the menu screen, as well as the status of the relay.

If the cycle number is less than 5, then plotflag is set to one. The plotflag is then tested, and if it is equal to 1 (ie. if nc is less than 5 or the soft key, CTRL-c, was pressed during the cycle) the "plotcycle" sub-program is called.

The "plotcycle" sub-program uses the stress data stored in the up(n) and dn(n) arrays to plot the stress-strain curve for the cycle. The axes are calculated from the stress and strain calibration variables.

Once the curve is plotted on the screen, the user may press CTRL-\ and the HERCPRIN program will dump the curve to the printer.

Pressing "y" clears the screen, and the "plotcycle" sub-program calls the "printout" sub-program.

The "printout" sub-program prompts the user to enter a string, po$. If po$ is "y" then "printout" prints the stress data to the printer.

The "sawtooth" sub-program then calculates the variables needed to test for failure from the data collected on the FOR...Next loops. It then tests whether the conditions indicating failure are met. If the conditions are met, ie. the specimen has failed , then "switch(0)", "savedata" and "printout" are called and the string variable, stp$, is set to "y".

"Switch (0)" switches the DC relay, and consequently, the KEPCO power supply, off. "Savedata" is a sub-program which saves the stress data of the cycle in a random access file. The name of the file is entered by the user at the beginning of the "sawtooth" sub-program. If the cycle is the last cycle , "savedata" saves the number of the cycle, the amplitude and offset voltage of the test and the stress and strain calibration factors to the file.

Similarly, if the overload flag is not zero, "switch (0)", "savedata" and "printout' are called and stp$ is set to "y'.

If the number of cycles is a multiple of 1000, "sawtooth" calls "savedata" and the cycle is saved to the random access file.

This completes a single cycle. If stp$ does not equal "y" then the DO...LOOP UNTIL loop is repeated. If stp$ equals "y" the program returns to the main module, the ITHACO interrupts are disabled, the ITHACO software driver file is closed and the program ends.

7.2.2 **Running the Fatigue Program**

When the program was started the desired offset voltage was entered, and a value of zero was entered for the amplitude. The stress and strain calibration factors, calculated for the specimen, were entered and the name of the file to which data should be saved was entered.

The computer switched the KEPCO power supply on and displayed the menu on the screen. With the amplitude set to zero, the computer generated a constant voltage, V_{ref}, and the lower magnet moved downwards until the strain LVDT output corresponded to V_{ref}. Then the loose jaw of the top specimen grip was screwed into place and tightened as much as possible.

With the stress LVDT output nulled, CTRL-a was pressed and the desired amplitude entered into the computer. The computer then generated a sawtooth voltage, V_{ref}, with the desired amplitude and the tester started fatiguing the specimen.

For the first five cycles, the computer plotted the cycle on the screen, so the hysteresis loop could be checked. These curves were printed out, if necessary, by pressing CTRL-\. Thereafter, the computer continued generating a sawtooth V_{ref}, saving the data every thousandth cycle and checking for overloading or failure.

The test continued until the magnets overloaded or the specimen failed. The last cycle was saved to the random access file, and the test was terminated.

The apparatus was switched off, the specimen removed from the grips and stored in a labelled glass tube.

7.3 **READING THE FATIGUE DATA**

A program, RAF.BAS, was written to read the stress-strain data stored in the random access file during the fatigue test.

The program is listed in Appendix 1. RAF.BAS is a QuickBASIC program and consists of a main module and a sub-program.

The main module declares the sub-program, dimensions the global arrays and declares the global variables. The program prompts the user to enter the name of the file wherein the data is stored, and then opens the file. It reads the number of the last cycle saved, the amplitude and offset voltage of the test, and the stress and strain calibration factors of the specimen. It prints all the information to the screen and the printer.

A FOR...NEXT loop reads each cycle from the file and stores the data in an array. The "plotcycle" sub-program is called from the loop, and plots the cycle on the screen. This sub-program is almost the same as the "plotcycle" sub-program in the FATGDIFF.BAS program. Once again, pressing CTRL-\ dumps the curve to the printer. The program then prompts the user to enter a string, prt$. If prt$ is "y", then the program prints the data to the printer.

Once all the cycles have been read, the random access file is closed and the program ends.

CHAPTER 8
TESTING OF COPPER AND GOLD SPECIMENS

8.1 INTRODUCTION

To demonstrate the present stage of development of the instrumentation of the fatigue tester, single crystals of pure copper and polycrystals of gold were fatigued to failure. The mechanical hysteresis loops are presented in Section 8.3.1. A Hitachi S-570 scanning electron microscope (SEM) was used to observe some of the characteristic features of fatigue failure in these specimens. The micrographs obtained are presented in Section 8.3.2. Attention is drawn to some problems with the specimen preparation and the operation of the tester, which remain to be resolved in the next stage of the project.

8.2 SPECIMEN PREPARATION

8.2.1 Copper Specimens

Copper single crystals prepared for tensile testing (Nathanson 1979) were available for testing. The single crystals were approximately 50mm long with a cross section of approximately 3mm × 3mm. The Schmid factor of the copper single crystals was 0.47 (Nathanson 1979). For the purposes of fatigue testing a gauge length 4mm long, with a cross-section of 3mm × 2mm, was prepared. The fatigue tester can accommodate gauge lengths from approximately 4mm to 10mm. Short gauge lengths minimise the risk of bending and buckling in compression. Figure 8.1 shows a typical copper specimen.

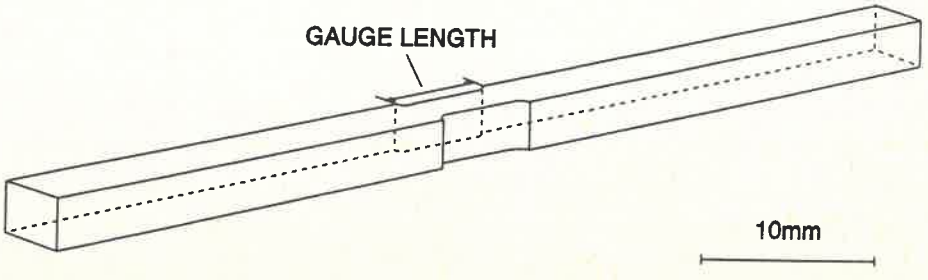

Figure 8.1 : Diagram of copper specimen showing gauge length.

The gauge length was prepared with a milling machine fitted with a 4mm diameter, 4-fluted side mill tool. Milling to a depth of 0.5mm on two opposite sides of the specimen formed a neck ~2mm wide, as shown Figure 8.1. During milling the specimen was clamped in a small stainless steel jig, designed for the purpose.

After milling, the specimens were annealed in an oxy-acetylene flame, and then quenched in cold water.It should be noted that the initial state of perfection of fatigue specimens is less important than that of specimens used for tensile tests. Fatigue into saturation always produces the same microstructure irrespective of initial perfection. The specimens were then cleaned in a solution of 40% nitric acid and 60% water to remove the soot and oxide produced during annealing. The specimens were electropolished in a 50% *ortho*-phosphoric acid - 50% distilled water solution. They were cleaned for 30 seconds at approximately 10V, and then polished for 4 minutes at 1.8V, at room temperature. They were washed first under running water, then in ethanol, and dried in a warm air stream.

The dimensions of the gauge length were measured using a travelling microscope and vernier calipers. Figure 8.2 shows the measurements taken. The length, l, is taken to be the average of the length of the two sides, as determined from measurements a,b,c and d. Note that a,b,c and d are the points where the crystal sides become parallel, so that the measured gauge length has a constant cross-section. The cross-sectional area, A, is the product of h and w, which were measured at intervals along the gauge length.

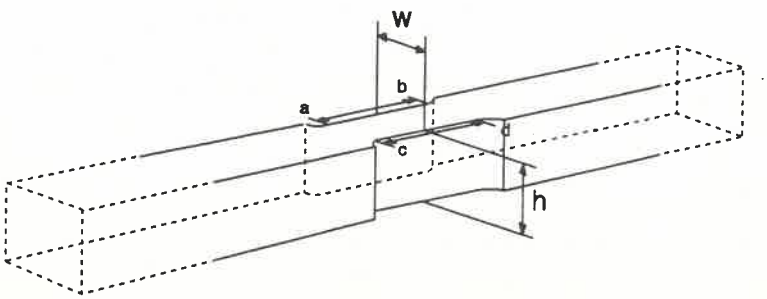

Figure 8.2 : Diagram of specimen showing measurements taken.

Using the values obtained for the length and cross-sectional area

of a specimen, the calibration factors for stress and strain were calculated as follows:

$$Stress\ cal.\ factor = \frac{(1000\mu V)\,(9.79 ms^{-2})}{(1.47\mu V/kg)\ A(mm^2)}\ MPa/mV, \qquad (8.1)$$

$$Strain\ cal.\ factor = \frac{100mV}{(0.705mV/\mu m)\ l(mm)}\ mV^{-1}. \qquad (8.2)$$

These values are entered into the computer when a test is run.

8.2.2 **Gold Specimens**

The fatigue tester was designed to hold specimens the shape and size of the copper crystals described above. It was therefore convenient to cast gold into specimens of similar size and shape. The casting technique was devised and carried out by Mr. A.C. Hill of the Physics Department Workshop.

The gold specimens were cast by the lost wax technique. This technique requires a wax model, of the exact size and shape of the desired specimen, to be made. A precision stainless steel mould was designed and machined to produce the necessary wax models. The wax models were then embedded in a substance called "investment", which is a plaster-of-paris type water-setting medium with a reinforcing agent. Attached to the wax model was a small cone shaped piece of wax, which protruded from the surface of the investment.

The solid body of the investment, with the wax model embedded in it, was subjected to a baking-out procedure. The investment was initially heated to 120°C in an oven to eliminate the wax by melting it. The temperature was then increased to 800°C for 5 hours, to expel the excess water in the investment and vapourize the remaining traces of wax. Finally, the temperature was reduced to 400°C and the investment allowed to cool to this temperature.

Next, the gold was melted under an oxy-acetylene flame in a carbon crucible. The mould was removed from the oven and the

molten gold poured into it immediately. This procedure was vacuum assisted. The mould was placed over an aperture in a metal box connected to a small vacuum pump. The vacuum pump was used to evacuate air from the mould as the gold was poured into it. This method relies on the porosity of the investment. As soon as the gold had solidified, the investment mould was quenched in cold water. When wet the investment disintegrated, so that the crystal could be withdrawn with ease.

The lost wax technique described above is a standard technique in jewellery manufacture and in dentistry.

The first specimens cast were 18ct yellow gold, which was supplied in error by Argen Precious Metals Ltd. After casting they were annealed in air in a temperature controlled oven for an hour at 800°C. The casting technique worked well but, due to the copper and silver impurities in 18ct gold, severe oxidation took place during casting and annealing. The oxide layer proved to be extremely difficult to remove. Several cleaning solutions were tried : nitric acid, aqua regia and sulphuric acid. None of these solutions removed the oxide layer, which was eventually removed using a commercially available abrasive metal polish.

A further supply of pure (fine) gold was purchased and cast as described above. Although no oxide formed during casting, the casting procedure proved unsuccessful. Several attempts were made to cast pure gold. However, the investment invariably cracked as the gold was poured in, and the specimens were incomplete or had fins where the investment had cracked. This is possibly because of the higher melting temperature of pure gold (1063°C) compared with the alloy (~950°C). Two specimens were produced and fatigued to failure. However, the first had a very unsatisfactory surface and after fatiguing, was melted down to produce the second specimen. The second specimen was hollow, but this was only discovered after it had been fatigued to failure.

The casting technique for pure gold needs to be further developed and this will be attended to in the next phase of the project.

8.3 RESULTS OF THE FATIGUE TESTS

Six copper single crystals, two 18ct gold polycrystals and two pure gold polycrystals were fatigued to failure.

8.3.1 The Mechanical Hysteresis Loops

Tests were first carried out on unmachined copper crystals to determine whether (a) the fatigue tester was working, and (b) the computer program and hardware were working properly. The program measures the stress one hundred times in each cycle and can plot a stress-strain curve on request. It was noted that at small strain amplitudes the curves exhibited signs of hysteresis. However, closer examination of these loops revealed that their shapes did not correspond to the expected shape of a loop exhibiting plastic strain. An example of one such apparent hysteresis loop is shown in Figure 8.3 (b). Increasing the strain amplitude gave rise to curves such as the loop shown in Figure 8.4(a).

In order to determine whether or not loops, like Figure 8.3 (b), were in fact genuine hysteresis loops due to plastic strain, the strain amplitude was gradually decreased until the observed loop was obscured by noise. It was found that the apparent hysteresis persisted until the stress amplitude was too small for the ITHACO lock-in amplifier to measure. This indicated that the apparent hysteresis was not due to plastic strain since, because even at the lowest strain amplitudes, the straight line associated with pure elastic strain did not materialise.

It was discovered that the apparent hysteresis at low strain amplitudes was due to a small phase lag in the response of the magnet control circuit. This lag also produced the unusual tapered loop shape shown in Figure 8.4(a) at higher strain amplitudes. The computer program was adapted to allow for this lag, which was found to be just less than 0.1 seconds. This was done by associating the control strain with the stress measured 0.1 seconds later. The adjustment was carried out after the

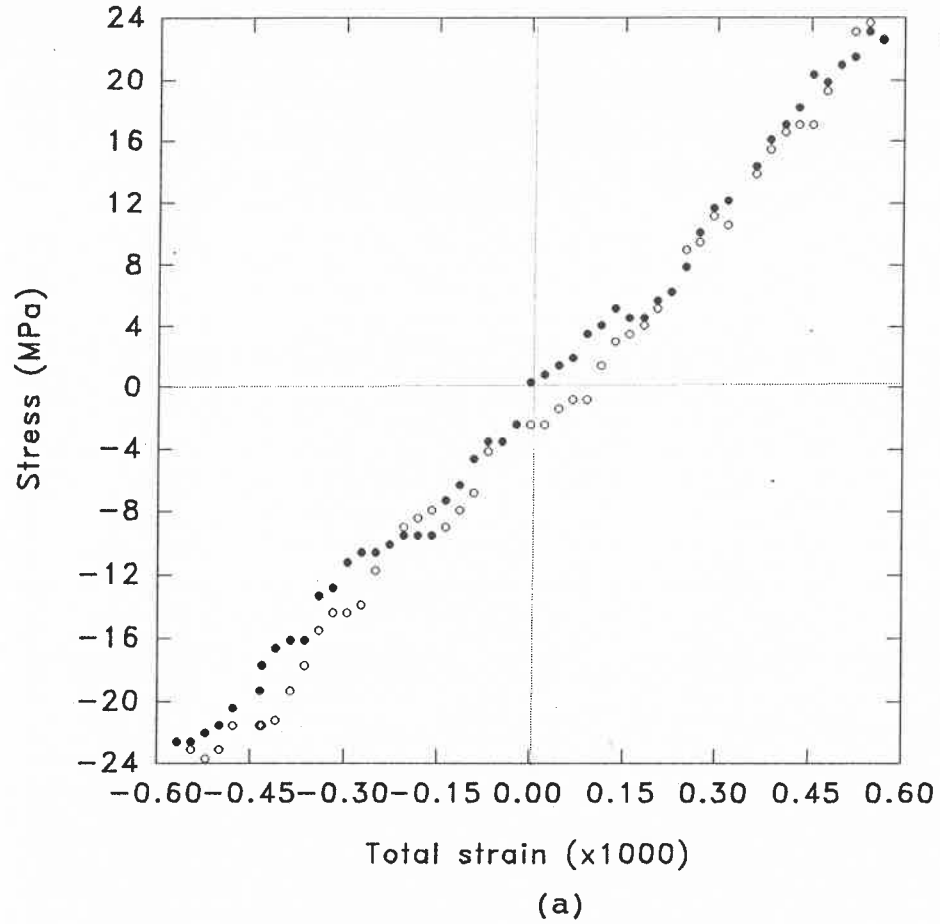

(a)

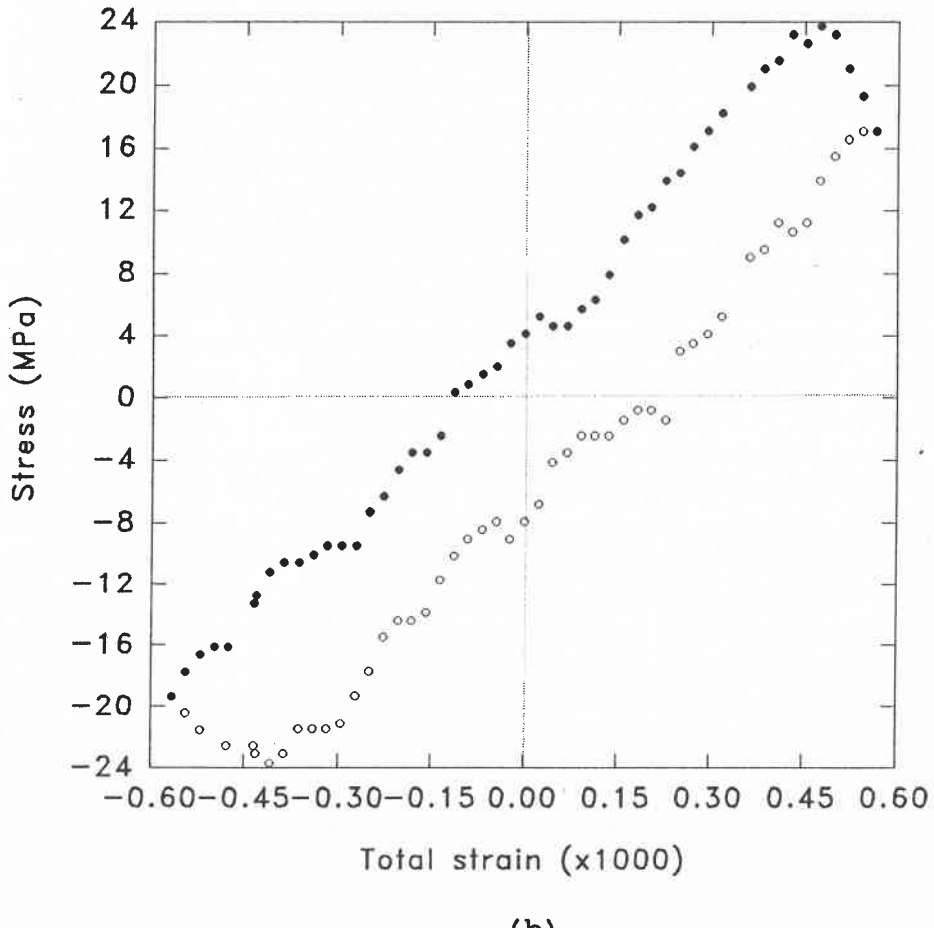

(b)

Figure 8.3 : Hysteresis loops (a) with and (b) without lag correction.

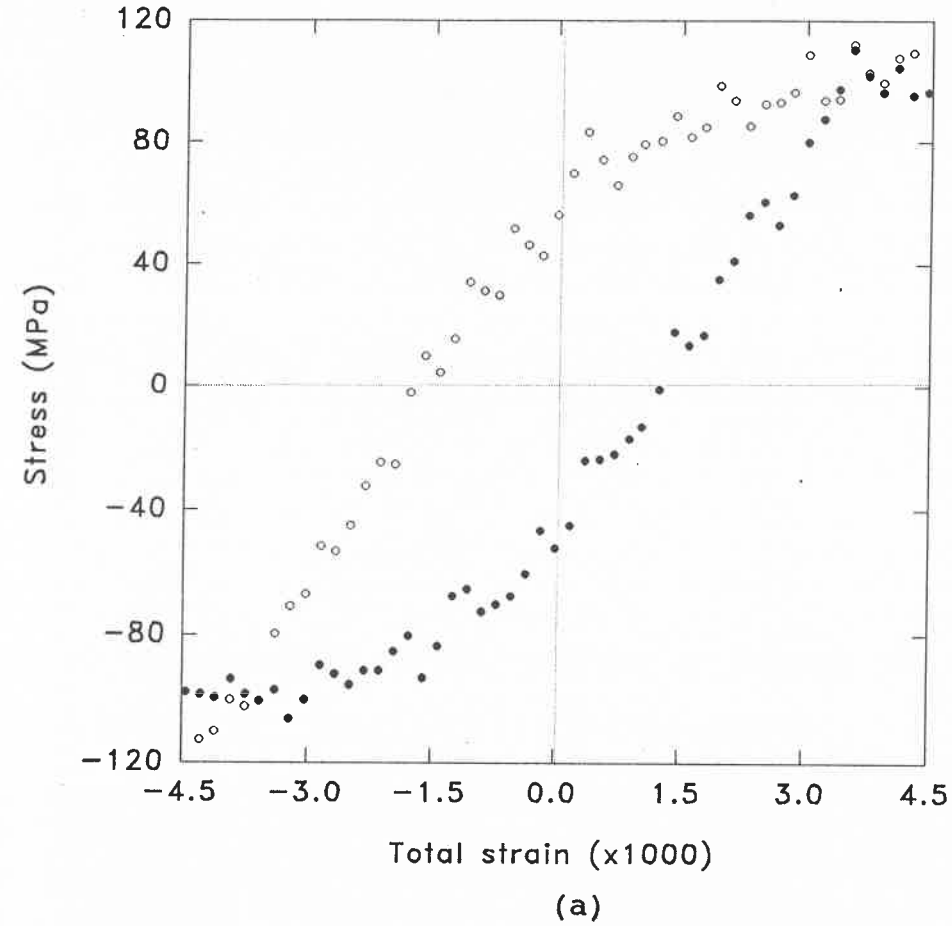

(a)

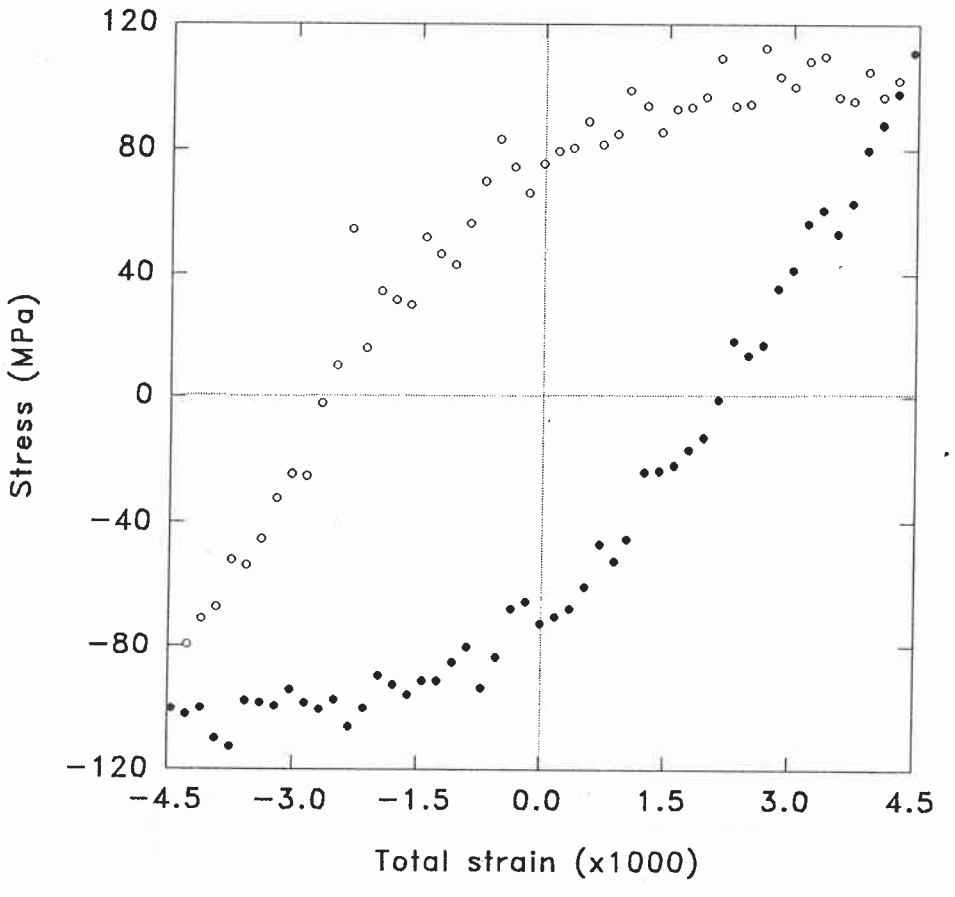

(b)

Figure 8.4 : Hysteresis loops (a) without and (b) with lag correction.

completion of a cycle. The loops in Figures 8.3(b) and 8.4(a) were corrected for lag to produce the loops in Figures 8.3(a) and 8.4(b) respectively. Thus, it can be seen that at the lower strain amplitude (Figure 8.3(a)) the stress-strain curve is a straight line indicating pure elastic strain. At the higher strain amplitude (Figure 8.4(b)) a true hysteresis loop is produced, indicating that the specimen is undergoing plastic strain (Section 1.1).

Once the lag problem was solved, copper single crystals and gold polycrystals were fatigued to failure. The fatigue data for all the specimens tested is given in Table 8.1 below. For each specimen, the axial plastic strain amplitude, ϵ_{pl}, the axial saturation stress amplitude, σ_s, the resolved plastic shear strain amplitude, γ_{pl}, the saturation shear stress amplitude, τ_s, and the fatigue life, N_f, are given. Specimens Cu1 to Cu6 were copper single crystals as described in Section 8.2.1. Specimens Au1 and Au2 were polycrystals of 18ct yellow gold, while Au3 and Au4 were polycrystals of pure gold, as described in Section 8.2.2. The specimens were fatigued in the following order: Cu1, Cu2, Cu3, Cu4, Au1, Cu5, Au2, Cu6, Au3 and Au4.

Figure 8.5 shows the hysteresis loops of a copper (Cu1) crystal; (a) early in life, N = 50 cycles, (b) later in the fatigue life, N = 4250 cycles, and (c) after failure has occurred, N_f = 32000. It can be seen that the specimen hardened before it reached the saturation stress (Section 1.2). The loops in figure 8.5(a) and (b) show the slightly flattened peaks characteristic of the plateau of the CSS curve and PSB formation. The curve in Figure 8.5(c) is characteristic of a fractured specimen. The characteristic horizontal section was used as a diagnostic indication that failure had occurred (Section 6.3.4)

The value of Young's modulus , Y, determined from the hysteresis loops of Cu1-Cu4 and Cu6, is ~40GPa. The slope of the hysteresis curve of Cu5 was 91GPa, more than twice the value obtained from

the other copper crystals. The expected Young's modulus of pure copper is 129.8GPa, more than three times larger than the average

obtained.

Table 8.1 : Data for the fatigued specimens.

Specimen	ϵ_{pl} ($\times 10^3$)	σ_s (MPa)	γ_{pl} ($\times 10^3$)	τ_s [6] (Mpa)	N_f
Cu1	1.77	103	3.77	49	32000
Cu2	3.14	115	6.88	54	19000
Cu3	0.72	98	1.54	46	177000
Cu4	2.11	108	4.49	51	32000
Cu5 [1]	0.71	270	1.51	127	19000
Cu6	3.80	150	8.09	71	11000
Au1 [2]	2.43	820	5.44	366	326000
Au2 [3]	2.00	800	4.48	357	33000
Au2 [4]	3.85	200	8.62	89	3000
Au4 [5]	4.70	169	10.53	75	1000

Notes:

[1] This crystal failed very quickly, even though the plastic strain amplitude was low. The saturation stress amplitude was very high compared with the other copper crystals fatigued.

[2] This specimen fractured below the gauge length.

[3] After this test the specimen grips were found to be out of alignment by ~1mm, so the crystal was bent.

[4] This polycrystal was badly cast and there may have been internal cracks present before fatiguing took place.

[5] This gold polycrystal was found to be hollow.

[6] The stress values are above the plateau value of 28 MPa. This may indicate that saturation was not reached before failure.

It is possible that the discrepancy between the observed and expected value of Y is the result of an error in the calibration of the stress or the strain, but the calibrations were rechecked

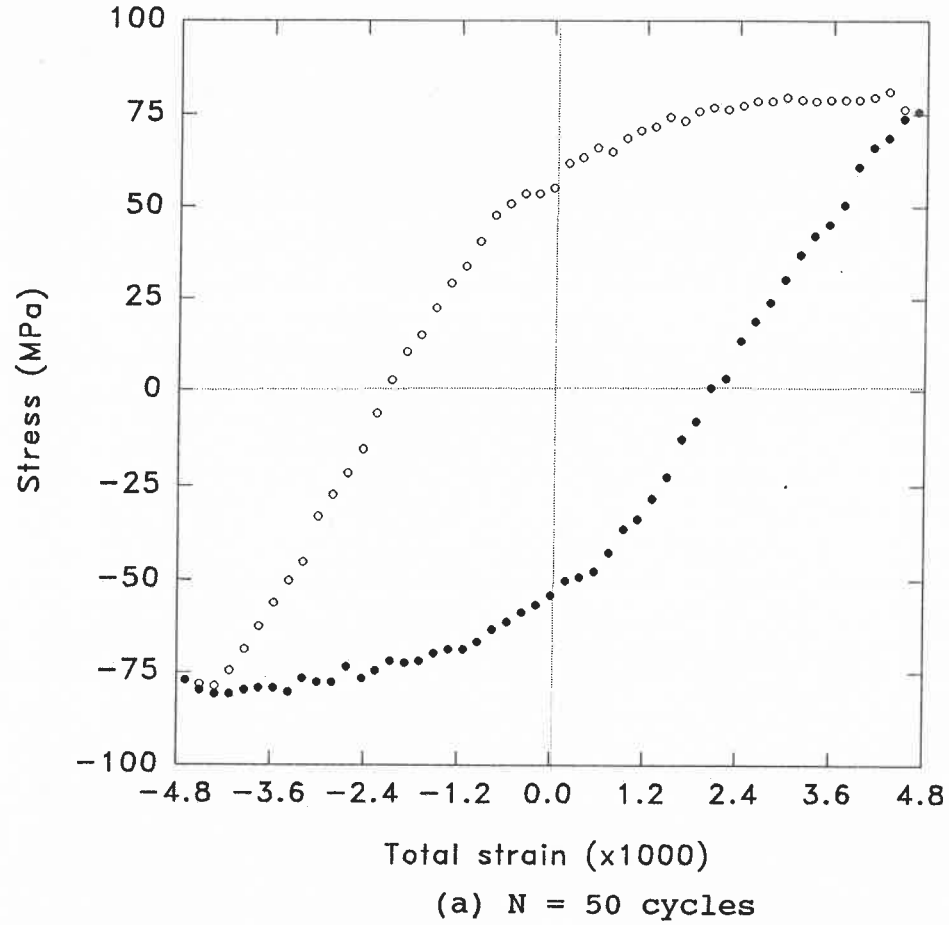

(a) N = 50 cycles

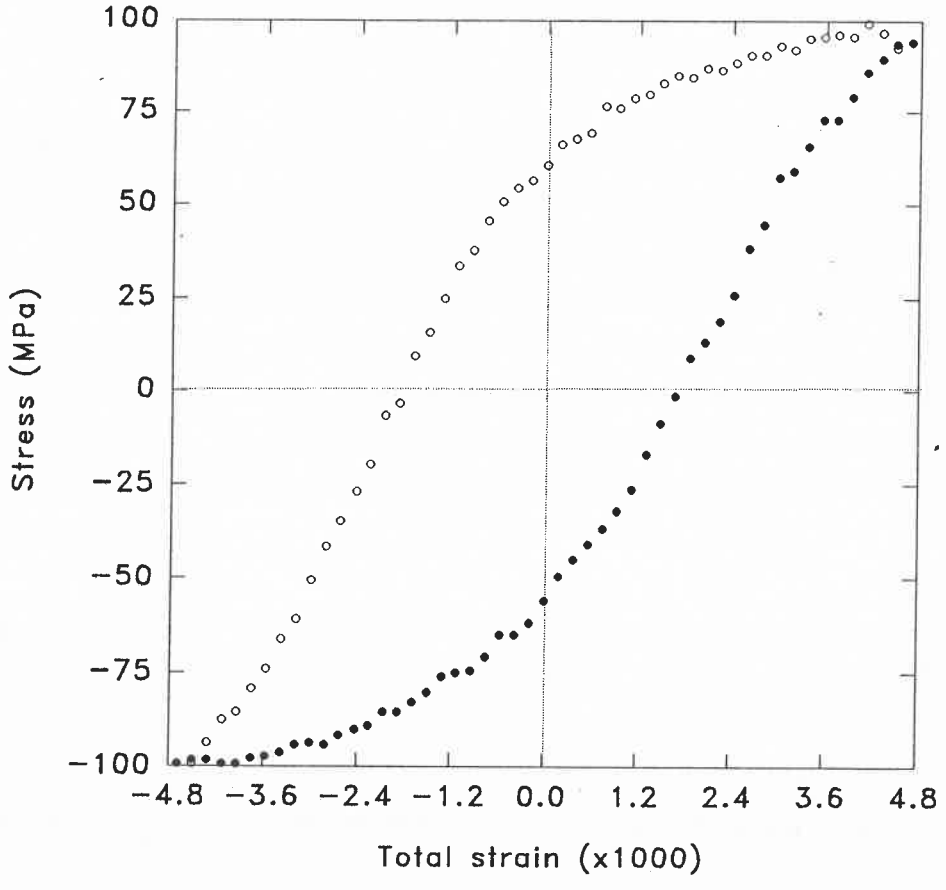

(b) N = 4250 cycles

Figure 8.5 : Hysteresis loops of copper single crystals (a) early in fatigue life, and (b) later in fatigue life.

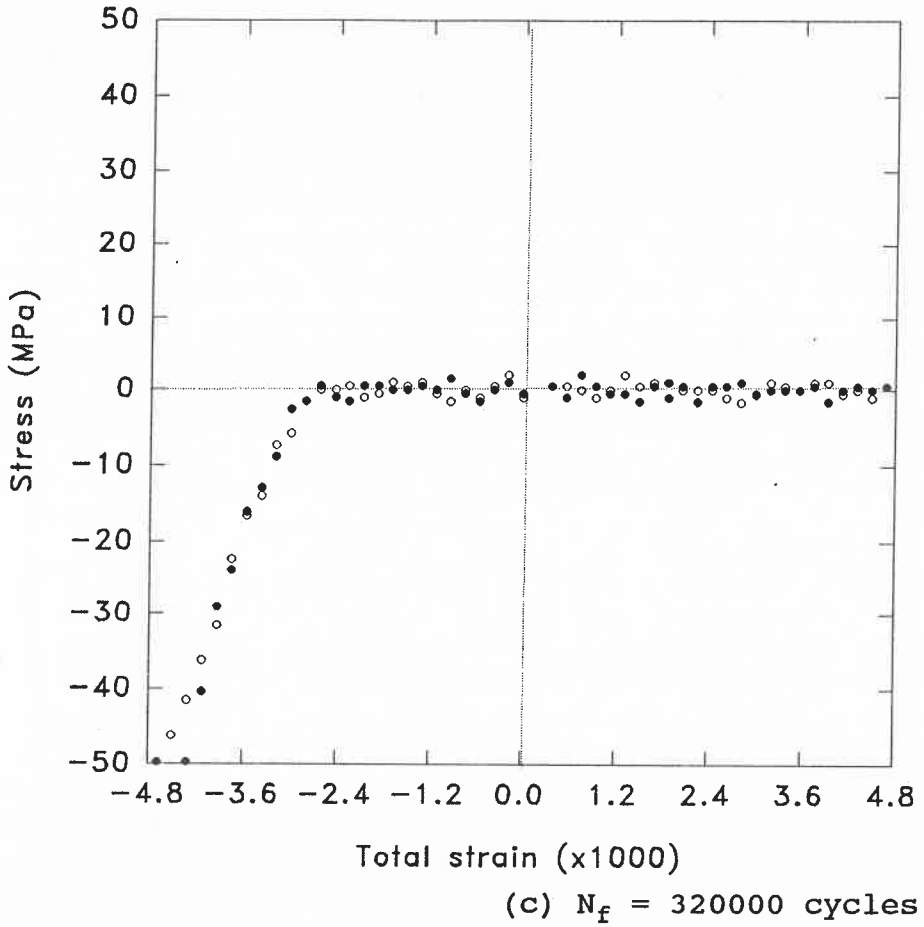

(c) N_f = 320000 cycles

Figure 8.5 (c) : Hysteresis loop of copper single crystals after failure.

and appeared to be correct. Another possible source of error is in the measurement of the gauge length of the crystals (Section 8.2.1). The gauge length was taken as the length of the milled length of constant cross-section. It has been calculated that if the gauge length were taken as the entire length of the milled neck (Figure 8.2) the error would not exceed 50%, which, although high, would not account for the discrepancy in Young's modulus. This discrepancy must be investigated further in the next phase of the project.

Figure 8.6 shows hysteresis loops of the 18ct gold polycrystal, Au1; (a) early in fatigue life, N = 15, and (b) much later in the fatigue life, N = 97000. The loads involved in fatiguing the gold alloy specimens were much higher than for copper (Table 8.1), and the hysteresis loops had a rather unexpected shape, as shown in Figure 8.6. At first glance these loops appear to be like the slim, pointed loops characteristic of fatigue in Region A of the

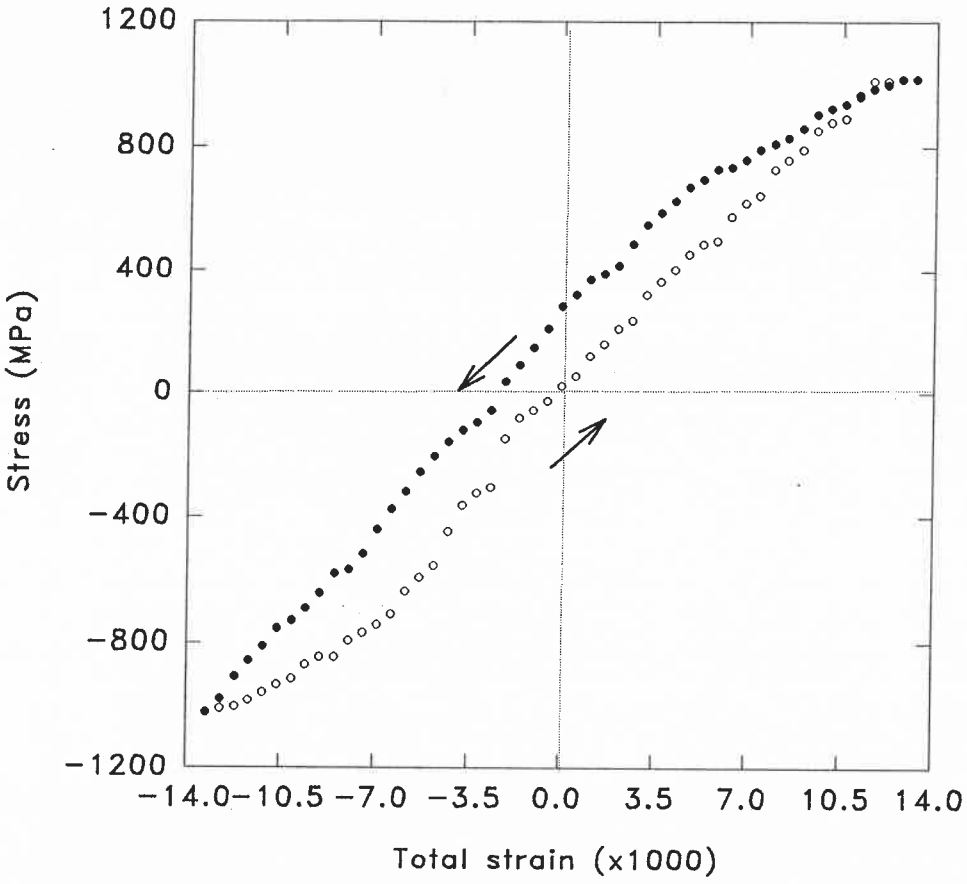

(a) N = 15 cycles

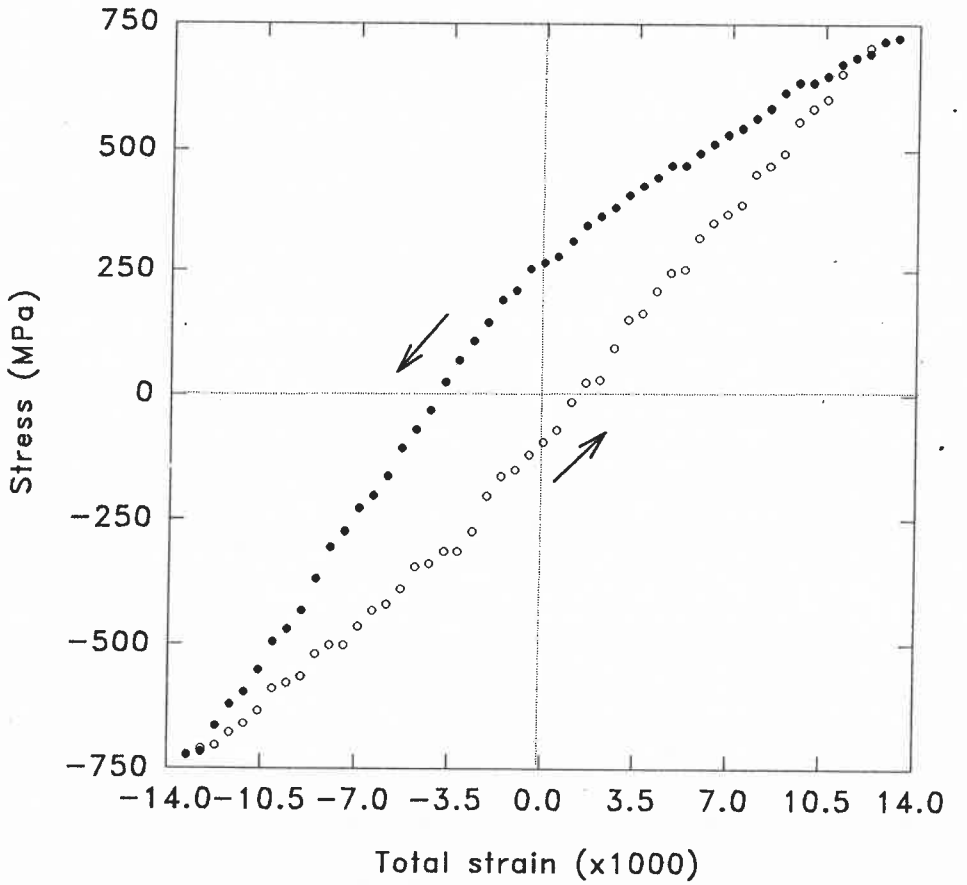

(b) N = 97000 cycles

Figure 8.6 : Hysteresis loops of 18ct gold polycrystals (a) early in fatigue life, and (b) later in fatigue life.

CSS curve of copper. However, the direction of cycling, as shown by the arrows in Figure 8.6, should be noted. This loop shape appears to indicate that, on increasing the strain amplitude, the gold becomes stiffer. However this is not physically possible. The fact that the gold alloy specimens were fatigued to failure implies that the specimens experienced some plastic strain, and the measured hysteresis curves should therefore have had the conventional shape.

It seems more likely that the anomalous shape of the observed hysteresis loops of the gold alloy may have been due to the elastic response of the fatigue tester to stresses and strains greatly in excess of the design parameters. The tester was designed to fatigue pure copper crystals (maximum stress amplitude of ~300MPa), so it is likely that the loads involved in fatiguing 18ct gold (~800MPa), which has a much higher yield stress than pure copper or gold, would result in overloading of the tester.

This overloading may have been the cause of the misalignment of the specimen grips, which was discovered after Au2 had been fatigued. It should be noted that Cu5 was fatigued after Au1 and before Au2. Thus, it is possible that the atypical behaviour of Cu5 (Table 8.1) was caused by bending due to the misalignment of the grips. The grips were realigned before Cu6 was fatigued.

The pure gold crystals that were fatigued had hysteresis loops similar to those of the copper crystals, with stress amplitudes similar to those of the copper tests. Thus, it would appear that the fatigue of pure gold specimens, if properly cast, would be well within the capabilities of the tester, and could prove a useful comparison with the fatigue of copper crystals. Ideally, pure gold single crystals would provide the best comparison with single crystals of pure copper, but their cost is prohibitive.

The hysteresis loops of most of the copper crystals and of the two pure gold crystals were found to be very noisy, as a result of noise in the stress measurements. A possible solution would be to try and reduce the noise in the stress measurement (which

was apparent during calibration) or to take the average of several hysteresis loops.

8.3.2. **Surface Observations**

Scanning electron micrographs were taken of the surfaces of the fatigued specimens at various magnifications. Micrographs showing features of interest are presented below.

All of the copper single crystals showed PSB and extrusion formation to varying degrees of intensity and development. Figure 8.7 shows well-developed extrusions forming along PSBs, on Cu1. Figure 8.8 shows extrusions along PSBs and micro-PSBs (Section 1.3.4), separated by areas relatively free of surface slip, on Cu3, which was fatigued at a lower plastic strain amplitude than Cu1. There was a higher PSB density evident on the surface of Cu1 than on Cu3, which would be expected because of the higher plastic strain amplitude of the Cu1 test.

Figure 8.9 shows extrusions on a high index face of the Cu2 single crystal, adjoining a side parallel to the cross glide plane. This specimen was fatigued at a higher plastic strain amplitude than Cu1 or Cu3, and the extrusions shown fall in a very wide PSB, or a collection of smaller PSBs not separated by matrix structure. It should be noted that Figure 8.9 is at the same magnification (× 2750) as Figure 8.7.

Figure 8.10 shows extrusions along PSBs which traverse a twinned region on the surface of Cu1. The presence of the twin indicates that some recrystallization of Cu1 must have occurred during annealing.

Figures 8.11 and 8.12 are micrographs of the surface of Cu5, and show grain boundaries, which indicate that Cu5 had also recrystallized on annealing. Both Figure 8.11 and 8.12 show intergranular cracks along grain boundaries and Figure 8.12, which is at a higher magnification than Figure 8.11, shows PSBs traversing as twinned boundary. It seems that the annealing

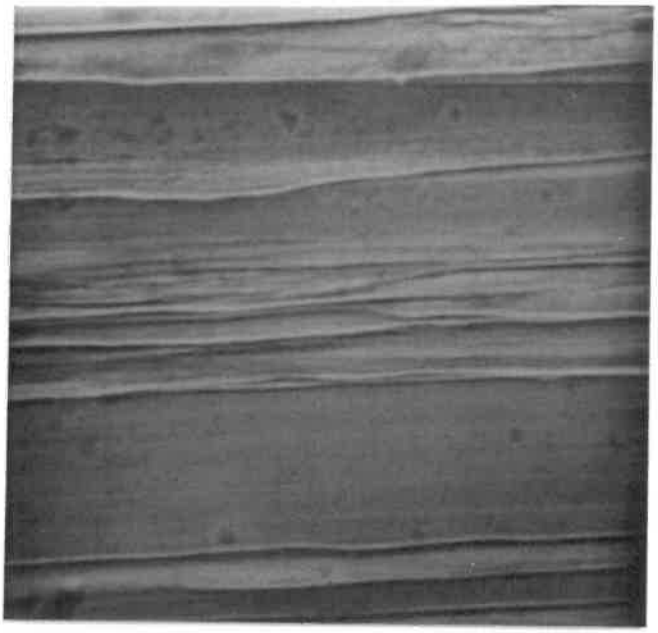

Figure 8.7 : Micrograph showing extrusions along PSBs in Cu1 (×2750).

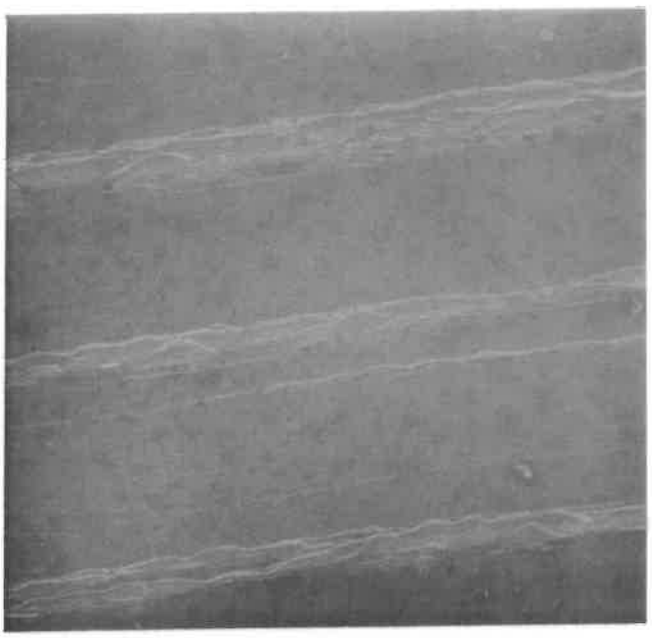

Figure 8.8 : Micrograph showing extrusions along PSBs in Cu3 (×925).

Figure 8.9 : Micrograph showing extrusions on a high index face of Cu2 (×2750).

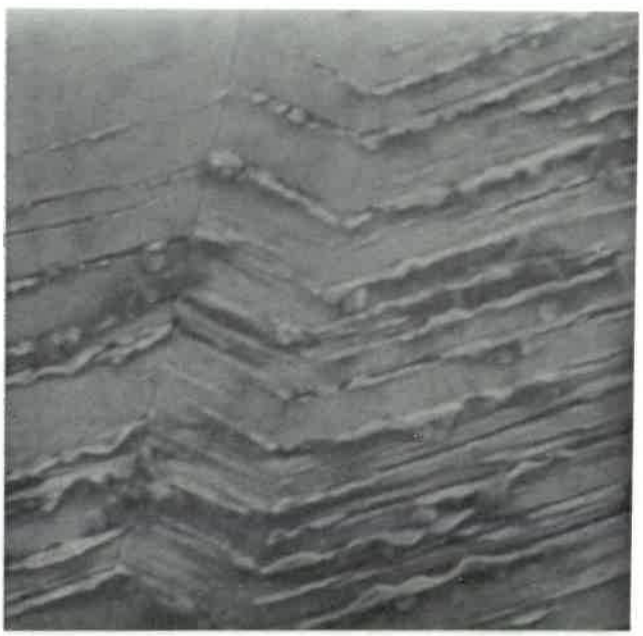

Figure 8.10 : Micrograph showing PSBs traversing a narrow twin in Cu1 (×2300).

Figure 8.11 : Micrograph showing grain boundaries and intergranular cracks on Cu5 (×1200).

Figure 8.12 : Micrograph showing intergranular cracks in Cu5 (×2300).

Figure 8.13 : Micrograph showing PSBs connected by secondary slip traces on Cu3 (×1850).

Figure 8.14 : Micrograph showing two active intersecting slip systems on Cu6 (×3200).

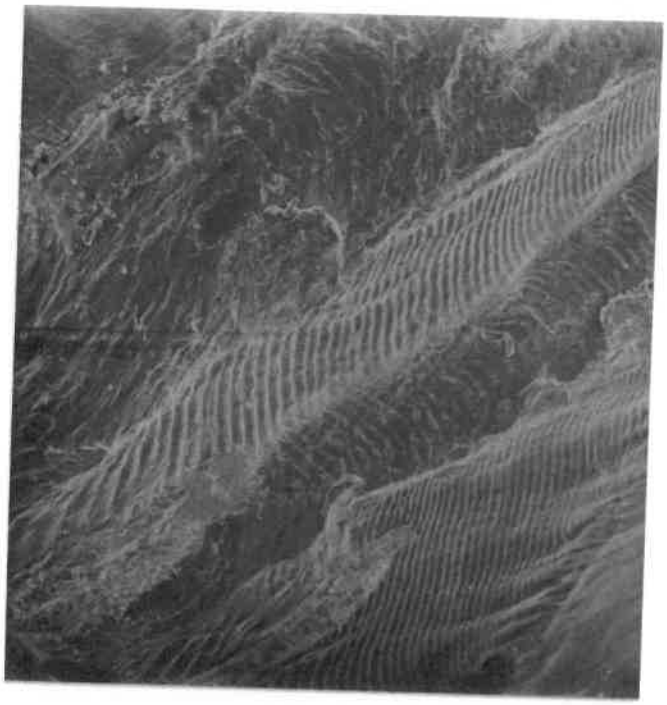

Figure 8.15 : Micrograph showing fatigue striations on the fractured surface of Cu2 (×325).

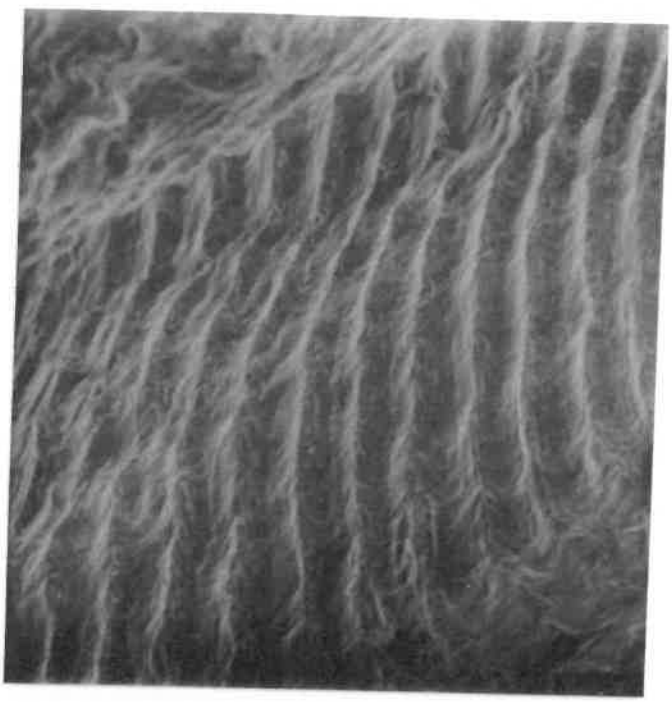

Figure 8.16 : Micrograph showing fatigue striations on the fractured surface of Cu2 (×1850).

process used should be revised to prevent such recrystallization in further investigations.

Figure 8.13 shows PSBs connected by secondary slip on the surface of Cu3. There appear to be long cracks or deep intrusions (I) associated with some of the PSBs. Figure 8.14 shows PSBs on two intersecting slip systems on the surface of Cu6, which was fatigued at a high plastic strain amplitude (Table 8.1). The extrusions do not appear to be very well developed, although the PSBs are closely spaced. This may be a result of the high strain amplitude and the short life time.

Figures 8.15 and 8.16 show the fractured surface of the copper single crystal, Cu2. They both show striations characteristic of fatigue failure. Figure 8.16 is at ~6× the magnification of Figure 8.15.

Figures 8.7 to 8.10 and Figure 8.13 and 8.14 show clearly the existence of PSBs and extrusions in the fatigued copper specimens, while Figure 8.15 and 8.16 show characteristic fatigue striations on the fracture surface.

Figures 8.17 and 8.18 show the fractured surface of the 18ct yellow gold specimen, Au1. Figure 8.17 is a low magnification (×30) micrograph of the fracture and shows that the specimen fractured below the gauge length. Figure 8.18 is a higher magnification micrograph of a portion of the fractured surface. No fatigue striations were visible, even at higher magnifications.

Figure 8.19 shows the surface of the Au2 gold alloy specimen. This micrograph is at the same magnification as Figures 8.7 and 8.9, but no PSBs are visible. Only very fine lines are visible, which are possibly fine slip lines. It should be noted, however, that in polycrystals PSBs usually form only in those surface grains orientated for single slip (Mughrabi 1984).

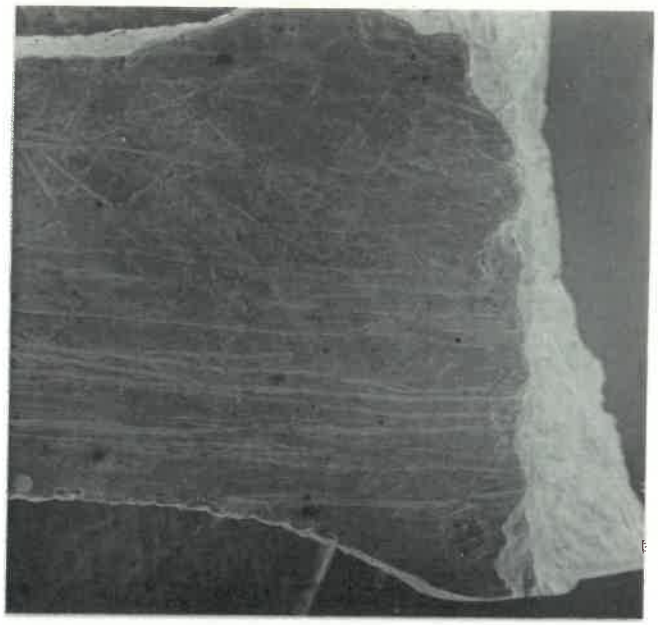

Figure 8.17 : Micrograph showing the fractured surface of Au1, which failed beyond the gauge length (×30).

Figure 8.18 : Micrograph showing a portion of the fractured surface of Au1 (×1000).

Figure 8.19 : Micrograph showing possible fine slip on the surface of Au2 (×2750).

8.4 **CONCLUSIONS**

The results presented demonstrate the present capabilities of the electromagnetic fatigue tester. The tester has been fully instrumented and the strain amplitude control could be easily adapted by suitable programming. In its present state, the tester is capable of fatiguing soft specimens, such as pure copper and pure gold, at constant total strain amplitude. Alloys such as the 18ct gold tested are however beyond the design capabilities of the tester.

In the next phase of this project it is intended to make a comparison of surface observations and hysteresis loops between pure copper and pure gold to determine what effect environment has on fatigue life and the fundamental mechanisms of fatigue. This will require an improvement of the noise levels of the hysteresis loops. This could perhaps be achieved by averaging between successive hysteresis loops, or between successive points on individual loops (statistical smoothing).

REFERENCES

Bairstow, L. (1910). *Philosophical Transactions of the Royal Society* 210 : 1910.

Barnett, N. (1988). *MSc. Thesis*. University of Natal : Pietermaritzburg.

Basinski, Z.S. (1959). *Philosophical Magazine* 4 : 393.

Basinski, S.J., Basinski, Z.S. & Howie, A. (1969). *Philosophical Magazine* 19 (161) : 899-924.

Basinski, Z.S., Korbel, A.S. & Basinski, S.J. (1980). *Acta Metallurgica* 28 (2) : 191-207.

Basinski, Z.S. & Basinski, S.J. (1982). In *Strengths of Metals and Alloys : Proceedings of the Sixth International Conference on the Strength of Metals and Alloys (ICSMA 6)*, ed. Gifkins, R.C., Vol. 2, pgs. 819-824. Pergamon Press : Oxford.

Basinski, Z.S. & Basinski, S.J. (1984a). In *Fundamentals of Deformation and Fracture : Eschelby Memorial Symposium*, ed Bilby, B.A., Miller, K.J. & Willis, J.R., pgs. 583-594. Cambridge University Press : Cambridge.

Basinski, Z.S. & Basinski, S.J. (1984b). *Scripta Metallurgica* 18 : 851-856.

Basinski, Z.S. & Basinski, S.J. (1985a). *Acta Metallurgica* 33 (7) : 1307-1317.

Basinski, Z.S. & Basinski, S.J. (1985b). *Acta Metallurgica* 33 (7) : 1319-1327.

Basinski, Z.S. & Basinski, S.J. (1988). In *Strengths of Metals and Alloys : Proceedings of the Eighth International*

Conference on the Strength of Metals and Alloys (ICSMA 8), ed. Kettunen, P.O., Lepistö, T.K. & Lehtonen, M.E., Vol. 1, pgs. 13-24. Pergamon Press : Oxford.

Basinski, Z.S. & Basinski, S.J. (1989). *Acta Metallurgica* 37 (12) : 3263-3273.

Charsley, P. (1981). *Materials Science and Engineering* 47 : 181.

Coffin, L.F. (1954). *Transactions of the American Society of Mechanical Engineers* 76 : 923.

Cortie, M.B. (1989). In *Advances in Fracture Research. Proceedings of the Seventh International Conference on Fracture (ICF7)*, ed. Salamara, K., Ravi-Chandar, K., Taplin, D.M.R. & Rama Rao, P., Vol. 2, pgs 1385-1393. Pergamon Press : Oxford.

Cottrell, A.H. & Hull, D. (1957). *Proceedings of the Royal Society* Series A, 242 : 211.

Descoins, M.J. (1992). *MSc Thesis*. University of Natal : Pietermaritzburg.

Essmann, U. & Mughrabi, H. (1979). *Phiosophical Magazine A* 40 : 731.

Essmann, U., Göselle, U. & Mughrabi, H. (1981). *Philosophical Magazine A* 44 : 405.

Ewing, J.A. (1889). *Reports. British Association* pg. 502.

Ewing, J.A. & Humfrey, J.C.W. (1903). *Philosophical Transactions of the Royal Society* Series A, 200 : 241-250.

Ewing, J.A. & Rosenhain, W. (1899). *Proceedings of the Royal Society* 67 : 85.

Feltner, C.E. & Laird, C. (1967). *Acta Metallurgica* 15 : 1621 &

1632.

Finney, J.M. & Laird, C. (1975). *Philosophical Magazine* 31 : 339-336.

Forsyth, P.J.E. (1953). *Nature* 171 : 172.

Gough, H.J. (1926). *The Fatigue of Metals*. Benn : London.

Grosskreutz, J.C. & Bowles, C.Q. (1965). In *Environment-Sensitive Mechanical Behaviour : Metallurgical Society Conference*, eds. Westwood, A.R.C. & Stoloff, N.S., Vol. 35, pgs. 67-105. Gordon & Breach : New York.

Helgeland, O. (1965). *Journal of the Institute of Metals* 93 : 570.

Jackson, P.J. (1989). *Materials Science and Engineering A* 119 : 1-6.

Kahn, M. (1970). *The Versatile Op Amp*, Chapters 1-5. Holt, Rinehart and Winston, Inc. : New York.

Laird, C. (1983). In *Dislocations in Solids*, ed. Nabarro, F.R.N., Vol. 6, pg. 56. North Holland Publishing Co. : Holland.

Laird, C., Charsley, P. & Mughrabi, H. (1986). *Materials Science and Engineering* 81 : 433-450.

Lepinoux, J. & Kubin L.P. (1985). *Philosophical Magazine A* 51 : 675-696.

Lisiecki, L.L. & Pedersen, O.B. (1991). *Acta Metallurgica Materialia* 39 (7) : 1449-1456.

Lukáš, P., Klesnil, M. & Polák, J. (1974). *Materials Science and Engineering* 15 : 239.

Ma, B. & Laird, C. (1989a) *Acta Metallurgica* 37 : 325-336.

Ma, B. & Laird, C. (1989b). *Acta Metallurgica* 37 : 337-348.

Manson, S.S. (1954). *National Advisory Committee of Aeronautics* Technical note 2933.

Mott, N.F. (1958). *Acta Metallurgica* 6 : 195.

Mughrabi, H. (1978). *Materials Science and Engineering* 33 : 207-223.

Mughrabi, H., Ackermann, F. & Herz, K. (1979). In *Fatigue Mechanisms*, ed. Fong, J.T., ASTM-STP 675, pgs. 69-105. American Society of Testing and Materials : Philadelphia.

Mughrabi, H. (1980). In *Strengths of Metals and Alloys : Proceedings of the Fifth International Conference on the Strength of Metals and Alloys (ICSMA 5)*, ed. Haasen, P., Gerold,V. & Kostorz, G., Vol. 3, pg. 1615. Pergamon Press : Oxford.

Mughrabi, H. & Wang, R. (1981). In *Proceedings of the Second Risø International Symposium on Metallurgy and Materials Science: Deformation of Polycrystals*, eds. Hansen, N., Horsewell, A., Leffers, T. & Lilholt, H., pg. 87. Risø National Laboratory : Roskilde.

Mughrabi, H. (1983). *Acta Metallurgica* 31 : 1367.

Mughrabi, H., Wang, R., Differt, K. & Essmann, U. (1983). In *Fatigue Mechanisms: Advances in Quantitative Measurement of Physical Damage*, eds. Lankford, J., Davidson, D.L., Morris, W.L. & Wei, R.P., ASTM-STP 811, 5. American Society of Testing and Materials : Philadelphia.

Mughrabi, H. (1984). In *Dislocations and Properties of real Materials*, ed. Loretto, M.H., pgs. 244-262. Bristol : J.W. Arrowhead Ltd.

Nathanson, P.D.K. (1979). *PhD. Thesis*. University of Natal :

Pietermaritzburg.

Neubert, H.K.P. (1975).*Instrument Transducer: an Introduction to their Performance and Design*. Clarendon Press : Oxford.

Neumann, P. (1983). In *Physical Metallurgy* eds. Cahn. R.N. & Haasen, P., Vol. 2, pg. 1553. Elsevier : Amsterdam.

Pohl, K., Mayr, P. & Mauerauch, E. (9180). *Scripta Metallurgica* 14 : 1167.

Pedersen, O.B. & Winter, A.T. (1982). *Acta Metallurgica* 30 : 711.

Pratt, J. (1967). *Acta Metallurgica* 15 : 319.

Roberts, W.N. (1969). *Philosophical Magazine* 20 : 675.

Snowden, K.U. (1963). *Journal of Applied Physics* 34 : 3150.

Thompson, N., Wadsworth, N.J. & Louat, N. (1956). *Philosphical Magazine* 1 : 113.

Thompson, N. & Wadsworth, N.J. (1958). *Advances in Physics* 7 : 72.

Usher, M.J. (1985).*Sensors and Transducers*. Macmillan : Hong Kong.

Wadsworth, N.J. & Hutchings, J. (1958). *Philosophical Magazine* 3 : 1154-1166.

Winter, A.T. (1974). *Philosophical Magazine* 30 : 719-738.

Winter, A.T., Pedersen, O.B. & Rasmussen, K.V. (1981). *Acta Metallurgica* 29 : 735.

Wood, W.A. & Segall, R.L. (1957). *Bulletin. Institute of Metals* 3 : 160.

Yamamoto, A. & Imura, T. (1981). In *Dislocation Modelling of Physical Systems*, eds. Ashby, M.F., Bullough, R., Hartley, C.S. & Hirth J.P., pg. 75. Pergamon Press : Oxford.

APPENDIX 1
COMPUTER PROGRAMS

This appendix contains the program listings of the two computer programs described in Chapters 6 and 7.

The first program, FATGDIFF.BAS, is used to run the fatigue tester. It generates the reference output voltage for the magnet control circuit and reads the stress from the ITHACO lock-in amplifier. It also generates hysteresis loops, saves data, and controls the dc relay for the Kepco power supply.

The second program, RAF.BAS, retrieves the data saved in random access files by the first program. It plots the corresponding hysteresis loops and prints the data.

```
DECLARE SUB init ()
DECLARE SUB lagcalc ()
DECLARE SUB menu ()                    '
DECLARE SUB plotcycle ()               'Declaring
DECLARE SUB printout ()                'subprograms
DECLARE SUB readstress (rs)            '
DECLARE SUB savedata ()
DECLARE SUB sawtooth ()
DECLARE SUB sendit ()
DECLARE SUB setup ()
DECLARE SUB softkey ()
DECLARE SUB startup ()
DECLARE SUB stressdn (D)
DECLARE SUB stressup (u)
DECLARE SUB switch (x)
DECLARE SUB voltout (v)
DECLARE SUB OPTOWARE (a%, b%, C%, BYVAL D%, BYVAL e%, BYVAL f%)

DIM SHARED posi%(15)                   '
DIM SHARED info%(15)                   'Dimensioning
DIM SHARED modi%(1)                    'arrays
DIM SHARED volt(20)                    '
DIM SHARED up(50)
DIM SHARED dn(50)
DIM SHARED upl(50)
DIM SHARED dnl(50)

COMMON SHARED addr%, cmd%, info%(), posi%()     '
COMMON SHARED modi%(), errs%                    'Setting
COMMON SHARED addr1%, addr2%, module%           'global
COMMON SHARED volt(), up(), dn()                'variables
COMMON SHARED upl(), dnl()                      '
COMMON SHARED nc, ov, aml, b, t
COMMON SHARED lag
COMMON SHARED stp$, kepco$, file$
COMMON SHARED plotflag
COMMON SHARED stresscal, straincal

CALL startup                    'open files

CALL init                       'initialize parameters

CALL setup                      'set initial conidtions

CALL softkey                    'set softkeys

CALL sawtooth                   'runs tester

IOCTL #2, "DSI "
CLOSE #2

END


plot:  LET plotflag = 1          'sets flag to plot
RETURN


volt:
        flag = 0                'changes offset voltage
        DO
                CLS
                LOCATE 5, 17
                INPUT "New offset voltage (-10V to 10V):"; nov
                nb = nov - aml
```

```
                nt = nov + aml
                IF nb >= -10 AND t <= 10 THEN flag = 1
        LOOP UNTIL flag = 1
        LET ov = nov
        LET b = ov - aml
        LET t = ov + aml
        CLS
        CALL menu
RETURN

amplitude:                          'changes strain amplitude
        flag = 0
        DO
                CLS
                LOCATE 5, 17
                INPUT "New amplitude:"; naml
                nb = ov - naml
                nt = ov + naml
                IF nb >= -10 AND nt <= 10 THEN
                        IF naml >= 0 THEN flag = 1
                END IF
        LOOP UNTIL flag = 1
        LET aml = naml
        LET b = ov - aml
        LET t = ov + aml
        CLS
        CALL menu

RETURN

pausecycle:                         'sets amplitude to zero
        LET oldaml = aml
        LET aml = 0
        LET b = ov - aml
        LET t = ov + aml
        CLS
        CALL menu
RETURN

restart:                            'resets amplitude to
        LET aml = oldaml            'original value
        LET b = ov - aml
        LET t = ov + aml
        CLS
        CALL menu
RETURN

stopcycle:                          'sets flag to stop
        INPUT "Do you want to stop the program? (y/n):"; stp$
        CLS
RETURN

SUB init                'initialises parameters
        errs% = 0
        FOR n = 0 TO 15
                posi%(n) = 0
                info%(n) = 0
                IF n = 0 OR n = 1 THEN modi%(n) = 0
        NEXT n
        addr1% = 0
        addr2% = 255
        module% = 0
END SUB

SUB lagcalc             'adjusts values for lag
        FOR nl = 1 TO 50
```

```
            IF (50 - nl) >= lag THEN upl(nl) = up(nl + lag)
            IF (50 - nl) < lag THEN upl(nl) = dn(100 - lag - nl)
        NEXT nl

        FOR nl = 0 TO 49
            IF nl >= lag THEN dnl(nl) = dn(nl - lag)
            IF nl < lag THEN dnl(nl) = up(lag - nl)
        NEXT nl

END SUB

SUB menu                    'prints menu on screen
        LOCATE 1, 17
        PRINT "#######  F A T I G U E   T E S T  #######"
        LOCATE 10, 17
        PRINT "################ M E N U ################"
        LOCATE 11, 17
        PRINT " (1) Change the output voltage:   CTRL-v"
        LOCATE 12, 17
        PRINT " (2) Change the amplitude:        CTRL-a"
        LOCATE 13, 17
        PRINT " (3) Pause:                       CTRL-p"
        LOCATE 14, 17
        PRINT " (4) Re-start cycle:              CTRL-r"
        LOCATE 15, 17
        PRINT " (5) Stop:                        CTRL-s"
        LOCATE 16, 17
        PRINT " (6) Plot a cycle:                CTRL-c"
        LOCATE 18, 17
        PRINT "No. of cycles ="
        LOCATE 19, 17
        PRINT "Offset voltage ="
        LOCATE 20, 17
        PRINT "amplitude ="
        LOCATE 18, 42
        PRINT "Kepco:"

END SUB

SUB plotcycle               'plots a hysteresis loop
        SCREEN 3
        CLS

        LET hi = -10
        LET low = 10
        FOR hl = 0 TO 50
                IF hl > 0 THEN
                        IF up(hl) > hi THEN hi = up(hl)
                        IF up(hl) < low THEN low = up(hl)
                END IF
                IF hl < 50 THEN
                        IF dn(hl) < low THEN low = dn(hl)
                        IF dn(hl) > hi THEN hi = dn(hl)
                END IF
        NEXT hl

        LET mid = (hi + low) / 2
        LET multiply = 170 / (hi - mid)

        CALL lagcalc

        FOR p = 0 TO 50
                LET xposi = p * 14 + 10
                IF p > 0 THEN
                    LET yposi = 172 - (upl(p) - mid) * multiply
                    LINE (xposi, yposi)-(xposi, yposi)
```

```
            CIRCLE (xposi, yposi), 3
        END IF
        IF p < 50 THEN
            LET yposi = 172 - (dnl(p) - mid) * multiply
            LINE (xposi, yposi)-(xposi, yposi)
            CIRCLE (xposi, yposi), 2
        END IF
NEXT p

LINE (10, 172)-(710, 172)
LINE (360, 1)-(360, 346)

PRINT "Ampl.="; aml; "V"
PRINT "Offset ="; ov; "V"
PRINT "Cycle no.="; nc
PRINT "Lag ="; lag
LOCATE 1, 27
PRINT "Stress (MPa)"
LOCATE 12, 1
PRINT "Strain (*1000)"

LET mv = multiply / 20000
FOR mark = 1 TO 20
        IF (mark * mv) <= 170 THEN
            ymarkpos = 172 - mark * mv
            LINE (355, ymarkpos)-(365, ymarkpos)
            LET ypos = ymarkpos / 14 + .5
            LOCATE ypos, 42
            LET yscale = mark * .05 * stresscal
            PRINT USING "####.###"; yscale
            LET ymarkpos = 172 + mark * mv
            LINE (355, ymarkpos)-(365, ymarkpos)
            LET ypos = ymarkpos / 14 + .5
            IF ypos + .5 < 24 THEN
                LOCATE ypos, 42
                PRINT USING "####.###"; -1 * yscale
            END IF
        END IF
        IF mark = 1 AND mv > 170 THEN
            LINE (355, 2)-(365, 2)
            LOCATE 1, 42
            PRINT USING "####.###"; (hi - mid) * stresscal
            LINE (355, 342)-(365, 342)
            LOCATE 23, 42
            PRINT USING "####.###"; (low - mid) * stresscal
        END IF
        NEXT mark

FOR xmark = 0 TO 4
        IF xmark <> 2 THEN
            xmarkpos = 10 + xmark * 175
            LINE (xmarkpos, 168)-(xmarkpos, 176)
            xpos = xmarkpos / 9 + .5 - xmark - 1
            LOCATE 14, xpos
            LET xscale = (x - 2) / 2 * aml * straincal
            PRINT USING "###.###"; xscale
        END IF
NEXT xmark

DO
LOOP UNTIL INKEY$ = "y"
CLS
CALL printout
LET plotflag = 0
CLS
CALL menu
```

```
END SUB

SUB printout              'prints out data of the cycle plotted
        CLS
        INPUT "Would you like to print out the cycle? (y/n)"; po$
        IF po$ = "y" THEN
           LPRINT "Ampl.="; aml; "V"
           LPRINT "Offset ="; ov; "V"
           LPRINT "Cycle no.="; nc
           LPRINT "Lag ="; lag
           LPRINT "Stress cal ="; stresscal
           LPRINT "Strain cal ="; straincal
           LPRINT
           FOR prnt = 1 TO 50
              LPRINT prnt; ")"; TAB(7);
              LPRINT USING "#.####"; upl(prnt) * stresscal; TAB(25);
              LPRINT prnt + 50; ")"; TAB(32);
              LPRINT USING "#.####"; dnl(50 - prnt) * stresscal
           NEXT prnt
        END IF
        CLS
END SUB

SUB readstress (rs)       'reads the stress from the ITHACO
        IOCTL #2, "CXC! "
        v$ = IOCTL$(#2)
        L = LEN(v$)
        p = INSTR(v$, " ")
        r$ = RIGHT$(v$, L - p)
        rs = -1 * VAL(r$)
END SUB

SUB savedata              'saves the data to a random acess file
        last = 0
        IF nc = INT(nc / 1000) * 1000 THEN
                LET savenum = INT(nc / 1000)
        ELSE
                LET savenum = INT(nc / 1000) + 1
                LET last = 1
        END IF

        CALL lagcalc

        OPEN "R", #3, file$, 8
        FIELD #3, 4 AS up$, 4 AS dn$
        FOR n = 1 TO 50
                LET uplag = upl(n) * 1000 * stresscal
                LET dnlag = dnl(n - 1) * 1000 * stresscal
                LSET up$ = MKS$(uplag)
                LSET dn$ = MKS$(dnlag)
                LET recnum = n + 50 * savenum
                PUT #3, recnum
        NEXT n
        IF last = 1 THEN
                LSET up$ = MKS$(savenum)
                LSET dn$ = MKS$(nc)
                PUT #3, 1
                LSET up$ = MKS$(aml)
                LSET dn$ = MKS$(ov)
                PUT #3, 2
                LSET up$ = MKS$(lag)
                LSET dn$ = MKS$(last)
                PUT #3, 3
                LSET up$ = MKS$(stresscal)
                LSET dn$ = MKS$(straincal)
                PUT #3, 4
```

```
        END IF
        CLOSE #3
END SUB

SUB sawtooth            'controls the strain cycles
        DO
                LOCATE 5, 17
                INPUT "Offset Voltage (-10V to 10V) ="; ov
                LOCATE 6, 17
                INPUT "Amplitude ="; aml
                        LET b = ov - aml
                        LET t = ov + aml
                LOCATE 7, 17
                INPUT "Set Lag ="; lag
                        LET lag = INT(lag)
                IF b >= -10 AND t <= 10 THEN
                        IF aml >= 0 AND lag >= 0 THEN flag = 1
                END IF
        LOOP UNTIL flag = 1
        stp$ = ""
        INPUT "Enter the stress calibration factor:"; stresscal
        INPUT "Enter the strain calibration factor:"; straincal
        INPUT "Enter the name of the data file:"; file$
        CLS
        CALL menu
        CALL switch(1)

        DO
                LET halfmax = -.001
                LET halfmin = .001
                LET overload = 0

                FOR n = 26 TO 50
                   LET f = n * (t - b) / 50 + b
                   CALL voltout(f)
                   CALL stressup(n)
                   IF n >= 26 + lag THEN
                         IF up(n) > halfmax THEN LET halfmax = up(n)
                         IF up(n) < halfmin THEN LET halfmin = up(n)
                   END IF
                   IF up(n) > .001 OR up(n) < -.001 THEN overload = 1
                NEXT n

                FOR n = 49 TO 0 STEP -1
                   LET f = n * (t - b) / 50 + b
                   CALL voltout(f)
                   CALL stressdn(n)
                   IF n > 25 - lag THEN
                         IF dn(n) > halfmax THEN LET halfmax = dn(n)
                         IF dn(n) < halfmin THEN LET halfmin = dn(n)
                   END IF
                   IF dn(n) > .001 OR dn(n) < -.001 THEN overload = 1
                NEXT n

                FOR n = 1 TO 25
                        LET f = n * (t - b) / 50 + b
                        CALL voltout(f)
                        CALL stressup(n)
                NEXT n

                IF aml > 0 THEN nc = nc + 1

                LOCATE 18, 33
                PRINT nc
                LOCATE 19, 34
                PRINT ov; "V"
```

```
                LOCATE 20, 29
                PRINT aml; "V"
                LOCATE 18, 48
                PRINT kepco$

                IF plotflag = 1 THEN CALL plotcycle

                LET maxdif = ((halfmax - halfmin) * 1000 * stresscal)
                IF maxdif < 5 AND maxdif > 0 AND aml > 0 THEN
                        CALL switch(0)
                        CALL savedata
                        CALL printout
                        LOCATE 21, 17
                        PRINT "The last cycle was "; nc
                        stp$ = "y"
                END IF

                IF overload > 0 AND aml <> 0 THEN
                        CALL switch(0)
                        CALL savedata
                        CALL printout
                        LOCATE 21, 17
                        PRINT "The system overloaded in cycle "; nc
                        stp$ = "y"
                END IF

                IF nc = INT(nc / 1000) * 1000 THEN
                        IF nc <> 0 THEN CALL savedata
                END IF

        LOOP UNTIL stp$ = "y"

END SUB

SUB sendit      'sends commands to OPTO driver
    LET e% = errs%
    LET ad% = addr%
    LET cm% = cmd%
    FOR r = 0 TO 15
        LET p%(r) = posi%(r)
        LET i%(r) = info%(r)
        IF r = 0 OR r = 1 THEN
            LET m%(r) = modi%(r)
        END IF
    NEXT r
    CALL OPTOWARE(e%, ad%, cm%, VARPTR(p%(0)), VARPTR(m%(0)), VARPTR(i%(0)))
    IF errs% < 0 THEN
        PRINT "There is an error (number "; errs%
        PRINT "The command Number was "; cmd%
        END
    END IF

END SUB

SUB setup               'sets up initial conditions
        cmd% = 102              'Set serial port to COM 2
        info%(0) = 2
        CALL sendit

        addr% = addr1%          'Analog
        cmd% = 0                'Power-up-clear
        CALL sendit

        addr% = addr1%          'Analog
        cmd% = 1                'Reset
        CALL sendit
```

```
        addr% = addr2%          'Digital
        cmd% = 0                'Power-up-clear
        CALL sendit

        addr% = addr2%          'Digital
        cmd% = 1                'Reset
        CALL sendit

        cmd% = 103              'Set number of retries at 6
        info%(0) = 6
        CALL sendit

        addr% = addr1%          'Analog
        cmd% = 8                'Configure module 1 as output
        posi%(0) = module%
        posi%(1) = -1
        CALL sendit

        addr% = addr2%          'Digital
        cmd% = 8                'Configure module 1 as output
        posi%(0) = module%
        posi%(1) = -1
        CALL sendit

        CALL voltout(0)         'Set output voltage as Zero


END SUB

SUB softkey             'sets up and enables softkeys
        KEY 15, CHR$(&H4) + CHR$(&H2E)    'c
        KEY 16, CHR$(&H4) + CHR$(&H2F)    'v
        KEY 17, CHR$(&H4) + CHR$(&H1E)    'a
        KEY 18, CHR$(&H4) + CHR$(&H19)    'p
        KEY 19, CHR$(&H4) + CHR$(&H13)    'r
        KEY 20, CHR$(&H4) + CHR$(&H1F)    's
        KEY(15) ON
        KEY(16) ON
        KEY(17) ON
        KEY(18) ON
        KEY(19) ON
        KEY(20) ON
        ON KEY(15) GOSUB plot
        ON KEY(16) GOSUB volt
        ON KEY(17) GOSUB amplitude
        ON KEY(18) GOSUB pausecycle
        ON KEY(19) GOSUB restart
        ON KEY(20) GOSUB stopcycle
END SUB

SUB startup             'opens files
        CLS

        OPEN "COM2: 19200,N,8,1,RS,CS,CD,DS" FOR RANDOM AS #1
        CLOSE #1

        OPEN "R", #2, "I3981D1"
        IOCTL #2, "ENI "
        IOCTL #2, "SIN1 "
END SUB

SUB stressdn (D)     'put stress into array for downstroke
                CALL readstress(r)
                dn(D) = r
END SUB
```

```
SUB stressup (u)        'puts stress into array for upstroke
                CALL readstress(r)
                up(u) = r
END SUB

SUB switch (x)          'switches KEPCO on/off

        IF x = 0 THEN
                addr% = addr2%
                cmd% = 11
                posi%(0) = module%
                posi%(1) = -1
                CALL sendit
                kepco$ = "OFF"
        END IF
        IF x = 1 THEN
                addr% = addr2%
                cmd% = 9
                posi%(0) = module%
                posi%(1) = -1
                CALL sendit
                kepco$ = "ON"
        END IF
END SUB

SUB voltout (v)         'Sets the reference voltage from OPTO
        addr% = addr1%
        cmd% = 35               'Set output voltage
        posi%(0) = module%
        posi%(1) = -1
        info%(0) = ((v + 10) / 20) * 4095
        CALL sendit
END SUB
```

```
DECLARE SUB plotcycle ()                    '
                                            'Dimensioning and
DIM SHARED upl(50)                          'declaring
DIM SHARED dnl(50)                          'subprogram
                                            'and variables
COMMON SHARED upl(), dnl()                  '
COMMON SHARED aml, ov, lag, nc              '
COMMON SHARED stresscal, straincal          '

CLS
INPUT "File name:"; file$                   '
OPEN "R", #1, file$, 8                      '
LPRINT "file name :"; file$                 '  Reading and
                                            '  printing
FIELD #1, 4 AS up$, 4 AS dn$                '  information
GET #1, 1                                   '  from the
LET lastnum = CVS(up$)                      '  random access
LET lcn = CVS(dn$)                          '  file
LPRINT "The last cycle was:"; lcn           '
PRINT "The last cycle was:"; lcn            '
                                            '
GET #1, 2                                   '
LET aml = CVS(up$)                          '
LET ov = CVS(dn$)                           '
LPRINT "Amplitude = "; aml                  '
LPRINT "Offset Voltage = "; ov              '
PRINT "Amplitude = "; aml                   '
PRINT "Offset Voltage = "; ov               '
                                            '
GET #1, 3                                   '
LET lag = CVS(up$)                          '
LET last = CVS(dn$)                         '
LPRINT "Lag = "; lag                        '
PRINT "Lag = "; lag                         '
                                            '
GET #1, 4                                   '
LET stresscal = CVS(up$)                    '
LET straincal = CVS(dn$)                    '
LPRINT "Stress calibration factor = "; stresscal; "Mpa/mV"
LPRINT "Strain calibration factor = "; straincal; "1000/V"
PRINT "Stress calibration factor = "; stresscal; "Mpa/mV"
PRINT "Strain calibration factor = "; straincal; "1000/V"

SLEEP 10
                                                '
FOR m = 1 TO lastnum                            '
        IF m = lastnum THEN                     '
                nc = lcn                        '
        ELSE nc = m * 1000                      '  Reading the
        END IF                                  '  stress values
        FOR n = 1 TO 50                         '  of each
                GET #1, n + 50 * m              '  cycle into
                LET upl(n) = CVS(up$)           '  arrays
                LET dnl(n - 1) = CVS(dn$)       '
                                                '
                LET upl(n) = upl(n) / 1000 / stresscal
                LET dnl(n - 1) = dnl(n - 1) / 1000 / stresscal
        NEXT n                                  '
        CALL plotcycle                          '  Plotting the
                                                '  cycle
        INPUT "Do you want to print?"; prt$     '
        IF prt$ <> "y" THEN GOTO 10             '  Printing the
        LPRINT                                  '  cycle on
        LPRINT "Cycle No.:";                    '  request
        LPRINT nc                               '
        FOR n = 1 TO 50                         '
```

```
                LET upl(n) = upl(n) * 1000 * stresscal
                LET dnl(n - 1) = dnl(n - 1) * 1000 * stresscal

                LPRINT "up"; n; ")"; upl(n); "     ";
                LPRINT "dn"; n - 1; ")"; dnl(n - 1)
        NEXT n                                          '
                                                        '
                                                        '
10 NEXT m                                               '
CLOSE #1

END

SUB plotcycle                   'subprogram to
        SCREEN 11               'plot a hysteresis
        CLS                     'loop

        LET hi = -10            'determining the min
        LET low = 10            'and max of the cycle
        FOR hl = 0 TO 50
                IF hl > 0 THEN
                        IF upl(hl) > hi THEN hi = upl(hl)
                        IF upl(hl) < low THEN low = upl(hl)
                END IF
                IF hl < 50 THEN
                        IF dnl(hl) < low THEN low = dnl(hl)
                        IF dnl(hl) > hi THEN hi = dnl(hl)
                END IF
        NEXT hl

        LET mid = (hi + low) / 2                'calculating
        LET multiply = 170 / (hi - mid)         'scale factor

        FOR p = 0 TO 50
                LET xposi = p * 14 + 10
                IF p > 0 THEN
                        LET yposi = 172 - (upl(p) - mid) * mulitply
                        LINE (xposi, yposi)-(xposi, yposi)
                        CIRCLE (xposi, yposi), 3
                END IF
                IF p < 50 THEN
                        LINE (xposi, yposi)-(xposi, yposi)
                        CIRCLE (xposi, yposi), 2
                END IF
        NEXT p

        LINE (10, 172)-(710, 172)
        LINE (360, 1)-(360, 346)

        PRINT "Ampl.="; aml; "V"                '
        PRINT "Offset ="; ov; "V"               '
        PRINT "Cycle no.="; nc                  'Printing
        PRINT "Lag ="; lag                      'cycle
        LOCATE 1, 27                            'information
        PRINT "Stress (MPa)"                    '
        LOCATE 12, 1                            '
        PRINT "Strain (*1000)"                  '
                                                        'Plotting
        LET mv = multiply / 20000                       'scales
        FOR mark = 1 TO 20                              '
                IF (mark * mv) <= 170 THEN              '
                        LET yposi = 172 - mark * mv
                        LINE (355, yposi)-(355, yposi)
                        LET ypos = yposi / 14 + .5
                        LOCATE ypos, 42
                        PRINT USING "####.###"; mark * .05 * stresscal
```

```
                        LET yposi = 172 + mark * mv
                        LINE (355, yposi)-(355, yposi)
                        LET ypos = yposi / 14 + .5
                        IF ypos + .5 < 24 THEN
                                LOCATE ypos, 42
                                LET yscale = -1 * mark * .5 * stress
                                PRINT USING "####.###"; yscale
                                END IF
                END IF
                IF mark = 1 AND mv > 170 THEN
                        LINE (355, 2)-(365, 2)
                        LOCATE 1, 42
                        PRINT USING "####.###"; (hi - mid) * stresscal
                        LINE (355, 342)-(365, 342)
                        LOCATE 23, 42
                        PRINT USING "####.###"; (low - mid) * stresscal
                END IF
                NEXT mark

        FOR xmark = 0 TO 4
                IF xmark <> 2 THEN
                        xmarkpos = 10 + xmark * 175
                        LINE (xmarkpos, 168)-(xmarkpos, 176)
                        xpos = (xmarkpos) / 9 + .5 - xmark - 1
                        LOCATE 14, xpos
                        LET xscale = (xmark - 2) / 2 * aml * straincal
                        PRINT USING "###.###"; xscale
                END IF
        NEXT xmark

        DO
        LOOP UNTIL INKEY$ = "y"
        CLS
END SUB
```

APPENDIX 2
BACKGROUND ELECTRONICS FOR CHAPTER 2

A2.1 The Operational Amplifier

An operational amplifier (op amp) is a multistage amplifier. It is termed "operational" because it can be used to perform mathematical operations such as addition, subtraction, integration and others.

The following discussion on op amps and feedback amplifiers is based on Chapters 1 to 5 of "*The Versatile Op Amp*" (Kahn, 1970).

The most commonly used op amp is the integrated circuit or IC op amp, which is fabricated on a single silicon chip. Op amps can be used as dc amplifiers, ac amplifiers, differential amplifiers, non-inverting amplifiers or inverting amplifiers.

The actual circuit of an op amp is complex (Kahn, 1970) and will not be discussed here. However, they can usually be treated simply as a single unit, using the "black box" approach. Figure A2.1 shows a schematic diagram of an op amp.

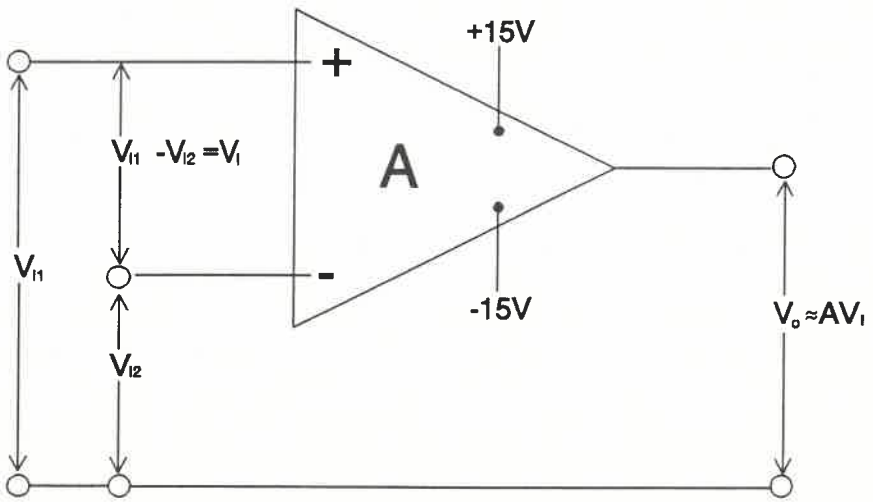

Figure A2.1 : Schematic diagram of an op amp.

An operational amplifier has two inputs and an output. One of the inputs is an inverting input and the other is a non-inverting input. The inverting input is so called because voltages applied

to this terminal will be inverted at the output; that is, the output will be 180° out of phase with the input. Similarly the non-inverting input voltage will not be inverted at the output, but will be in phase with the output.

Most commonly available op amps are powered by a +15V and a -15V dc power supply. The difference between the two inputs is amplified at the output. If V_{I1} and V_{I2} are the two input voltages and V_o is the output voltage, then to a good approximation

$$V_o = A(V_{I1}-V_{I2}) \qquad (A2.1)$$
$$= AV_I,$$

where A is the *gain* of the op amp,
and $V_I=V_{I1}-V_{I2}$, is the *difference voltage*.

This proportionality only holds while V_o is between the limits of saturation. These limits are determined by the magnitude of the dc voltage supplied to the op amp. The positive and negative saturation voltages will be slightly smaller in magnitude than the supply voltage. Figure A2.2 shows graphically how the output voltage, V_o is related to the difference voltage, V_I.

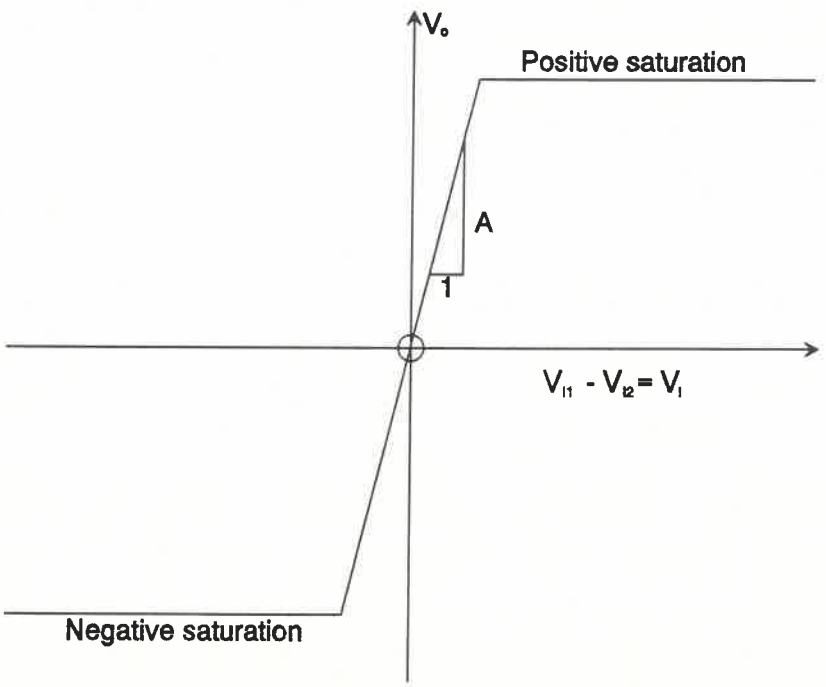

Figure A2.2 : The voltage transfer characteristic of an op amp.

In practice there may also be a sum or error term, and

$$V_o = A_D(V_{I1} - V_{I2}) + \frac{A_c}{2}(V_{I1} + V_{I2}) \quad , \qquad \text{(A2.2)}$$

where $A_D = V_o/(V_{I1}-V_{I2}) = V_o/V_I$, is the *differential gain* of the op amp, and $A_c = V_o/V_{I1}$ when $V_{I1}=V_{I2}$ ie. $V_I=0$. A_c is called the *common mode gain*.

The *common mode rejection ratio* C is defined as follows :

$$C = \frac{A_D}{A_c} \quad . \qquad \text{(A2.3)}$$

In an ideal amplifier, A_c should be zero. C would then be infinite and A would be equal to A_D. In practice the op amp circuit is designed to maximise C. In the discussion below it is assumed that C is large and that the error term is correspondingly small.

A2.2 **The Negative Feedback System**

In an ideal op amp the gain would be constant. In practice, external influences such as temperature can cause the gain to vary. In addition, due to mass production of IC op amps, the gain of individual op amps may vary considerably from the stated or nominal gain.

Negative feedback is used to reduce the effects of this uncertainty in the gain. The basic feature of feedback involves feeding a portion of the output voltage back to the inverting input of the op amp.

If only one input of the op amp has a voltage source connected to it, then there are two possible configurations for negative feedback. Figure A2.3(a) shows a non-inverting feedback amplifier, and Figure A2.3(b) shows an inverting feedback amplifier. The output of the non-inverting amplifier is in phase with the input (source) voltage, while the output of the

inverting amplifier is 180° out of phase with the source voltage, V_s.

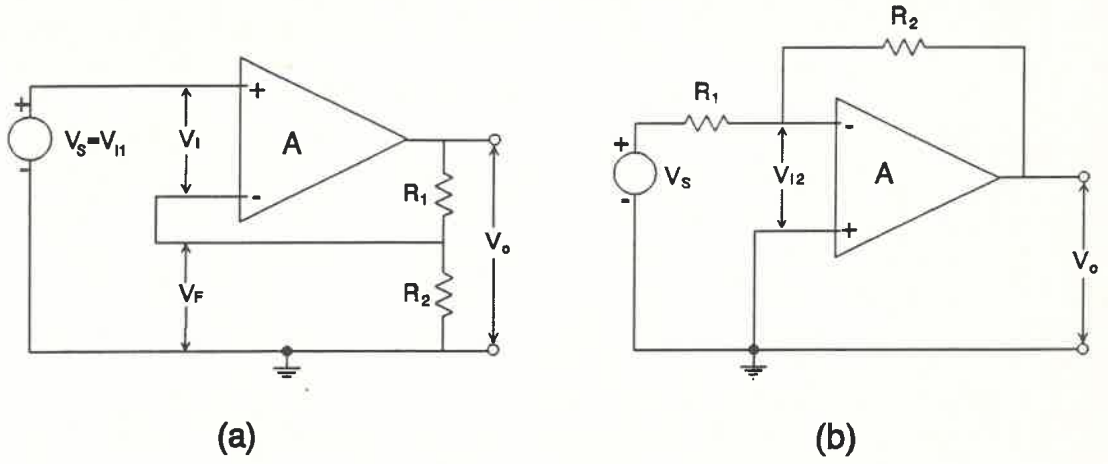

Figure A2.3 : Schematic diagram of (a) a non-inverting feedback amplifier, and (b) an inverting feedback amplifier.

The gain of the amplifier with feedback, A_F, which is equal to the ratio of the output voltage to the source voltage, is called the *closed loop gain*. A_o, the gain without feedback, is called the *open loop gain*. It can be shown (Kahn, 1970) that for a general feedback system

$$A_F=\frac{A_o}{1+A_o\beta} \quad , \tag{A2.4}$$

where β is defined as the *feedback factor*,
and $A_o\beta$ is defined as the *loop gain*.

If $A_o\beta$ is much greater than one then

$$A_F=\frac{A_o}{1+A_o\beta}\approx\frac{A_o}{A_o\beta}=\frac{1}{\beta} \quad . \tag{A2.5}$$

The term $1/\beta$ is called the *ideal closed loop gain*.

For the non-inverting system shown in Figure A2.3(a)

$$A_o=A \tag{A2.6}$$

and

$$\beta = \frac{R_2}{R_1 + R_2} \quad . \qquad \text{(A2.7)}$$

For the inverting feedback system shown in Figure A2.3(b)

$$A_o = \frac{R_2 A}{R_1 + R_2} \qquad \text{(A2.8)}$$

and

$$\beta = \frac{R_1}{R_2} \quad . \qquad \text{(A2.9)}$$

Thus, the *ideal closed loop gain* for the feedback systems are

$$\frac{1}{\beta} = \frac{R_1 + R_2}{R_2} \qquad \text{(A2.10)}$$

for the non-inverting system, and

$$\frac{1}{\beta} = -\frac{R_2}{R_1} \qquad \text{(A2.11)}$$

for the inverting system. The negative sign in equation A2.11 indicates that the phase is inverted by the amplifier.

If $A_o\beta >> 1$, the gain of the amplifier as a whole depends only on the values of the resistors used in the circuit. This means that the overall gain of the feedback system is not dependent on external influences, such as temperature. The gain can be adjusted very easily by using different resistors, as long as the basic assumptions are not compromised, that is, $A_o\beta >> 1$.